

STATUS OF THESIS

Title of thesis

REMOVAL AND RECOVERY OF BORON FROM PRODUCED
WATER BY ELECTROCOAGULATION AND
HYDROTHERMAL MINERALIZATION

I, EZERIE HENRY EZECHI
hereby allow my thesis to be placed at the Information Resource Center (IRC) of
Universiti Teknologi PETRONAS (UTP) with the following conditions:

1. The thesis becomes the property of UTP
2. The IRC of UTP may make copies of the thesis for academic purposes only.
3. This thesis is classified as

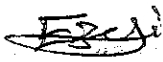
☐ Confidential

☒ Non-confidential

If this thesis is confidential, please state the reason:

The contents of the thesis will remain confidential for _____ years.

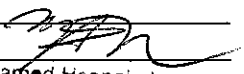
Remarks on disclosure:



Signature of Author

Permanent address: Ichi-Nta,
Umuajuju Village, Isiala Ngwa
South L.G.A., Abia State, Nigeria,
West Africa.

Date : 19/2/2013



Dr Mohamed Hasnain Isa
Associate Professor
Civil Engineering Department
Universiti Teknologi PETRONAS
Bandar Seri Iskandar, 31750 Tronoh
Perak Darul Ridzuan, MALAYSIA

Signature of Supervisor

Name of Supervisor
AP. Dr. Mohamed Hasnain Isa

Date : 19/2/2013

UNIVERSITI TEKNOLOGI PETRONAS


REMOVAL AND RECOVERY OF BORON FROM PRODUCED WATER BY
ELECTROCOAGULATION AND HYDROTHERMAL MINERALIZATION

by

EZERIE HENRY EZECHI

The undersigned certify that they have read, and recommend to the Postgraduate
Studies Programme for acceptance this thesis for the fulfillment of the requirements
for the degree stated.


Signature:


Dr Mohamed Hasnain Isa
Associate Professor
Civil Engineering Department
Universiti Teknologi PETRONAS
Bandar Seri Iskandar, 31750 Tronoh
Perak Darul Ridzuan, MALAYSIA

Main Supervisor:

AP. Dr. Mohamed Hasnain Isa

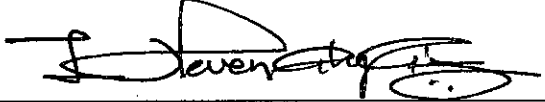
Signature:


Dr. Shamsul Rahman Mohamed Kutty
Associate Professor
Civil Engineering Department
Universiti Teknologi PETRONAS
Bandar Seri Iskandar, 31750 Tronoh
Perak Darul Ridzuan, MALAYSIA

Co-Supervisor:

AP. Dr. Shamsul Rahman Kutty

Signature:



Head of Department:

AP. Ir. Dr. Mohd Shahir Liew

Date:

Assoc. Prof. Ir. Dr Mohd Shahir Liew
Head
Civil Engineering Department
Universiti Teknologi PETRONAS
Bandar Seri Iskandar, 31750 Tronoh
Perak Darul Ridzuan, MALAYSIA

**REMOVAL AND RECOVERY OF BORON FROM PRODUCED WATER BY
ELECTROCOAGULATION AND HYDROTHERMAL MINERALIZATION**

by

EZERIE HENRY EZECHI

A Thesis

Submitted to the Postgraduate Studies Programme

as a Requirement for the Degree of

MASTER OF SCIENCE

CIVIL ENGINEERING

UNIVERSITI TEKNOLOGI PETRONAS

BANDAR SERI ISKANDAR,

PERAK

FEBRUARY 2013

DECLARATION OF THESIS

Title of thesis

REMOVAL AND RECOVERY OF BORON FROM PRODUCED
WATER BY ELECTROCOAGULATION AND
HYDROTHERMAL MINERALIZATION

I EZERIE HENRY EZECHI

hereby declare that the thesis is based on my original work except for quotations and citations which have been duly acknowledged. I also declare that it has not been previously or concurrently submitted for any other degree at UTP or other institutions.



Signature of Author

Permanent address: Ichi-Nta,
Umuajuju Village, Isiala Ngwa
South L.G.A., Abia State, Nigeria,
West Africa.

Date : 19/2/2013



Witnessed by Dr. Mohamed Hasnain Isa
Associate Professor
Civil Engineering Department
Universiti Teknologi PETRONAS
Bandar Seri Iskandar, 31750 Tronoh
Perak Darul Ridzuan, MALAYSIA

Signature of Supervisor

Name of Supervisor
AP. Dr. Mohamed Hasnain Isa

Date : 19/2/2013

DEDICATION

TO MY BELOVED PARENTS AND SIBLINGS.

ACKNOWLEDGEMENT

I would like to express my sincere gratitude to my supervisor: Ap. Dr. Mohamed Hasnain Isa and my Co-supervisor; Ap. Dr. Shamsul Rahman Bin Mohamed Kutty for their guidance, support, advice and encouragement throughout the course of this programme without which this work wouldn't have been a success.

I would like to thank Universiti Teknologi PETRONAS (UTP) for her financial assistance as graduate assistant during the course of this programme. Indeed, I am very grateful. My gratitude also goes to all the UTP technicians who in one way or the other helped me during this programme. I am also indebted to all my friends who supported and encouraged me during this programme.

My profound gratitude goes to my family in entirety for their support, love and encouragement during this programme. I am very grateful to my parents and siblings who stood by me during this programme.

Finally, I would like to thank all my friends whom in one or the other encouraged and supported me during this programme.

ABSTRACT

Produced water is the largest wastestream of oil and gas exploration and a major supplement to the increased limited freshwater supply. It is therefore necessary to ensure that the quality of produced water meets the appropriate standard for use as potable water. This study investigated the removal and recovery of boron from produced water by electrocoagulation and hydrothermal mineralization. The efficiency of the study was investigated in both the batch and continuous mode using aluminum and iron electrodes. Preliminary studies were conducted with synthetic wastewater and the obtained optimum conditions applied to produced water. Different operating parameters were investigated. They include pH, current density, initial concentration, electrolysis time, inter-electrode spacing, flow rate, retention time. pH played a significant role in removal efficiency with the best removal efficiency around pH 7 for both electrodes. Increase in current density also increased removal efficiency. When the initial concentration was increased, removal efficiency decreased. Increase in electrolysis time increased removal efficiency. However, when the spacing between electrodes was increased, removal efficiency decreased. The removal efficiency decreased when the flowrate was increased. Increase in retention time also resulted in increase in removal efficiency. A removal efficiency of 98% and 88% were observed for the batch and continuous mode study respectively using aluminum electrode while a removal efficiency of 97% and 78% were observed for the batch and continuous mode study, respectively using iron electrode.

The adsorption kinetic study was evaluated with four kinetic models; Lagergren pseudo first order kinetics, Ho pseudo second order kinetics, Intra-particle diffusion and Elovich model. The adsorption isotherm was evaluated by Langmuir isotherm and Freundlich isotherm. The thermodynamics of the process was evaluated by Gibbs free energy equation. The adsorption kinetic study revealed that the adsorption of boron onto $\text{Al}(\text{OH})_3$ and $\text{Fe}(\text{OH})_3$ followed the Ho pseudo second order kinetic. The adsorption isotherm study showed that Langmuir isotherm fits the experimental data

better than the Freundlich isotherm and suggest monolayer coverage. Conversely, the thermodynamic study revealed that adsorption of boron onto $\text{Al}(\text{OH})_3$ and $\text{Fe}(\text{OH})_3$ was spontaneous across all the temperature range investigated. The standard enthalpy and entropy indicates that the adsorption is chemisorptions, endothermic and had consistent dispersal of particles. The continuous mode study proved that electrocoagulation can be applied in industrial scale.

The recovery study was conducted using the EC floc and $\text{Ca}(\text{OH})_2$ as a mineralizer at specific temperature. The SEM and XRD results obtained from the recovery study showed the possibility of recovering rare hydrate borate compounds from EC floc. Parasibirskite, Inyoite, Vimsite, Nifontovite and Takedaite were all identified by the XRD result. This result indicates that produced water could be a potential source of rare hydrated borate minerals.

The objective of this study is to remove boron from produced water by electrocoagulation to meet the World Health Organization (WHO) stipulated limit in potable water and recover boron by hydrothermal mineralization from electrocoagulation flocs.

ABSTRAK

Penghasilan air terbesar daripada sisa bahan buangan minyak dan gas merupakan salah satu masalah utama bagi kekurangan bekalan sumber air tawar. Oleh itu, adalah penting untuk memastikan bahawa penghasilan air tersebut mempunyai kualiti dan memenuhi piawai yang sesuai untuk tujuan pengairan. Kajian ini meneliti penyingkiran dan pemulihan boron daripada penghasilan air oleh sisa bahan buangan dengan menggunakan konsep penggumpalan elektrik dan pemineralan hidroterma. Kebersanan kajian ini telah disiasat dalam kedua-dua kelompok dan mod berterusan menggunakan aluminium dan elektrod-elektrod. Kajian awal telah dijalankan dengan air buangan sintetik dan memperolehi syarat-syarat optimum digunakan ke atas menghasilkan air termasuklah menggunakan parameter yang berbeza. Parameter tersebut adalah seperti pH, ketumpatan arus, konsentrasi awal, masa elektrolisis, jarak antara elektrod, kadar aliran, kawasan elektrod dan masa. pH memainkan peranan penting dalam kecekapan penyingkiran dengan kecekapan penyingkiran terbaik sekitar pH 7 untuk kedua-dua elektrod-elektrod. Peningkatan dalam ketumpatan arus juga meningkat kecekapan penyingkiran. Apabila konsentrasi awal dinaikkan, kecekapan penyingkiran menurun. Peningkatkan jangka masa elektrolisis telah menambah kecekapan penyingkiran. Bagaimanapun, apabila jarak antara elektrod-elektrod telah ditambah, kecekapan penyingkiran menurun. Kecekapan penyingkiran mengurang apabila kadar arus air dinaikkan. Terdapat sedikit peningkatan dalam kecekapan penyingkiran apabila kawasan elektrod meningkat. Peningkatan tempoh masa juga menyebabkan peningkatan dalam kecekapan penyingkiran. Kecekapan penyingkiran adalah sebanyak 98% dan 94% telah diperhatikan untuk kelompok dan kajian mod berterusan masing-masing menggunakan elektrod aluminium manakala kecekapan penyingkiran 97% dan 86% telah diperhatikan untuk kelompok dan kajian mod berterusan masing-masing menggunakan elektrod besi.

Penyerapan tenaga kinetik dinilai dengan empat model kinetik; Lagergren tertib pertama ilmu kinetik, Ho tertib peringkat kedua ilmu kinetik, resapan Intra- zarah dan

Elovich model. Isoterma penjerapan dinilai oleh isoterma Langmuir dan isoterma Freundlich. Penyerapan kajian kinetik mendedahkan bahawa penyerapan boron ke atas $\text{Al}(\text{OH})_3$ dan $\text{Fe}(\text{OH})_3$ mengikuti H_0 tertib peringkat kedua kinetik. Kajian menunjukkan isoterma penjerapan isoterma Langmuir itu sesuai data percubaan lebih baik daripada isoterma Freundlich dan mencadangkan liputan ekalapisan. Kajian termodinamik dinilai dengan persamaan tenaga bebas Gibb mendedahkan bahawa penyerapan boron ke atas $\text{Al}(\text{OH})_3$ dan $\text{Fe}(\text{OH})_3$ adalah spontan merentasi semua julat suhu. Entalpi standard dan entropi menunjukkan bahawa penyerapan yang telah berlaku adalah serapan kimia, endoterma dan telah menambah kerawakan kajian. Kajian mod berterusan membuktikan bahawa penggumpalan elektrik dapat diaplikasikan dalam piawaian industri.

Kajian pemulihan telah dijalankan menggunakan flok SPR dan $\text{Ca}(\text{OH})_2$ kerana satu pemineral di suhu tertentu. Hasil kajian SEM dan XRD diperolehi dan menunjukkan pemulihan borat hidrat daripada bahan flok SPR. Parasibirskite, inyoite, vimsite, nifontovite dan takedaite kesemuanya dikenal pasti oleh hasil XRD. Hasil ini menunjukkan bahawa penghasilan air mungkin daripada bahan buangan sisa adalah mustahil dan mempunyai potensi luar biasa terhadap mineral borat.

Objektif kajian ini ialah untuk membuang boron dari menghasilkan air oleh penggumpalan elektrik bertemu Pertubuhan Kesihatan Sedunia (WHO) menetapkan had dalam air minuman dan pulih boron oleh pemineralan hidroterma dari electrocoagulation flocs.

In compliance with the terms of the Copyright Act 1987 and the IP Policy of the university, the copyright of this thesis has been reassigned by the author to the legal entity of the university,

Institute of Technology PETRONAS Sdn Bhd.

Due acknowledgement shall always be made of the use of any material contained in, or derived from, this thesis.

© Ezerie Henry Ezechi, 2013

Institute of Technology PETRONAS Sdn Bhd

All rights reserved.

TABLE OF CONTENTS

ABSTRACT.....	vii
ABSTRAK.....	ix
LIST OF FIGURES	xvii
LIST OF TABLES.....	xix
CHAPTER 1 INTRODUCTION	1
1.1 Chapter overview.....	1
1.2 Produced water	1
1.2.1 Boron.....	2
1.2.2 Electrocoagulation in wastewater treatment.....	3
1.3 Problem Statement.....	3
1.4 Significance of the study	5
1.5 Objectives of the study	6
CHAPTER 2 LITERATURE REVIEW	7
2.1 Chapter Overview.....	7
2.2 Chemistry of boron.....	7
2.2.1 Applications of boron.....	8
2.2.2 Toxicity and deficiency of boron in plants.....	8
2.2.3 Health challenges associated with boron	10
2.3 Overview of treatment methods.....	11
2.3.1 Membrane treatment technologies	11
2.3.1.1 Reverse Osmosis (RO).....	12
2.3.2 Electrodialysis (ED)	13
2.3.3 Adsorption.....	14
2.3.4 Ion exchange	16
2.3.5 Biological treatment process	16
2.3.6 Coagulation/flocculation	17
2.4 Fundamentals of electrocoagulation.....	18
2.4.1 Definition of electrocoagulation.....	19
2.4.2 Destabilization mechanism of electrocoagulation.....	20
2.4.3 Power Source.....	21

2.4.4 Electrocoagulation Reactor	22
2.4.4.1 Types of electrocoagulation reactors	23
2.4.5 Design of an EC reactor	25
2.4.5.1 Physical design of EC cell	25
2.4.5.2 Chemical design of EC reactor	26
2.4.6 Electrodes	27
2.4.7 Electrode reactions	29
2.4.8 Gas bubble generation	32
2.4.9 Operating parameters for electrocoagulation	32
2.4.9.1 Current density	32
2.4.9.2 Sample pH.....	33
2.4.9.3 Inter-electrode spacing.....	33
2.4.9.4 Conductivity.....	34
2.4.9.5 Temperature	34
2.4.9.6 Electrocoagulation cell voltage.....	34
2.4.10 Previous wastewater studies with electrocoagulation	36
2.4.11 Advantages of electrocoagulation	40
2.4.12 Disadvantages.....	41
2.5 Boron recovery	41
2.5.1 Solvent extraction.....	42
2.5.2 Ion exchange	43
2.5.3 Hydrothermal mineralization	44
2.6 Adsorption kinetics.....	45
2.6.1 Mass transfer	45
2.6.1.1 Diffusion	45
2.6.1.2 Convection	46
2.6.1.3 Migration.....	46
2.6.2 Lagergren pseudo first order rate equation	46
2.6.3 Ho pseudo second order rate equation	47
2.6.4 Intra-particle diffusion.....	48
2.6.5 Elovich model	49
2.7 Adsorption Isotherm	50

2.7.1 Freundlich adsorption isotherm.....	50
2.7.2 Langmuir adsorption isotherm	51
2.7.3 Thermodynamics	51
2.7.4 Kinetic model test.....	52
CHAPTER 3 METHODOLOGY	53
3.1 Chapter overview.....	53
3.2 Electrode type	53
3.2.1 Operating parameters	53
3.2.2 Synthetic wastewater preparation.....	54
3.2.3 Produced water sampling	54
3.3 Electrochemical Set-up.....	55
3.3.1 Batch study	56
3.3.2 Continuous Mode Study.....	57
3.3.3 Determination of boron in aqueous solution	58
3.3.4 Collection of EC flocs from the reactor	59
3.3.5 Hydrothermal mineralization of EC flocs	59
3.3.6 Apparatus used for both Batch and Continuous mode study	61
3.3.7 Materials used for batch and continuous mode study	62
3.3.8 Materials used for hydrothermal mineralization	63
3.4 Adsorption study.....	63
3.5 Thermodynamic study	64
CHAPTER 4 RESULTS AND DISCUSSION.....	66
4.1 Chapter overview.....	66
4.1.1 Justification of parameters	66
4.2 Synthetic wastewater batch study result.....	67
4.2.1 Effect of initial solution pH.....	67
4.2.1.1 Aluminum electrodes	67
4.2.1.2 Iron electrodes.....	71
4.2.2 Effect of current density	73
4.2.2.1 Aluminum electrodes	74
4.2.2.2 Iron electrodes.....	77
4.2.3 Effect of Initial Boron Concentration.....	80

4.2.3.1 Aluminum electrodes	80
4.2.3.2 Iron electrodes.....	81
4.2.4 Effect of Treatment time	82
4.2.4.1 Aluminum electrodes	82
4.2.4.2 Iron electrodes.....	83
4.3 Produced water batch study result	84
4.3.1 Effect of Inter-electrode spacing	84
4.3.1.1 Aluminum electrodes	85
4.3.1.2 Iron electrodes.....	85
4.4 Continuous Mode Study	87
4.4.1 Effect of Flowrate.....	87
4.4.1.1 Aluminum electrodes	87
4.4.1.2 Iron electrodes.....	89
4.4.2 Effect of Concentration	90
4.4.2.1 Aluminum electrodes	90
4.4.2.2 Iron electrodes.....	91
4.4.3 Effect of Retention time	92
4.4.4 Residue concentration of electrode materials.....	92
4.5 Adsorption Kinetics	93
4.5.1 Lagergren pseudo first order kinetics	94
4.5.1.1 Aluminum electrodes	95
4.5.1.2 Iron electrodes.....	96
4.5.2 Ho Pseudo Second Order Kinetic.....	97
4.5.2.1 Aluminum electrodes	98
4.5.2.2 Iron electrodes.....	99
4.5.3 Intra-particle diffusion.....	100
4.5.3.1 Aluminum electrodes	101
4.5.3.2 Iron electrodes.....	102
4.5.4 Elovich Model	104
4.5.4.1 Aluminum electrode.....	104
4.5.4.2 Iron electrodes.....	105
4.5.5 Test of Kinetics	107

4.6 Adsorption Isotherm	108
4.6.1 Langmuir Isotherm.....	108
4.6.1.1 Aluminum electrode.....	108
4.6.1.2 Iron electrode	109
4.6.2 Freundlich Isotherm	110
4.6.2.1 Aluminum electrode.....	110
4.6.2.2 Iron electrode	111
4.7 Thermodynamics	112
4.7.1 Aluminum electrodes	113
4.7.2 Iron electrodes	114
4.8 Analysis of EC flocs	116
4.8.1 Percent recovery of boron (Aluminum electrode).....	116
4.8.1.1 XRD and SEM results for aluminum electrodes.....	116
4.8.2 Percent recovery of boron (Iron electrode)	119
4.8.2.1 XRD and SEM results for Iron electrodes	119
4.8.3 Produced water as a potential source of hydrated borate minerals ...	121
4.9 Analysis of other parameters	123
CHAPTER 5 CONCLUSIONS AND RECOMMENDATIONS	124
5.1 Conclusions	124
5.2 Recommendations for future work	127
REFERENCES.....	128
APPENDIX A.....	143
APPENDIX B.....	151
APPENDIX C.....	153
APPENDIX D.....	156

LIST OF FIGURES

Figure 2.1: Reaction mechanism of electrocoagulation.....	20
Figure 2.2: Image of clay particles prior to electrocoagulation.....	21
Figure 2.3: Image of aggregates after electrocoagulation.....	22
Figure 2.4: Schematic diagram of electrocoagulation reactor	23
Figure 2.5: Schematic diagram of monopolar electrode pattern.....	28
Figure 2.6: Schematic diagram of a bipolar electrode pattern	29
Figure 2.7: Summary of electrocoagulation reaction.....	31
Figure 2.8: Distribution of H_3BO_3/H_2BO_3 in water as a function of pH	33
Figure 2.9: Close circuit: Voltage and current.....	35
Figure 2.10: Open circuit: voltage but no current.....	35
Figure 2.11: Cell removal: No voltage and no current	36
Figure 3.1: Experimental setup for batch study	57
Figure 3.2: Electrochemical setup for continuous mode study.....	58
Figure 3.3: Experimental setup for dissolution of EC floc	60
Figure 3.4: Experimental setup for hydrothermal mineralization.....	61
Figure 3.5: Experimental Flow chart	65
Figure 4.1: Effect of initial pH (Aluminum).....	68
Figure 4.2: Boron removal at different initial pH values (Aluminum).....	69
Figure 4.3: Plot of final pH vs initial pH at different current density (Aluminum).....	70
Figure 4.4: Effect of initial pH (Iron).	72
Figure 4.5: Boron removal efficiency at different initial pH values; (Iron).....	72
Figure 4.6: Plot of final pH vs. initial pH at different current densities. (Iron).....	73
Figure 4.7: Amount of metal ions dissolved (g) at different current; (Aluminum).....	74
Figure 4.8: Effect of current density (Aluminum).....	75
Figure 4.9: Boron removal efficiency at different current densities: (Aluminum).....	76
Figure 4.10: Amount of metal ions dissolved (g) at different current, (Iron).....	78
Figure 4.11: Effect of current density (Iron).....	78
Figure 4.12: Boron removal efficiency at different current densities: (Iron).	79
Figure 4.13: Effect of initial boron concentration; Batch study (Aluminum).	80

Figure 4.14: Effect of initial boron concentration; Batch study (Iron).	82
Figure 4.15: Effect of electrolysis time (Aluminum and Iron).	83
Figure 4.16: Effect of inter-electrode spacing (Aluminum).	85
Figure 4.17: Effect of inter-electrode spacing (Iron).	86
Figure 4.18: Effect of flowrate (Aluminum).	88
Figure 4.19: Effect of flowrate (Iron).	90
Figure 4.20: Effect of initial concentration; Continuous mode (Aluminum).	91
Figure 4.21: Effect of initial concentration; Continuous mode (Aluminum).	92
Figure 4.22: Lagergren pseudo first order plot (Aluminum).	95
Figure 4.23: Lagergren pseudo first order plot (Iron).	97
Figure 4.24: Ho pseudo second order plot (Aluminum).	99
Figure 4.25: Ho pseudo second order plot (Iron).	100
Figure 4.26: Intra particle diffusion plot (Aluminum).	102
Figure 4.27: Intra-particle diffusion plot (Iron)	103
Figure 4.28: Elovich model plot (Aluminum).	105
Figure 4.29: Elovich model plot (Iron).	106
Figure 4.30: Langmuir plot (Aluminum).	109
Figure 4.31: Langmuir plot (Iron).	110
Figure 4.32: Freundlich plot (Aluminum).	111
Figure 4.33: Freundlich plot (Iron).	112
Figure 4.34: Thermodynamic plot (Aluminum).	114
Figure 4.35: Thermodynamics Plot (Iron).	115
Figure 4.36: XRD of EC floc before hydrothermal mineralization (Aluminum)	117
Figure 4.37: SEM of EC floc after hydrothermal mineralization (Aluminum).	118
Figure 4.38: XRD of EC floc after hydrothermal mineralization (Aluminum).	118
Figure 4.39: XRD of EC floc before hydrothermal mineralization (Iron).	120
Figure 4.40: SEM of EC floc after hydrothermal mineralization (Iron).	120
Figure 4.41: XRD of EC floc after hydrothermal mineralization (Iron).	121

LIST OF TABLES

Table 2.1: Boron tolerance of different plants	9
Table 2.2: Health hazard implications of boric acid	10
Table 2.3: Reactivity series of metals	28
Table 3.1: Range of parameters	54
Table 3.2: Characteristics of produced water	55
Table 4.1: Energy consumption at different current densities (Aluminum)	76
Table 4.2: Energy consumption at different current densities (Iron)	79
Table 4.3: Lagergren pseudo first order kinetic constants (Aluminum)	96
Table 4.4: Lagergren pseudo first order kinetic constants (Iron)	97
Table 4.5: Ho pseudo second order kinetic constants (Aluminum)	98
Table 4.6: Ho pseudo second order kinetic constants (Iron)	100
Table 4.7: Intra-particle diffusion constants (Aluminum)	102
Table 4.8: Intra-particle diffusion constants (Iron)	103
Table 4.9: Elovich model constants (Aluminum)	104
Table 4.10: Elovich model constants (Iron)	106
Table 4.11: Langmuir Isotherm Constants (Aluminum)	108
Table 4.12: Langmuir Isotherm constants (Iron)	109
Table 4.13: Freundlich Isotherm constants (Aluminum)	111
Table 4.14: Freundlich Isotherm constants (Iron)	112
Table 4.15: Thermodynamics constants (Aluminum)	113
Table 4.16: Thermodynamics constants (Iron)	115
Table 4.17: Other parameters analyzed (Aluminum)	123
Table 4.18: Other parameters analyzed (Iron)	123

CHAPTER 1

INTRODUCTION

1.1 Chapter overview

This chapter discusses produced water and its generation during oil and gas operation. It also discusses the sources of boron in the environment and health effects of boron at high concentrations to living organisms. The use of electrocoagulation as a treatment technology is also discussed as well as the significance and objectives of this study.

1.2 Produced water

As the limited freshwater sources continue to reduce, attention is turned to produced water in many countries as a supplement, especially in arid areas, for irrigation purposes. Produced water is a by-product of oil well operation which is trapped in underground formation and is brought to the surface along with oil and gas during drilling. It is separated from crude oil above ground in an oil/water separator. As the demand for crude oil increases, the production of produced water increases proportionately. Produced water has unique characteristics which differentiates it from other wastewater.

Produced water composition varies and depends on geological conditions, storage formation and type of recovery method [1]. Produced water generation is usually low in the early stages of oil and gas operation but can rise to as high as 80% during the later years of oil and gas operation [2]. Produced water is reportedly the largest waste-stream of oil and gas exploration with an estimated 250 million barrels per day of produced water generation compared with about 80 million barrels per day of oil

production [3]. Produced water presents several environmental challenges because it is produced in large volumes and often contains constituents in concentrations and forms that are toxic to receiving system biota [4]. Produced water may comprise of flow from above or below the hydrocarbon zone, flow from fluids injected during operation, flow from within the hydrocarbon zone and addition of additives during production. The hydrocarbon content of produced water includes organic acids, polycyclic aromatic hydrocarbons (PAHs), phenols and volatiles [5]. Aquatic toxicity occurs when these compounds combine together [6]. The treatment chemicals used during oil and gas production are complex mixtures of various molecular compounds which can also increase the potential toxicity of produced water [7]. The potential environmental impacts of produced water vary across the locations where it is discharged. When produced water is discharged into small streams, its environmental impact may be higher than when discharged into big streams possibly due to dilution. Most on-shore or near shore locations have been prohibited from receiving produced water discharges due to the environmental implications of untreated produced water [4].

The chemical composition of produced water varies when compared with surface water because produced water is constrained within an aquifer for a long time [8]. Naturally, produced water contains various microorganisms which result in microbial corrosion of the inner surfaces of pipes and related systems conveying the water. Such microbial corrosion process occurs by formation of biofilms on the metal surfaces [9]. In addition, produced water also contains high range of environmental and health constituents of concern like chlorides, light metals and low amount of heavy metals. Therefore, thorough characterization of produced water is vital to identify the environmental risk compounds associated with this water especially when it is to be used as a supplement for fresh water supply.

1.2.1 Boron

Boron is a commonly known drinking water contaminant which presents serious challenges to living organisms at high concentration [10]. In nature boron appears

mostly as boric acid (H_3BO_3) and borax ($\text{Na}_2\text{B}_4\text{O}_7 \cdot 10\text{H}_2\text{O}$). In aquatic systems, it exists primarily as undissociated boric acid and borate ions [11]. The main sources of boron in surface water are urban wastewater containing detergents and cleaning products, industrial effluents, and chemical products used in agriculture [12]. When water with high boron concentration is used for irrigation, boron compounds form complexes with heavy metals like Pb, Cu, Co, Ni, Cd and increase the potential toxicity of these heavy metals. Serious health and environmental problems are caused when these complexes pass to groundwater [13, 14]. The potential toxicity of boron to the environment made the World Health Organization (WHO) propose a boron permissible limit of 0.5 mg/L in potable water which has remained a challenge to many treatment technologies [10]. Therefore effective technologies should be used to meet this stringent limit.

1.2.2 Electrocoagulation in wastewater treatment

The use of electric current in the treatment of wastewater is increasingly gaining global acceptance due to its reported efficiencies and cost effectiveness. Electrocoagulation relies on the scientific theory of response of water contaminants to strong electric field during an oxidation/reduction reaction. Electrocoagulation involves the destabilization of suspended, emulsified or dissolved contaminants in an aqueous medium by introducing an electric current into the medium [15]. Electrocoagulation has been widely used in the removal of water contaminants and presents similar advantages to chemical coagulation. In addition, it produces lesser amount of sludge and requires no chemicals addition. Thus, electrocoagulation presents itself as an important treatment technology.

1.3 Problem Statement

Wastewater treatment has been a remedy to supplement limited freshwater resources in many countries. Various industries produce different wastewater and the produced wastewater is characterized in terms of their physical, biological and chemical compositions. Three significant methods can be used to treat wastewater, which

include primary, secondary and tertiary/advanced treatment methods. Primary method is used to separate suspended solids and grease from water; secondary method is used to remove biodegradable waste while tertiary method is used to remove non-biodegradable waste. Non-biodegradable contaminants present severe health and environmental challenges. Tertiary wastewater treatment processes like reverse osmosis, ion exchange, chemical coagulation, electrodialysis, and adsorption can be used to treat these contaminants. However, most of these conventional methods are expensive and require some level of expertise. In addition, most of these methods have their setbacks which affect their efficiency [16].

For humans, boron can present reproductive dangers and developmental malfunctions. An investigative study conducted with boron in rats, mice and rabbits demonstrated several developmental abnormalities [11]. In humans, symptoms of boron toxicity include diarrhea, nausea, dermatitis, weight loss, vomiting, and lethargy [17]. In plants, boron tolerance limit varies. While some plants can tolerate high boron concentration, others do not. Boron is readily leached by rainfall and needs to be frequently replaced through an alternative process like irrigation in order to retain the properties of the soil and meet the requirements of the crops [18]. However, care is required with the use of irrigation water on plants because the range between boron deficiency and toxicity in plants is narrow [17].

The cost of conventional wastewater treatment methods and their various constraints in boron removal led to the search for an environmentally friendly approach which is cheap and shows consistent removal efficiency. Most conventional methods require high personnel training, high operational cost and produce high amount of sludge. Electrocoagulation is an environmentally friendly approach which requires minimal personnel training and no chemical addition or expensive membranes. In an attempt to solve the cost and efficiency problem of conventional methods in boron removal, electrocoagulation was applied with aluminum and iron electrodes. Electrocoagulation is solely based on the oxidation of the sacrificial anode under the influence of electric current in an oxidation/reduction process. The electrodes are cheap and readily available, they can be used over a certain number of

experiments when thoroughly washed and dried, they release metal ions which adsorb wastewater particles to form flocs.

The volume of industrial and domestic wastes in many countries has been increasing. Landfills have been the method used in disposing sludge. The health and environmental dangers landfills pose to their surrounding environments cannot be overemphasized. In addition, many landfill sites are already filled up, and finding new sites is challenging. It has been observed that sludge makes up about 46% of industrial waste [19]. Therefore it is important to find ways to recover boron as a recyclable precipitate from sources with high boron concentration rather than discharging the waste into the environment. Due to the use of boron compounds in diverse industrial applications, the world boron consumption is increasing and is greater than 1.5 million ton/year in terms of B_2O_3 [20]. In an effort to address the sludge disposal issue, an attempt to recover boron as a recyclable precipitate using hydrothermal mineralization was made. Hydrothermal mineralization involves the use of a mineralizer to recover boron from the flocs produced during electrocoagulation at specific temperature. Evaluation of aluminum and iron electrodes was carried out for the removal of boron from produced water and subsequent recovery with hydrothermal mineralization.

1.4 Significance of the study

Much work on the use of aluminum, iron, zinc, and titanium electrodes has been reported with electrocoagulation. However, about 92% of the works reported on boron removal with electrocoagulation have mainly been with synthetic wastewater in batch study with few operating parameters. Literature on boron removal by continuous mode process is scarce. Many researchers have opted for batch study using electrocoagulation. Although the optimal parameters obtained from batch study are useful in providing information about the interaction of the adsorbent-adsorbate system, the data may not be applicable to most continuous flow treatment systems. Electrocoagulation on continuous flow reactor is quite preferable since it can be easily scaled up from the laboratory results. Therefore, there is the need to perform both batch and continuous flow experiments with electrocoagulation. A total of eight

operating parameters were studied for both the batch and continuous mode experiments. In addition, no work has attempted the recovery of boron as a recyclable precipitate from produced water using the combined methods of electrocoagulation and hydrothermal mineralization.

1.5 Objectives of the study

The main objectives of this study are to remove boron from produced water and subsequently recover boron as a recyclable precipitate from EC floc. The specific objectives are to:

- a) Determine the efficiency of boron removal from produced water in batch and continuous mode study using aluminum and iron electrodes with electrocoagulation.
- b) Determine the effects of operating parameters on the electrocoagulation process
- c) Determine the adsorption kinetic model, adsorption isotherm and thermodynamics parameters for both aluminum and iron electrodes.
- d) Investigate the recovery of boron as a recyclable precipitate from electrocoagulation flocs.

CHAPTER 2

LITERATURE REVIEW

2.1 Chapter Overview

The focus of this chapter is the description of boron, an overview of different processes that have been used in boron treatment, an overview of recovery processes, a detailed explanation of electrocoagulation process setup and the adsorption kinetics, adsorption isotherm, thermodynamics studied in this research.

2.2 Chemistry of boron compounds

Boron is one of the essential micro-nutrients for living organisms. It has an average atomic weight of 10.81 and is widely distributed in oceans, sedimentary rocks, coal, shale and soils [21]. Boron has two stable isotopes (^{10}B and ^{11}B) with a relative abundance of 19.8% and 80.2% respectively [22]. Boron as a metalloid possesses properties of a metal as well as a non metal and belongs to group IIIA of the periodic table [21]. Boron has many oxidation states in compounds but the most common is +3. The lower oxidation states +1, 0 or less than 0 are present only in compounds such as higher boranes (e.g. B_5H_9), subvalent halides (e.g. B_4Cl_4), metal borides (Ti_2B) or in some compounds containing multiple B-B bonds [17]. Structural studies have also indicated that in borates, the boron atom usually combines with either three or four oxygen atoms forming $[\text{BO}_3]$ or $[\text{BO}_4]$ groups. Consequently, the electronic orbitals are hybridized to a planar SP^2 or a three-dimensional SP^3 structure [23].

Boron acts as a Lewis acid [24]. The dissociation of boric acid occurs at various pKa. At low pH, boron exists in water as boric acid (H_3BO_3) and from pH 10, the

borate anion $[B(OH)_4]^-$ predominates. From about pH 11, highly water soluble polyborate ions such as $B_3O_3(OH)_4^-$, $B_4O_5(OH)_4^-$ and $B_5O_6(OH)_4^-$ are formed [11, 25]. The dissociation of boric acid in water can be described as follows [26] :



Total boron (tB) is comprised of all species of boron and is expressed in terms of the molecular weight of the atom.

$$tB = [H_3BO_3] + [H_2BO_3^-] + [HBO_3^{2-}] + [BO_3^{3-}] \text{ as mg/L B} \quad (2.4)$$

2.2.1 Applications of boron compounds

Boron compounds have been widely used for industrial applications. These applications have increased the demand for boron compounds. Boron compounds are used in nuclear technology, rocket engines as fuels, production of heat resistant materials such as refractories and ceramics, high quality steel, heat-resistant polymers, catalysts, manufacture of glass, pharmaceuticals, corrosion inhibitors in anti-freeze formulations for motor vehicle and other cooling systems, dyestuff production, cosmetics, flame retardants, mild antiseptics, soaps, detergents, neutron absorber for nuclear installations, fertilizers, disinfectants and food preservatives [19, 27-30]. Studies conducted by *Ozdemir and Kipcal* [20] revealed that clay wastes containing boron can be used as cement additives. Various researchers have found that boron is one of the elements of the periodic table with high industrial applications and uses almost similar to carbon [29].

2.2.2 Toxicity and deficiency of boron compounds in plants

Boron is an essential micro-nutrient for plants. Boron is one of the minor elements dissolved in natural water and one of the seven essential micronutrient elements

required for the normal growth of most plants. Boron has marked effects on plants in terms of both nutrition and toxicity [12]. Boron plays an important role in plant carbohydrates degradation, hormonal action, function of the apical meristem and function of the biological membrane structure. Boron deficiency in plants may result in reduced growth, yield loss, and even death of plant depending on the severity of the deficiency [31]. On the other hand, boron toxicity symptoms include yellowing of leaf tips progressing into the leaf blade, death of chlorotic tissue, leaf loss, loss of photosynthetic activities and loss in plant productivity [32]. Boron is required in very low concentration in irrigation water for certain metabolic activities. However, if it is present in amounts higher than required, it becomes toxic [19, 33].

The ability of plants to absorb boron differs. Some plants can tolerate boron at high concentrations while some require boron at low concentrations. Table 2.1 shows the various plant tolerance of boron.

Table 2.1: Boron tolerance of different plants [31]

Sensitive 1 mg/L in irrigation water	Semi-sensitive 2 mg/L in irrigation water	Resistant 4 mg/L in irrigation water
Walnut	Sunflower	Asparagus
Plum	Potato	Palm
Pear	Cotton	Date-palm
Apple	Tomato	Sugar beet
Fig	Olive	Clover
Grape	Pea	Broad bean
Cherry	Barley	Bean
Peach	Wheat	Onion
Apricot	Corn	Turnip
Orange	Gruel	Cabbage
Grapefruit	Cruet	Lettuce
Lemon		Carrot

2.2.3 Health challenges associated with boron

Boron poses dangerous health challenges when it is present above the minimum permissible limit. Long-term consumption of water and food products with high boron content results in malfunctioning of cardiovascular, nervous, alimentary, and sexual systems of humans and animals. Blood composition undergoes changes; physical and intellectual progress of children decelerates and risk of pathological births increases [11]. According to medico-biological investigations, boron compounds are reported to belong to the second class of toxicological danger [29]. For humans, boron can present reproductive dangers and has suspected teratogenetic properties as shown in Table 2.2 [11].

Table 2.2: Health hazard implications of boric acid [11]

Health hazards	Activities responsible for health hazards
Acute health effects	Direct contact with solution may cause eye irritation. Boric acid may be absorbed through broken or abraded skin. Breathing mists may cause respiratory tract irritation
Inhalation exposure	Inhalation-breathing mist may cause irritation to the respiratory tract
Eye contact	May cause mild irritation upon prolonged exposure
Skin contact	Not irritating to skin. May be absorbed through injured skin and cause poisoning
Oral ingestion	May cause headaches; weakness and in coordination; nausea, vomiting, dizziness, diarrhea, drowsiness. May cause kidney damage
Chronic health effects	Reproduction/teratogenicity: a human study of occupationally exposed borate workers showed no adverse reproductive effects. Animal studies of inorganic borates showed reproductive effects in males. Mutagenicity: negative results of in vitro tests. Carcinogenicity: this substance has no evidence of carcinogenic properties. Health warnings: this product has low toxicity. Only large quantities may have adverse impact on human health. Target organs: kidneys

2.3 Overview of treatment methods

Many treatment technologies have been used in the removal of boron from wastewater. While few of these technologies have been effective with little disadvantage, some have shown high inadequacies in boron removal with enormous challenges. A comprehensive discussion of these technologies as related to boron removal is outlined below.

2.3.1 Membrane treatment technologies

One common problem associated with all membrane treatment technologies is membrane fouling and degradation. Membrane fouling results from interactions between dissolved and suspended solutes in the feed and the membrane surface. Membrane properties such as hydrophobicity, charge and roughness also affect the degree of rejection of dissolved species [34]. Other factors which affect membrane treatment technologies include pH, and pressure. In a comparative study conducted by *Koseoglu et al.* [35] using three membrane processes (Seawater reverse osmosis membrane (SWRO), brackish water reverse osmosis membrane (BWRO) and nanofiltration membrane (NF), they observed that the permeate boron concentration was high upto about 4.5 mg/L when nanofiltration membranes were used. SWRO and BWRO showed better removal efficiency with permeate boron concentration of about 2 mg/L respectively at an applied pressure of 15.5 bars and pH 8. However, when the applied pressure was increased to 40.3 bars and 20 bars for SWRO and BWRO, permeate boron concentration reduced to about 0.7 mg/L and 1.2 mg/L, respectively. The obtained result from these membranes did not meet the stipulated WHO guideline for boron in potable water at the pH of geothermal water. However when pH was increased to 10.5, permeate boron concentration of about 0.04 mg/L was achieved for both SWRO and BWRO. However, the impact of high pH in membrane treatment processes cannot be overemphasized. It includes chemical addition, membrane degradation, membrane fouling, scale formation, flux reduction. In a related study conducted by *Smith et al.* [36], they investigated the efficiency of boron removal using polymer assisted ultrafiltration membrane. They observed a permeate boron

concentration of about 2 ppm from an initial boron concentration of about 10.5 ppm. The above literature shows that different factors affect boron removal by membrane processes. These factors must be considered while considering membrane treatment.

2.3.1.1 Reverse Osmosis (RO)

Reverse osmosis is a method of producing pure water by passing the solvent through a semi-permeable membrane in a direction opposite to that for natural osmosis with the application of a hydrostatic pressure greater than the osmotic pressure [37]. Reverse osmosis makes up about 36% of the world desalination capacity and is effective in rejecting salts and suspended solids. However, boron rejection in reverse osmosis membrane is extremely less than that of salt [30]. It is reported that Japanese standards for water quality can be achieved except for boron [38]. This is because boron can pass through reverse osmosis membranes in a non-ionic way, similar to that of carbonic acid or water at low pH [39]. According to *Pastor et al.* [40], boron can form bridges of hydrogen with active groups of the membrane at low pH and diffuse in a similar way to that of carbonic acid or water. Above pH 9, the dominant boron species in water is the borate ions and rejection of boron increases during reverse osmosis treatment. However, at high pH, potential precipitation of Magnesium hydroxide and Calcium carbonate present in solution occurs. Magnesium hydroxide and Calcium carbonate precipitates cause membrane fouling and enhanced scale formation on the surfaces of seawater reverse osmosis membranes [41]. The above mentioned conditions could be the reason why the efficiency of boron removal by conventional reverse osmosis (RO) membranes is reportedly about 40-78% [42]. Single stage RO membranes are able to turn seawater of boron concentration 4-5 mg/L into permeate water with boron concentration of about 0.9-1.8 mg/L [16]. Several factors affect the efficiency of reverse osmosis membrane in boron rejection. These factors include pH, operating pressure, permeate flux and flow velocity. However, pH is the most significant factor [41]. *Koseoglu et al.* [41], investigated the impact of pH, feed concentration, pressure and flow velocity in boron removal from seawater using high rejection seawater reverse osmosis membranes. They observed that at seawater pH of 8.2, boron removal efficiency was about 85-90% but rose

above 98% when the pH was increased to 10.5. At high pH, there is stronger repulsion between membrane active surface and the charged borate ions, which leads to enhanced boron rejection [43]. Applied pressure also affects reverse osmosis membrane processes. Increase in applied pressure also improves reverse osmosis membrane treatment efficiency [44]. However, newly produced seawater reverse osmosis membranes are claimed to have boron removal efficiency of 91-93% [45].

For every reverse osmosis process, a careful review of the wastewater characteristics is necessary. In order to prevent membrane fouling, scaling or other membrane degradation, a pre-treatment stage may be needed [46]. The advantages of reverse osmosis process in wastewater treatment include [46] :

- a) Ability to reject all contaminant ions and most dissolved non-ions
- b) Operation is fast
- c) Requires small space and has a modular type construction that can easily be expanded

The disadvantages of reverse osmosis membrane treatment process include

- a) High cost of power
- b) High maintenance cost
- c) Periodic monitoring of membrane

2.3.2 Electrodialysis (ED)

Electrodialysis is a treatment process in which ions migrate through ion selective semi permeable membranes as a result of attraction to two electrically charged electrodes. A typical electrodialysis is composed of a membrane stack with a number of cell pairs, each consisting of a cation transfer membrane, demineralized flow spacer, ion transfer membrane and a concentrate flow spacer [46]. Electrodialysis has high rejection for total dissolved solids, ions and colloids [46]. However, electrodialysis has low rejection for boron. Few studies conducted with electrodialysis reported that conventional electrodialysis is only capable of removing about 42-75% of boron [47]. Several factors also affect boron removal efficiency with electrodialysis. Among these

factors is interference of ions. Transport of boron in an electrodialytic chamber is influenced by the nature of cations and anions present in solution. *Barbara et al.* [48], in their study of boron removal with electrodialysis, reported that in the presence of chloride, percent removal of boron decreased and operation time increased. In the presence of sulfate, percent removal of boron did not change but operation time became longer. The difference in transport property of boron in the presence of sulfate/chloride was attributed to the hydrated radius of several anions present in the aqueous medium. *Kabay et al.* [49], in their study of removal of boron from water by electrodialysis, observed that more than 90% of chloride ions were removed from the solution in 18 minutes while only 20% of boron was removed along with chloride. After 42 minutes of operation time, almost all chloride ions were removed from the solution while about 40% of boron still remained in the solution. Another factor which affects electrodialysis is pH. At low pH, removal efficiency of boron is low but at high pH, boron removal efficiency increases. This is because at low pH, boric acid is the dominant boron species while at high pH, borate ions predominate [50]. The advantages of electrodialysis include [46] :

- a) High rejection of contaminants
- b) Low pressure requirement (Lower than RO)
- c) Requires minimal supervision in a remote setting
- d) Prevents scaling.

The disadvantages of electrodialysis include:

- a) High capital and operating cost
- b) High level of pre-treatment
- c) Frequent electrode replacement.

2.3.3 Adsorption

Adsorption is a process through which boron is adsorbed onto different kinds of particles. Many adsorbents have been used in adsorption process. They include Al_2O_3 based materials (siral 30 and pural) [13], iron-rich natural clays [14], activated sludge

[19], activated alumina [25], neutralized red mud [28], cerium [33], activated carbon prepared from coconut shell impregnated with calcium and barium chlorides, citric and tartaric acids [51], activated carbon impregnated with salicylic acid [52], and composite magnetic particles [53]. Several factors affect adsorption of boron. They include loss of adsorbent, diffusion rate, adsorbent dose and kinetics of the surface reactions [33]. The pH of the sample also affects boron removal by adsorption [54]. Depending upon the nature of adsorbents, *Irawan et al.* [55], reported that boron concentration in the solution and its adsorption are both pH-dependent and the optimum pH for boron adsorption is 2 for fly ash, 6.0 for composite magnetic particles, 7 for neutralized red mud, and 9 for layered double hydroxide. This was also supported by *Wei et al.* [56], who reported that solution pH affects both boron speciation and surface properties of the adsorbent. The amount of boron removed increases with increasing adsorbent dose due to the increase in the total available surface area of the adsorbent particles [47]. Studies have shown that different adsorbents have different adsorption capacities [13, 25, 33]. *Fujita et al.* [19], in their study of boron adsorption onto activated sludge reported that activated sludge has a limited capacity to remove boron from water. They observed that boron was adsorbed onto activated sludge rather than absorbed into the activated sludge because boron concentration in the activated sludge decreased within several days indicating a desorption process. *Bouguerra et al.* [25], in their study of boron removal by adsorption onto activated alumina and by reverse osmosis reported that for initial boron concentration of 5 and 50 mg/L, a maximum removal efficiency of 40% and 65% was observed at adsorbent dose of 0.8 and 5g, respectively. Using iron-rich natural camlica bentonites CB1 and CB2, *Seyhan et al.* [14], observed boron removal efficiency of 80% and 30% for CB1 and CB2 adsorbents, respectively. However, adsorbent loss during the adsorption process affects the overall process efficiency [57]. Adsorption process may be cheap and feasible but its efficiency depends on the type of adsorbent as well as the operating parameters.

2.3.4 Ion exchange

Ion exchange has recorded tremendous improvement in boron removal from wastewater. Ion exchange mechanism is based on exchanging mobile ions attached to an immobile functional acid or base group with solute ions which have greater affinity for the immobile functional group on a solid phase [46]. Some investigations into the efficiency of boron removal using ion exchange method revealed that conventional ion exchange method was not effective in boron removal due to poor ionization of boron [29]. However, the use of the newly produced selective ion exchange resins (purolite and Diaion) has not only been effective in removing boron from wastewater but also in recovering it from wastewater [58]. The most commonly used resins are the Amberlite IRA-743, otherwise known as Amberlite XE-243 and Diaion CRB 02 and Dowex XUS 43594.00 [59]. These resins are macroporous polystyrenic based resin, with functional groups specially designed for the selective removal of boron from aqueous solutions. They are effective for solutions over a wide range of pH values, and over a wide range of boron concentrations. These boron selective resins show great elimination performance. The resin performance is not affected by temperature variations, by pH value or by the background salinity of the water to be treated. Selective sorption of boron by these sorbents is as a result of formation of stable complexes like ethers or complex anions with polyoxocompounds. These resins used in ion exchange systems have a macroporous polystyrene backbone and a very specific functional group based on N-methyl glucamine, which has a tertiary amine end and a polyol end and makes a very stable complex with boric acid [60]. Boron removal efficiency here is reported to be about 93-98% [29]. However, the cost of resins regeneration is a major setback.

2.3.5 Biological treatment process

Little work has been done in this area concerning boron removal. Because boron is a non-biodegradable compound, there is not much literature on boron removal with anaerobic or aerobic treatment processes. From literature, it is reported that conventional biological process removes only little amount of boron [61]. According

to *Linares-Hernandez et al.* [62], conventional biological treatments have not been effective enough to reduce boron to its standard limit level for irrigation. *Kabay et al.* [49], also reported that conventional biological treatment process cannot be used for boron removal because inorganic boron compounds are antiseptics.

2.3.6 Coagulation/flocculation

Coagulation and flocculation processes have been in existence for over several decades. Different wastewaters have been treated with coagulation and flocculation method. This method depends on the strength of added coagulants to react with particles in water. In coagulation and flocculation, the two major materials used are [63-65]:

1. Inorganic and organic coagulants which include mineral additives (calcium, lime, salts etc), hydrolyzing metal salts (aluminum sulfate, ferric sulfate, ferric chloride) and polyelectrolytes which aid in coagulation.
2. Organic flocculants which include cationic and anionic polyelectrolytes, non-ionic polymers, amphoteric and modified polymers as well as naturally occurring flocculants (starch derivatives, guar gums, tannins, chitosan, alginates)

Some literature has reported that biopolymers are effective in removing water contaminants and are more environmental friendly than the conventional coagulation salts. Among the wastewater particles effectively removed by coagulation/flocculation are colloid particles, heavy metals and suspended solids [66-67]. The mechanism of coagulation involves the neutralization of charges on negatively charged colloids through the hydrolysis of cationic products and agglomeration of impurities in an amorphous hydroxide precipitate otherwise known as sweep floc [65,68]. The most widely used inorganic salts in conventional wastewater treatment are aluminum and iron salts. The efficiency of alum in wastewater treatment has been proved beyond doubt and is admired for its low cost, availability and ease of use. However, it produces large volume of sludge and there are questions about its health implications [64]. Most studies have used synthetic

coagulants of organic polymer origin. These polymers are effective in wastewater treatment and have some advantages over alum which include low coagulant dose, larger agglomerate sizes of the solid particles, produces smaller volume of sludge and improved settleability. However, these synthetic polymers are associated with high cost and polymer toxicity [63-64]. Many biological products has also been proposed and studied as coagulants and flocculants for the replacement of conventional materials [69-71]. These bioflocculants polymers (starch, chitosan and alginates) are safe, biodegradable, cheap and produce no secondary pollution [72-73]. However, literature on the removal of boron using these coagulants is scarce. *Yilmaz et al.* [74], investigated the efficiency of boron removal using aluminum chloride. From their results, conventional coagulation using aluminum chloride (alum) did not yield good result in boron removal. The optimum conditions were pH 8 and aluminum dose of 7.45 g/L. After a 2 minute rapid mix at 120 rpm and a 25 minute slow mix at 25 rpm and 60 minutes settling time, a boron removal efficiency of only 24% was observed. In another study, *Golder et al.* [75] investigated boron and nickel removal by coagulation/flocculation process using ferric chloride and aluminum sulfate. They observed that coagulation was not effective in boron removal. A removal efficiency of 41.9% and 33.1% was observed for ferric chloride and aluminum sulfate respectively

2.4 Fundamentals of electrocoagulation

In 1882, *Schulze* [76] showed that colloidal systems could be destabilized by the addition of ions which have a charge opposite to the charge of the colloid. This observation is based on the known principle that unlike charges attract while like charges repel. Under the influence of a spatially uniform electric field, dispersed particles in water tend to move to the electric pole of opposite charge. This motion of the dispersed particle is the bedrock of the present day electrochemistry. Electrochemical technologies were neglected for over a century because of the relatively large capital investment and the expensive electricity consumption. However, extensive research in the United States and the former USSR during the following century has accumulated abundant amount of knowledge and

electrocoagulation has tremendously regained its role as an effective treatment technology [77].

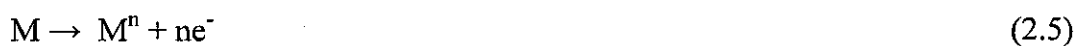
2.4.1 Definition of electrocoagulation

Electrocoagulation is the process of destabilizing suspended, emulsified or dissolved contaminants in an aqueous medium by the introduction of an electric current [15]. When direct current passes through water solution, it destabilizes the colloids in the medium. The destabilized colloids can aggregate together and subsequently be removed by sedimentation and/or flotation. The three major mechanisms of electrocoagulation are [78] :

- a) Formation of coagulants by electrolytic oxidation of sacrificial electrodes.
- b) Destabilization of the contaminants, particulate suspension and breaking of emulsions.
- c) Aggregation of the destabilized phases to form a floc.

Electrocoagulation process is operated with different parameters. The efficiency of electrocoagulation depends on the best combination of these parameters. Parameters such as pH, current density, treatment time, concentration, electrode gap, surface area, flow rate, temperature, electrode type, electrode pattern, applied potential etc. are all important electrocoagulation parameters. A power source of direct current is used. During the electrocoagulation process, metal ion generation takes place at the anode while hydrogen bubble is released at the cathode. The hydrogen bubble is responsible for the flotation of formed flocs to the surface of the water where the flocs are concentrated and removed. The oxidation of a metal (M) in an electrocoagulation process can be represented as :

Anode reaction



Cathode reaction



The metal ions released from the anode combine with the hydroxyl ion released from the cathode to form a highly charged coagulant. The mechanism of electrocoagulation process can be represented in Figure 2.1

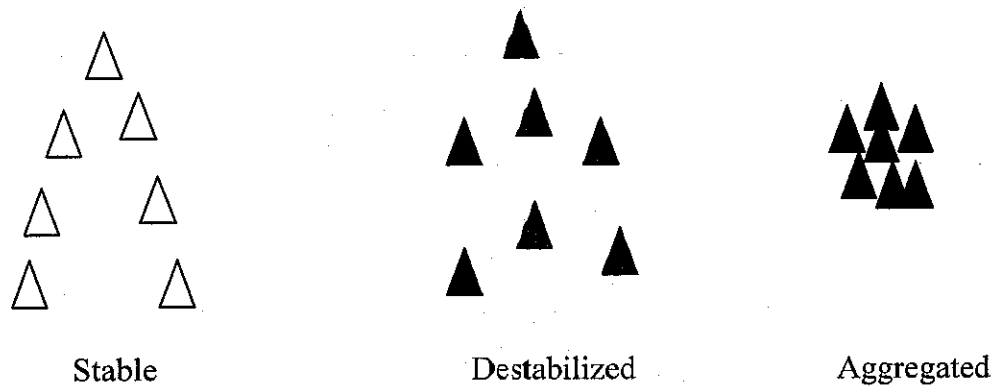


Figure 2.1: Reaction mechanism of electrocoagulation

2.4.2 Destabilization mechanism of electrocoagulation

When direct current is passed through aqueous solution, it destabilizes the colloids. This destabilization causes electrophoretic migration of the ions in the solution. This motion of the dispersed ions in water results in attracting unlike charges together to form a floc. The destabilization mechanism of electrocoagulation can be summarized as [27] :

- a) Compression of the diffuse double layer around the charged species by the interactions of ions generated by oxidation of the sacrificial anode.
- b) Charge neutralization of the ionic species present in water by counter ions produced by the electrochemical dissolution of the sacrificial anode. These counter ions reduce the electrostatic interparticle repulsion to the extent that the van der Waals attraction predominates, thus causing coagulation. A zero net charge results in the process.
- c) Floc formation: The floc formed as a result of coagulation creates a sludge blanket that entraps and bridges colloidal particles still remaining in the aqueous medium. The solid oxides, hydroxides and oxyhydroxides provide active surfaces for the adsorption of the polluting species.

Using light microscopy, *Holt et al.* [79] showed the microscopic images of clay particles before and after electrocoagulation as depicted in Figure 2.2. and 2.3 respectively. Before the electrocoagulation process, the size and shape of the clays particles were observed to be small, stable and behaves like a colloid. After the electrocoagulation process of 12 minutes at 1.0 A, the clay particles formed larger clusters. This illustrates further the destabilization and aggregation mechanism of electrocoagulation. Colloidal particles are destabilized by high charged cations through the formation of polyvalent poly hydroxide complexes with high adsorption properties aggregating with pollutants. This aggregate is referred to as the floc which is removed either through sedimentation or flotation with the aid of hydrogen bubble.

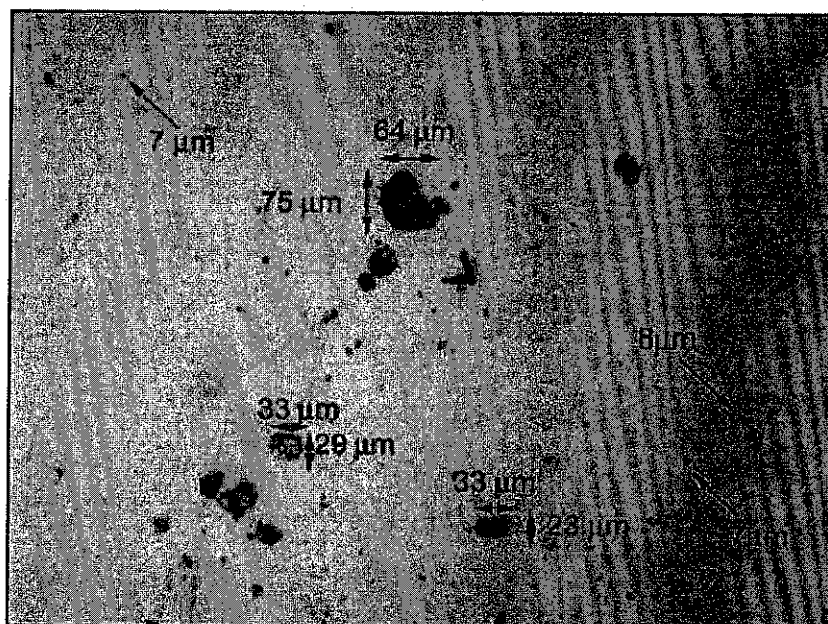


Figure 2.2: Image of clay particles prior to electrocoagulation [79]

2.4.3 Power Source

Electrocoagulation can be conducted by both alternating current and direct current. Majority of the work on electrocoagulation has preferred direct current to alternating current because of the cost associated with alternating current. Direct current can be supplied using a direct current power supply. This direct current power supply converts alternating current to direct current and reduces the energy consumption

during electrocoagulation process. Direct current is easy to operate, poses none or minimal risk and can be accurately controlled with the aid of a voltmeter and ammeter.

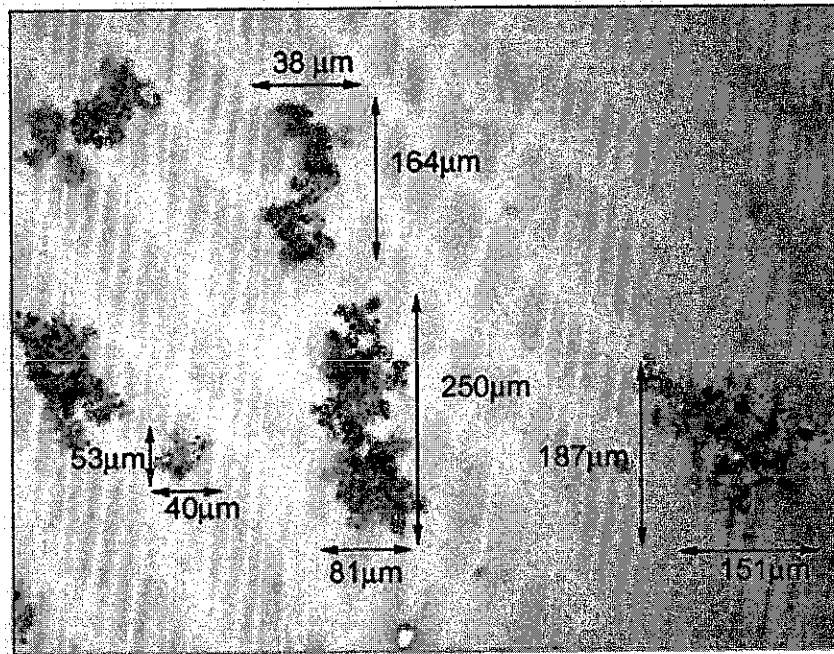


Figure 2.3: Microscopic image of aggregates from electrocoagulation reactor at 12 minutes [79]

2.4.4 Electrocoagulation Reactor

Different reactors can be used to conduct an electrocoagulation experiment. Majority of the work on electrocoagulation was conducted in the batch study using small beakers. However, few studies have attempted the continuous mode operation with electrocoagulation. In the continuous mode, the reactor design depends on the volume of wastewater to be treated. Different compartments may be included in the reactor design to separate the flocs from the treated water. Generally, laboratory scale electrocoagulation reactor is cheap to construct. A schematic diagram of electrocoagulation reactor is depicted in Figure 2.4.

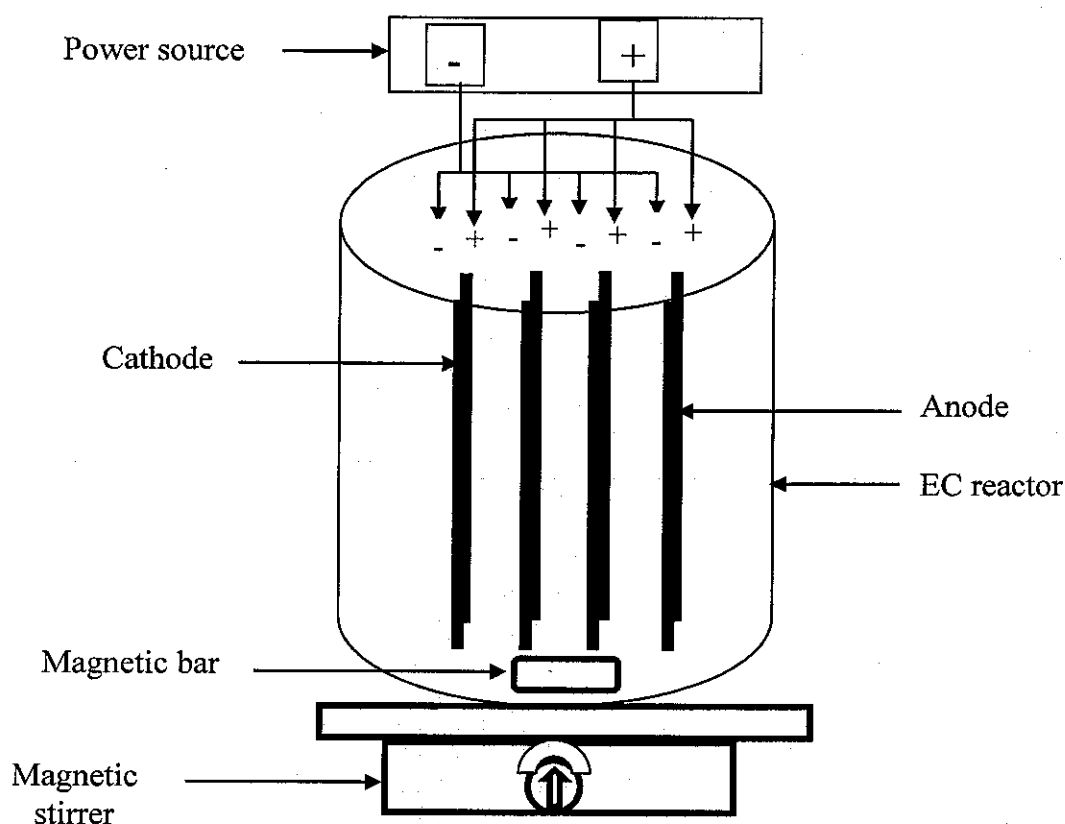


Figure 2.4: Schematic diagram of electrocoagulation reactor

However, the design of Electrocoagulation cell affects process efficiency. The following factors must be considered while designing an electrocoagulation cell [80].

- i. Minimization of the IR-drop between the electrodes.
- ii. Minimization of accumulated O_2 and H_2 gas bubble nucleates at the surface of the electrodes.
- iii. Favorable distances between electrodes must be investigated

2.4.4.1 Types of electrocoagulation reactors

a) Tall vertical plate reactor [81]

This type of reactor uses electrodes made from flat steel plates with vertical dimension bigger than horizontal dimension. The arrangement of the plates is in a non-conductive case which may be open or closed at the top. Electrical contact in the open case is above the solution level while the closed case requires a submerged

contact. In a closed case, the flow of liquid in this reactor is usually from the bottom to the top and the cell assembly is done through welding. Sometimes, corrosion locks the plates to the case if the plates are contained in slots within the case. For open case, welding is not required because the case uses contact above the solution. These reactors are effective in electrocoagulation but may be expensive to use.

b) Long horizontal plate reactor [80]

The pattern of arrangement of plate in this reactor is horizontal lying either flat or on edge. A rectangular non-conductive case with slots maintaining spacing is designed to install the plate. Gas bubbles rise within the stream and causes resistance at the bottom of the upper plate when the solution begins to move between the plates if the plates are installed in a flat pattern. Oxygen is produced in this arrangement and this causes short circuiting between the plates. Vertical arrangement of the plates enables for easy separation of the phases of the solution (solid, liquid and gas). However, the plates may not be removable once corrosion occurs.

c) Short horizontal plate reactor [80]

This reactor is designed with a spacer or grooves within the non-conductive case which allows the solution to pass between all spaces between plates. The plates used in this reactor are roughly squared, parallel, horizontal and are separated by the spacers. The solution can pass through both anode and cathode in a single pass. The reactor's configuration enables easy change of polarity. However, the contacts are made within the case which requires some innovation to allow the electrical contacts without welding.

d) Perforated plate reactor [80]

In this reactor, the flow of water passes through the plates rather than between them. This pattern of reactor configuration allows for accumulation of solids on the plates which causes short circuiting. These solids can only be removed by acid washing or disassembly. However, this reactor is effective in treating wastewater but doubts still abound if the assemblage will not leak at high pressure.

e) Solid tube reactor [80]

Solid tube reactor has two concentric tubes used as sacrificial surfaces. These sacrificial surfaces are contained in a third non conductive tube. These tubes are separated from each other by non-conductive cords. The voltage and fluid velocity is controlled by the spacing between the annular. One tube serves as the anode and another tube as the cathode. However, these reactors are difficult to prevent from leakage.

2.4.5 Design of an EC reactor

Typical design of EC cell is important because several factors affect removal efficiency during electrocoagulation process. The EC cell can be physically or chemical designed. Whichever method is used, it is important to consider certain factors which will affect process efficiency if not properly taken care of. The physical factors include reactor geometry and reactor scale up while the chemical factor involves electrode material and passivation.

2.4.5.1 Physical design of EC cell

The construction of EC cell requires technical knowledge of the process of electrochemistry because the design of EC affects its operation and efficiency.

a) Reactor geometry

Reactor geometry obviously deals with the properties of the reactor and how the parameters can effectively relate to increase efficiency within the reactor. The formation of floc, flow of liquid, settling characteristics, bubble path and flotation effectiveness are all affected by the geometry of the reactor. If the flow of solution is from the bottom of the reactor, the direction of flotation will differ from a reactor which solution flows from the top.

b) Reactor scale up

The reactor scale up is important because some parameters like surface area to volume ratio (As/V) are affected by the size of the reactor. The electrode area influences current density, rate of bubble and coagulant dosing. It is important to include this in the design of EC reactor.

2.4.5.2 Chemical design of EC reactor

The effectiveness and interactions of particles during electrocoagulation is further affected by chemical factors like electrode material and passivation.

a) Electrode materials

The choice of electrode material for electrocoagulation process is very important and affected by some factors. Several reported literatures on electrocoagulation has opted for aluminum and iron electrode because these two electrodes are readily available, effective and cheap. However, other electrode materials have also been used like magnesium, titanium, zinc etc. These electrodes are expensive and are not readily available. However, one chemical factor that is used to categorize these electrodes is the electrode must have adequate mechanical strength to withstand chemical and physical attack from the electrolytes, reactants and products.

b) Passivation

Passivation of electrode is one of the major challenges of electrocoagulation process. Passivation occurs as a result of the deposition of a layer of oxide on the surface of electrode materials reducing the efficiency of the electrocoagulation process. It prevents metal ion dissolution and electron transfer. In addition, the amount of metal ions released into the water sample reduces. Passivation normally occurs with the cathode while the anode undergoes electrochemical corrosion. Passivation of electrode can be reduced during electrocoagulation process by

i. Alternating the polarity of the electrode materials

- ii. Cleaning of the electrodes after several runs of experiment with appropriate cleaning agents.
- iii. Drying the electrodes after cleaning to remove any remaining surface impurity.

2.4.6 Electrodes

Different kinds of electrodes can be used in electrocoagulation study. They include aluminum, iron, magnesium, titanium, zinc anode etc. All these electrodes are effective when used in electrocoagulation process. These electrodes can be made from metal plates or even from metal scraps such as iron or aluminum millings, cuttings, etc. and can be made of different sizes [77]. However, various electrodes have different oxidation potential [82]. According to the reactivity series, the position of the metal in the reactivity series determines its strength. Moving from the bottom of the reactivity series to the top, the metals increase in reactivity, lose electrons more easily and become stronger reducing agents. The two most used electrodes are aluminum and iron. This is because of their availability, price, and efficiency. The significance of the reactivity series is that all metals above hydrogen will readily displace/liberate hydrogen from water/acid while those below it will not displace hydrogen. Therefore, the choice of electrode material is also an important factor. However, efficiency, cost, availability are the major indices for the choice of anode and cathode materials. The reactivity series is represented in Table 2.3

Electrodes can be arranged in bipolar or monopolar patterns [15]. Figure 2.5 and 2.6 shows monopolar and bipolar electrode connections respectively.

Monopolar electrode connections are cell connections made between pairs of anode and cathode electrodes. The current passes through the individual electrodes each connected to the power source by a separate power connection. The space between the anodes and cathodes causes electrolysis when the solutions flow between them. Series of connection can be made on one input connection in a parallel configuration. The polarity of each electrode set is defined by the connection polarity i.e anode electrodes are connected to the positive pole while cathode electrodes are connected to the negative poles [83]

Table 2.3: Reactivity series of metals

Metals	Reactivity
Potassium	<div>(Most reactive metals)</div> <div>↓</div> <div>Decreasing chemical reactivity</div> <div>↑</div> <div>(Least reactive metals)</div>
Sodium	
Calcium	
Magnesium	
Aluminum	
Zinc	
Iron	
Tin	
Lead	
Hydrogen	
Copper	
Mercury	
Silver	
Gold	
Gold	

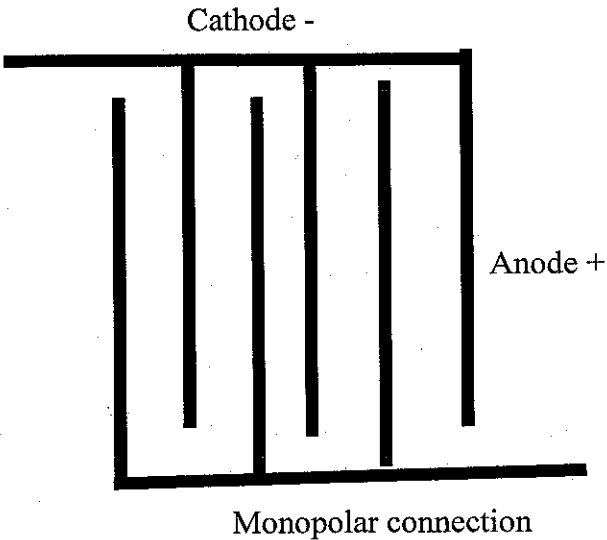


Figure 2.5: Schematic diagram of monopolar electrode pattern [84].

In bipolar electrode connections, current flows from one feeder electrode through the solution, into and out of each of the bipoles and subsequently to the second feeder electrode. Each electrode serves as both an anode and a cathode. The bipolar electrode pattern has a feeder electrode for the positive and negative power inputs points [84].

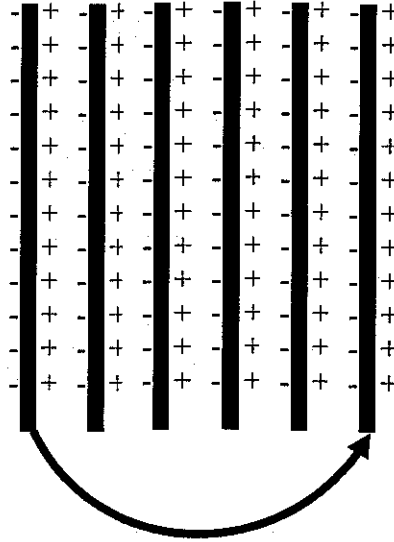


Figure 2.6: Schematic diagram of a bipolar electrode pattern [84]

2.4.7 Electrode reactions

The electrode reaction in electrocoagulation depends on the type of electrode. Each electrode reacts in a stepwise process to form metal hydroxide which reacts with contaminants to form flocs. For aluminum and iron electrodes, their reactions in water can be summarized as follows [85] :

Anode

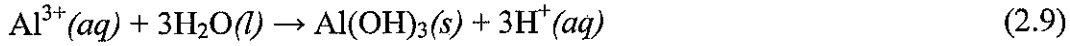


Cathode



Aluminum forms polymeric species during oxidation of the sacrificial anode. These polymeric species $\text{Al}_6(\text{OH})_{15}^{3+}$, $\text{Al}_7(\text{OH})_{17}^{4+}$, $\text{Al}_8(\text{OH})_{20}^{4+}$, $\text{Al}_{13}\text{O}_4(\text{OH})_{24}^{7+}$,

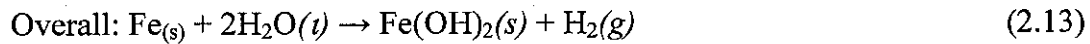
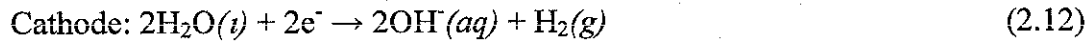
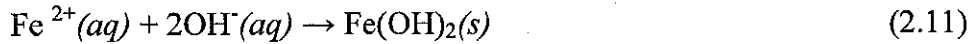
$\text{Al}_{13}(\text{OH})_{34}^{5+}$, transform finally into $\text{Al}(\text{OH})_3(s)$ according to the following equation [82].



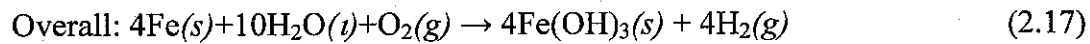
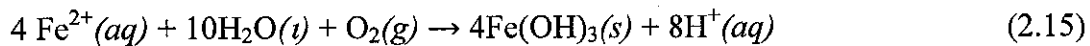
This newly formed $\text{Al}(\text{OH})_3(s)$ occurs as sweep floc having large surface area and is active in adsorption of organic compounds and trapping of colloidal particles. The formed floc is separated from aqueous medium by sedimentation or H_2 flotation.

Iron oxidation in an electrolytic system produces iron hydroxide, $\text{Fe}(\text{OH})_n$ where $n = 2$ or 3 . Two mechanisms for the production of metal hydroxide are shown below [86] :

Mechanism I



Mechanism II



Particles that interact with the insoluble metal hydroxides of iron are removed by surface complexation or electrostatic attraction [86]. The electric field enables electrophoretic migration of particles and increases the tendency of charges in suspension to interact with each other. The summary of electrocoagulation reaction is shown in Figure 2.7.

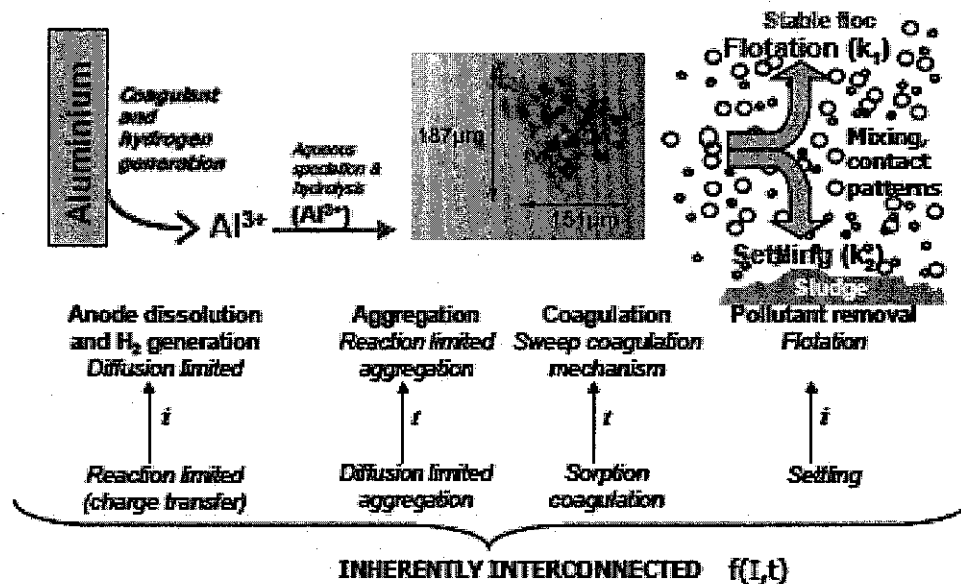


Figure 2.7: Summary of electrocoagulation reaction [79]

The amount of metal ions released from the respective electrode can be calculated using the Faraday equation [87].

$$W = \frac{ItM}{ZF} \quad (2.18)$$

where

w = quantity of electrode material dissolved (g);

I = current in amperes (A);

t = time (s);

M = molecular weight of the electrode material

Z = number of electrons involved in the redox reaction

F = Faraday constant (96500 C/mol of electrons)

The energy consumption during electrocoagulation can be calculated using the equation :

$$E = \frac{UIT}{V} \quad (2.19)$$

Where

E = energy consumption (kwh/m³)

U = voltage (V)

I = current in amperes (A)

T = time in hours (h)

V = volume of sample (L)

2.4.8 Gas bubble generation

At the start of electrocoagulation process, the sacrificial anode oxidizes while the cathode releases hydrogen gas bubbles. These hydrogen gas bubbles are responsible for the flotation of formed flocs to the surface of the reactor. However, gas bubble generation increases with increase in current. At high current, bubble generation rate favors flotation while at low current, bubble generation favors sedimentation [88].

2.4.9 Operating parameters for electrocoagulation

There are different operating parameters used in electrocoagulation process. Many studies have reported the role of these operating parameters in the efficiency of electrocoagulation process. Below is a review of some important operating parameters.

2.4.9.1 Current density

Current density is current per unit surface area of the electrode (anode). It is a parameter which controls the dissolution of the sacrificial anode on one hand and the formation of hydrogen bubble on the other [89]. Current density directly affects process performance and operating cost as well as determines the amount of ions released from the respective electrodes [77]. Literature on electrocoagulation has proved that current density is an important parameter and is responsible for the oxidation of the sacrificial anode and generation of gas bubbles. The degree of anodic dissolution of the electrode material increases with increase in current density [90].

2.4.9.2 Sample pH

The pH of a solution in electrocoagulation controls the process performance and the solubility of the analyte. The pH of an electrocoagulation process depends mainly on the nature of the contaminant [77]. For boron, pH determines the ionic form of boron (borate ions). At low pH, boric acid is the dominant form of boron in solution but at high pH, the borate ions dominate [91]. Figure 2.8 shows the form of boron at different pH values.

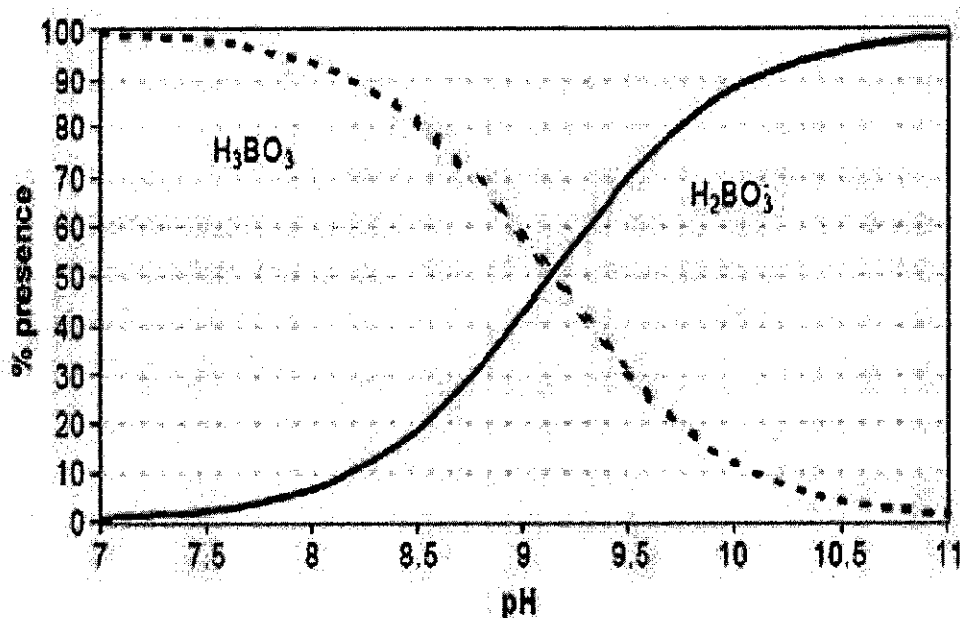


Figure 2.8: Distribution of H_3BO_3/H_2BO_3 in water as a function of pH [92]

2.4.9.3 Inter-electrode spacing

Inter-electrode spacing is the gap between electrodes. Some literatures have reported the effects of inter-electrode spacing in electrocoagulation process. Inter-electrode spacing is a measure of how the movement of the released metal ions affects process efficiency. It is important to maintain an appropriate spacing between electrodes during electrocoagulation. The appropriate spacing can only be determined through experimental process. When the inter-electrode spacing doesn't favor the reaction, electrical resistance occurs and reaction rate reduces.

2.4.9.4 Conductivity

Wastewater conductivity is an important parameter in electrocoagulation. Wastewater conductivity is a parameter which measures the ability of water to pass an electric current. When wastewater conductivity is high, the rate of oxidation of electrode material is rapid. Wastewater conductivity is measured in micromhos per centimeter ($\mu\text{mhos/cm}$) or microSiemens per centimeter ($\mu\text{S/cm}$). Wastewater conductivity is a function of the amount of dissolved solids present in the sample. The conductivity of different wastewater varies and can easily be measured using a conductivity meter. Knowledge of sample conductivity is important especially in electrochemical study because reaction is faster when the conductivity is high. However, samples with low conductivity can be enhanced by addition of some electrolytic substance to increase the electrical conduction. In addition, energy consumption reduces when wastewater conductivity is high because reactions are rapid and spontaneous [93].

2.4.9.5 Temperature

Temperature is an important parameter in electrocoagulation and indicates different energy levels during a reaction process. Sample temperature can vary across different wastewaters. Some wastewater contaminants are poor conductors of heat at room temperature and require elevated temperature. Temperature also gives a better knowledge of the adsorption and thermodynamic process of electrocoagulation. Wastewater temperature can be easily measured using a thermometer.

2.4.9.6 Electrocoagulation cell voltage

The use of current density in electrocoagulation cell is determined by the measured potential. The electric potential, often referred to as "push or force of electricity" is an important parameter which drives the current to flow. The potential of an electrocoagulation cell can be referred as a measure of the energy carried by a charge. The potential is responsible for the flow of current. In many EC cells, it is possible to have a potential without a current but current cannot flow without the potential. The

importance of potential is further illustrated in Figure 2.9 -2.11. Figure 2.9 shows a cell with a closed circuit which allows the current to flow. Due to the closed switch, potential and current work together. Figure 2.10 shows a cell with an open circuit. The cell possesses only the potential with no current. Due to the opening of the switch, the circuit is broken and current cannot flow. The cell works with potential only. Figure 2.11 shows the importance of the cell. When the cell is removed, there is no source of voltage and current cannot flow. The Figures illustrates the importance of cell potential in electrocoagulation.

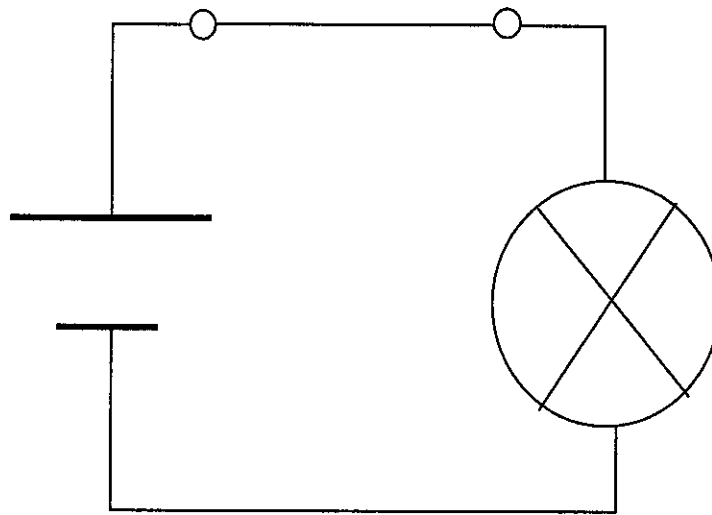


Figure 2.9: Close circuit: Voltage and current

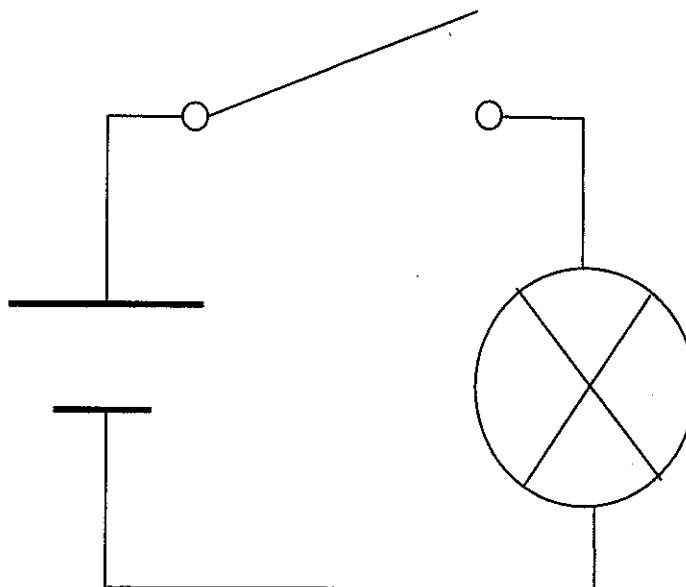


Figure 2.10: Open circuit: voltage but no current

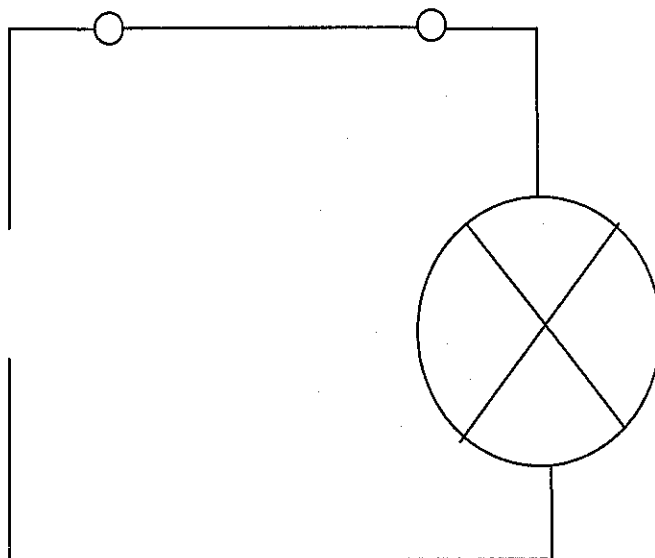


Figure 2.11: The cell is removed: No voltage and no current

The potential required to get a specific current density is defined as the sum of three components :

$$\eta_{AP} = \eta_k + \eta_{Mt} + \eta_{IR} \quad (2.20)$$

Where:

η_{AP} is the applied overpotential (V).

η_k is the kinetic overpotential (V).

η_{Mt} is the concentration overpotential (V).

η_{IR} is the overpotential caused by solution resistance or IR drop (V).

2.4.10 Previous wastewater studies with electrocoagulation

Many studies have successfully used electrocoagulation in wastewater treatment. These studies were done with different wastewaters and different operating parameters. As the study of electrocoagulation continues to gain wider acceptance, more operating parameters are being discovered to improve the process. Various wastewaters possess different composition and characteristics. This makes optimal operating parameter to differ from one wastewater to another. Therefore in the study of electrocoagulation, it is important to understand the characteristics and composition of the wastewater sample.

Yilmaz et al. [31], studied boron removal from geothermal wastewaters with electrocoagulation using aluminum electrodes. Current density, pH and temperature were the selected operating parameters. Boron removal efficiency increased with increase in pH. A removal efficiency of 95% was observed from an initial boron concentration of 24 mg/L after a 30 minute treatment time.

Schulz et al. [76], investigated the ability of electrocoagulation to remove scale forming species from industrial process water in bench and pilot scale. Aluminum and iron electrodes were used in this study at inter-electrode spacing of 4 mm. The study observed that there was frequent formation of gel on the surfaces of aluminum electrode more than iron electrode in the pilot scale study. This was attributed to aluminum dosing from the electrodes. It was observed that aluminum dosing was more in the bench scale than in the pilot scale. Silica removal in excess of 80% was achieved with electrocoagulation but less than 40% calcium and magnesium was removed.

Ghosh et al. [82], studied the removal of Fe(II) from tap water using electrocoagulation technique using aluminum electrode. The operating parameters varied were current density and inter-electrode spacing while pH, conductivity and salt concentration were kept constant. The study showed that increase in current density improved removal efficiency while removal efficiency was highest for the lowest inter-electrode distance. A removal efficiency of 99.2% was observed from an initial Fe(II) concentration of 25 mg/L after a 35 minute treatment time.

Merzouk et al. [88], investigated turbidity removal and separation of heavy metals using electrocoagulation-electroflotation technique. Effects of operating parameters were investigated using synthetic wastewater in a batch study. The optimal operating parameters were applied to textile wastewater. pH, current density, initial concentration, treatment time, inter-electrode distance and conductivity were investigated in this study. The electrochemical unit was a 1.5L reactor with aluminum electrodes installed in the reactor. Suspended solids removal efficiency of 86.5%, turbidity 81.56%, BOD 83%, COD 68%, and color 92.5% was observed at optimal operating conditions of current density 11.55 mA/cm², retention time 10 minutes and inter-electrode distance 1 cm. The study concluded that adsorption of pollutants by

electrocoagulation is rapid and that the kinetics of adsorption can be achieved within 15 minutes while the removal rate reaches 95%.

Chen et al. [94], studied the separation of pollutants from restaurant wastewater using electrocoagulation with aluminum electrodes in a continuous mode study. Different wastewater samples were collected from different restaurants in this study. The parameters investigated in this study included pH, current density, charge loading and conductivity. Efficiency was measured with respect to oil and grease, COD, BOD and suspended solids removal. Except the wastewater from one restaurant (America fast food restaurant), the overall efficiencies of the removal of oil and grease was about 94.4-99.9%, suspended solids 84.1-99.0%, COD 68.0-94.5% and BOD 59.3-93.4%. Electrocoagulation was observed to act as a pH neutralizer in this study. It was reported that when the influent pH is above 9.0, a pH drop occurs in the effluent sample. For a typical restaurant wastewater influent pH of 6-10, the effluent pH range is around pH 6-9 which makes the effluent usable. In this study, electrocoagulation was effective in removing the water pollutants.

Raju et al. [95], investigated wastewater treatment from a synthetic textile industry by electrocoagulation-electrooxidation. Aluminum and mild steel rod electrodes were used as anode and kept at 6 mm apart from each other in a 3L acrylic tank. Removal of suspended solids and COD was monitored to ascertain the efficiency of electrocoagulation. Initial concentration of suspended solids and COD were 830 mg/L and 1316 mg/L, respectively. A removal efficiency of 99% was observed for suspended solids after 5 minutes treatment time. In addition, 62% COD removal was observed after the electrocoagulation process for aluminum electrode. Using mild steel anode, COD removal efficiency of 53% was observed after 5 minutes. Comparing the efficiencies of aluminum and mild steel electrodes, the authors concluded that aluminum electrode was more effective than mild steel electrode.

Balasubramanian et al. [96], studied arsenic removal with electrocoagulation in a batch study using aluminum and mild steel electrodes. The study was modeled with response surface methodology (RSM). A four factor level of (A) current density (B) concentration (C) time and (D) pH was investigated in this study. The result of this

study indicates that a 98% arsenic removal was observed at current density of 1.5 A/dm^2 and treatment time of 55 minutes.

Bennajah et al. [97], investigated the removal of fluoride from Morocco drinking water by electrocoagulation/electroflotation in an electrochemical external loop airlift reactor. A batch and continuous mode study was conducted with aluminum electrodes in this study. Current density, pH, treatment time and concentration were varied in this study. The result indicated that a low fluoride concentration of 1.5 mg/L can be achieved from an initial fluoride concentration of 10 and 20 mg/L at current density of 6 mA/cm^2 and pH 5.

Malakootian et al. [98], evaluated the performance of electrocoagulation process in hardness removal using iron rod electrodes in drinking water. The parameters investigated were pH, voltage and treatment time. A removal efficiency of 98.2% and 97.4% was observed for calcium and total hardness removal respectively at voltage of 12V and reaction time of 60 minutes. Removal efficiency increased with increase in cell voltage. Increase in pH increased the removal efficiency. This is because pH has a significant effect on forming metal hydroxide species and removal mechanism of ion and pollutants.

Ricordel et al. [99], also investigated the viability of using electrocoagulation-electroflotation process as a surface water treatment process for industrial uses. Aluminum electrode was used for this study. It was reported that 50% of the suspended matter present in the sample were removed within 30 minutes.

Kilic et al. [100], compared electrocoagulation and coagulation process using ultrafine quartz suspensions. Aluminum anode and stainless steel cathode was used as electrode for electrocoagulation while aluminum sulfate was used as coagulant for conventional coagulation. The operating parameters investigated were solution pH, electrical potential, current density, treatment time and aluminum dosing. Turbidity removal from ultrafine quartz suspension was used to measure the efficiency of both methods. The study observed that at the same aluminum dosage, both treatment methods were effective for the removal of quartz particles from suspension. The optimum pH for the removal of quartz from suspension was found to be 9 in this

study for electrocoagulation with a turbidity removal efficiency of 92% at a current density of 87 A/m^2 . For coagulation, the value of the optimum coagulant dosage was 15 mg Al/L with a turbidity removal efficiency of 93% at a wider pH range of 6-9.

Solak et al. [101, 102], studied removal of suspended solids and turbidity from marble processing wastewaters by electrocoagulation. The study focused on the comparison of electrode material and electrode connection systems. Aluminum and iron electrodes connected in parallel and serial connections were used. pH, current density and electrolysis time were investigated. A 100% removal efficiency was reported for suspended solids with electrocoagulation using monopolar aluminum electrodes in parallel and serial connections at the optimum conditions of pH 9, current density 15 A/m^2 , and electrolysis time of 2 minutes. For iron electrode, a suspended solid removal efficiency of 99.86% and 99.94% was observed for serial and parallel connections respectively at optimum conditions of pH 8 and electrolysis time of 2 minutes.

Apayin et al. [102] investigated the treatment of tannery wastewater with electrocoagulation. Iron plate electrode was used in the batch study. COD and sulfide removal were used to assess the efficiency of electrocoagulation process. A COD and sulfide removal efficiency of 46% and 90% were observed within 5 minutes respectively.

2.4.11 Advantages of electrocoagulation

- i. Electrochemical setup is made up of simple equipment
- ii. It produces small amount of sludge as compared to conventional coagulation. In addition, the sludge easily settles.
- iii. Removes smallest colloidal particles because the strong electric field sets all particles present in motion.
- iv. It eliminates the addition of chemicals and also limits the chances of secondary pollution.
- v. The release of gas bubbles from the cathode enables flotation of pollutants to the surface of the reactor where it is concentrated and collected.

- vi. The maintenance of electrochemical set up is low since all the parts are stable.
- vii. In rural areas, a solar panel can be used to operate an electrochemical setup in the absence of electricity.

2.4.12 Disadvantages

- i. EC requires periodic cleaning and replacing of the sacrificial anode after a series of experiments
- ii. Passivation caused by the formation of impermeable oxide on the surface of the cathode can affect EC efficiency
- iii. Wastewater sample requires high conductivity for effective coagulation to occur.
- iv. Residue concentration of electrode material may increase after treatment especially with aluminum electrode

2.5 Boron recovery

Boron is among the inorganic compounds facing worldwide depletion challenges due to its increasing demand in electrical, magnetic and advanced engineering materials. Such precious compounds dissolved in wastewater can be collected rather than promote their discharge into the environment [103]. Boron can be recovered as a recyclable precipitate in order to mitigate its adverse consequences when discharged into the environment [104]. Over the years, there has been growing concern over the environmental challenges, ecotoxicological effect and the economic implication of the endless discharge of boron into the environment from treatment facilities and mining operations. The new European chemicals legislation, registration, evaluation, authorization and restriction of chemicals (REACH) places strong emphasis on chemical safety assessment of boron compounds in the European market because boron compounds are high production volume chemicals [105]. The widespread applications of boron compounds, its toxicological effects and solubility variations have raised serious concerns about these compounds especially for surface waters

where most boron are discharged into. During the production of boron compounds, boron is introduced into the environment as waste. Boron minerals like Borax, Ulexite ($\text{NaCaB}_5\text{O}_9 \cdot 8\text{H}_2\text{O}$), Colemanite ($\text{Ca}_2\text{B}_4\text{O}_8 \cdot 5\text{H}_2\text{O}$), Pandermite ($\text{CaB}_6\text{O}_9 \cdot 7\text{H}_2\text{O}$), and Tincal ($\text{Na}_2\text{B}_4\text{O}_7 \cdot 10\text{H}_2\text{O}$), are normally mined as hydrated borate minerals [106]. Considerable experimental investigations have been carried out to find the best way of solving the boron problem in treatment facilities as well as in mining industries. With the ever growing scarcity of landfills, the need to select an alternative method to handle the waste-stream is of paramount importance. Few methods have been used in boron recovery and they include solvent extraction, ion exchange using selective ion exchange resins and hydrothermal mineralization. While solvent extraction has been used to recover boron in the form of boric acid, investigations in the use of ion exchange are in view. Hydrothermal mineralization has been used to recover boron in the form of hydrated borate minerals.

2.5.1 Solvent extraction

Solvent extraction is a method of boron recovery that has been used in a few studies [106-107]. One of the advantages of solvent extraction is that boron can be recovered from both wastewater and boronic waste using a leaching agent. This process has been used to recover boron from different waste-streams like borogypsum, reactor waste, boronic sludge, waste mud and concentrator waste. The major disadvantage of this process is the choice of a leaching agent. Many of the above mentioned studies [106-108] have used sulfur dioxide and nitric acid as leaching agent. However, frequent exposure to sulfur dioxide can cause pulmonary impairment in humans due to bronchoconstriction. Another challenge of using sulfur dioxide is that it requires some level of skill and expertise to avoid casualties while working in the laboratory. In addition, nitric acid is corrosive and can easily burn the skin or cause explosion if not properly handled. The cost and dangers associated with the leaching agents have reduced the popularity of this method.

Demirbas et al. [106], investigated the recovery of boron from waste samples such as borogypsum, reactor waste, boronic sludges, waste mud and concentrator

waste by solvent extraction using distilled water, sulfur dioxide and carbon dioxide saturated water. Effect of temperature, stirring time and solid-liquid ratio was investigated. It was observed that increase in temperature and stirring time resulted in increase in boron recovery. Increase in solid-liquid ratio also increased boron recovery but lower than that of temperature and stirring time. They observed that about 90% of B_2O_3 was recovered in the form of boric acid from boron waste. They also observed that Water saturated by SO_2 , is a more effective leaching solvent than that saturated by CO_2 for the boronic wastes. *Boncukcuoglu et al.* [107], also investigated the recovery of boron oxide (B_2O_3) from trommel sieve waste (TSW) using solvent extraction. Sulfur dioxide (SO_2) saturated water was used as the leaching agent. They observed that about 90% of boron oxide (B_2O_3) was recovered from trommel sieve waste.

2.5.2 Ion exchange

The use of boron selective chelating ion exchange resins is gaining wider acceptability in wastewater treatment. These chelating ion exchange resins are macroporous polystyrenic based resin, with functional groups specially designed for the selective removal of boron from aqueous solutions. They are effective for such solutions over a wide range of pH values, and over a wide range of boron concentrations. The hydroxyl functional group at the Cis position is responsible for the high selectivity and sorption rate of the resins [109]. This method involves a series of reaction steps with hydrochloric acid and sulfuric acid as the commonly used eluting agents. However, these boron selective chelating ion exchange resins are expensive and the problem of regeneration of resin which is synonymous with ion exchange system hinders the wide acceptability of this method. In addition, ion exchange process requires the mastering of adequate technical skill for operation and has not been used for boron recovery from waste products. *Kabay et al.* [109], investigated the feasibility of boron recovery from geothermal wastewater. After removing boron from geothermal wastewater using Diaion CRB 02 N-glucamine-type chelating resins, a weak base anion-exchange resin Diaion WA 30 was used for the column mode separation of boron from H_2SO_4 . The chemical composition of the

mixture was obtained after separating boron from H_2SO_4 . The concentration of boron in the acidic eluate before separation was about 773 mg/L and about 517 mg/L of boron was successfully separated from H_2SO_4 using Diaion WA 30 anion-exchange resin. Based on the chemical composition, they [109] concluded that boric acid could be produced from this mixture by crystallization.

2.5.3 Hydrothermal mineralization

Hydrothermal mineralization is a method of boron recovery from wastewater to produce reusable borate which is analogous to the formation of borate ore in nature. Research into this area of boron recovery is scarce but very promising. Hydrothermal mineralization can be used to recover boron both in wastewater and the produced sludge of a treatment facility. Its principle is based on the extraction of boron using a thermal system. The process uses cheap and affordable mineralizers of the alkali or alkali earth compounds for the mineralization of boron. The most common used mineralizers are calcium hydroxide and magnesium hydroxide. Hydrothermal mineralization provides uniform heating to the sample at a specific temperature. In addition, hydrothermal mineralization can be conducted with thermal instruments like conventional oven [110] or microwave [111]. Efficiency of hydrothermal mineralization also depends on the temperature of the system and the mineralizer used. The costs of these mineralizers are cheap and the thermal instruments are readily available in the laboratory. In addition, the process has not been associated with any health risk hazard and does not require any technical skill for operation. *Itakura et al.* [110], investigated boron recovery from model wastewater using conventional oven. Boron concentration of 500 ppm was prepared and 30 ml of the sample was used for the study. They observed that about 99% of boron was recovered as a precipitate after 14 hrs treatment time. The recovered precipitate was identified as a calcium borate compound called parasirbiskite. *Tsai and Lo* [111], also investigated boron recovery from concentrated wastewater using microwave hydrothermal method and conventional heating with calcium hydroxide as a mineralizer. They observed that more than 90% of boron was recovered as a precipitate in both methods. They

concluded that the main mechanism of boron recovery is the mineralization of parasirbiskite by calcium hydroxide and boric acid.

2.6 Adsorption kinetics

The determination of the rate limiting step in an experiment is very important. The adsorption of a solute in an experiment can be controlled by one or more steps. To investigate the adsorption kinetics of this study, experimental data were fitted into different kinetic models. The following kinetic models were studied in the present work to determine the model that best fits the data.

2.6.1 Mass transfer

The theory of mass transfer involves a group of separation operations based on the transfer of materials from one homogenous phase to another. The mechanism of mass transfer involves the reduction of concentration of a given component (reactants) in one stream and the subsequent increase of the concentration of another component (products) in another stream. The separation between the two components of reactants and products is identified as equilibrium phase, because at equilibrium condition, the transfer of a component ceases [112]. In wastewater treatment, the most important mass transfer operations include the transfer of materials across gas-liquid interface, removal of unwanted gaseous constituents by air stripping and removal of unwanted constituents by adsorption onto solid surfaces. In electrochemical process, the supply of reactant and removal of product from electrode surface are important to chemical change and current. In general, mass transfer can occur in three forms namely diffusion, convection and migration.

2.6.1.1 Diffusion

Diffusion involves the movement of species due to concentration gradient. It is a physical process which involves the movement of species from a region of high concentration to a more dilute region until the concentration is uniform. Diffusion

occurs very often in electrochemical process because the transfer of electrons results to lowering of the reactant concentration and increase in product concentration. This transport mechanism is found to be important and inevitable in electrochemical process.

2.6.1.2 Convection

Convection involves the movement of species as a result of external mechanical force. Different forms of convection can be introduced during an experimental process. Natural convection can occur in process as result of vibrations in the laboratory or small density gradient from both concentration and temperature changes within the layer adjacent to the electrode associated with electron transfer. Convection can also be introduced by shaking the cell, stirring the solution or moving the electrode.

2.6.1.3 Migration

Migration is an electrostatic phenomenon which involves the movement of charged species due to a potential gradient. The flow of current through two electrodes requires the existence of a potential gradient. Migration allows the charged species to pass through the solution. Migrations may not be an important transport mechanism in laboratory experiments. This is because in laboratory solutions with high inert electrolytes, charge species are mainly carried by the ions in solution. However, in industrial electrolysis cell, the reactant may be charge and present in high concentration, then migration of the reactant must be considered.

2.6.2 Lagergren pseudo first order rate equation

Lagergren pseudo first order rate equation has been widely used to analyze different experimental data. The Lagergren pseudo first order rate equation is shown below :

$$\frac{dq_e}{dq_t} = k_1 (q_e - q_t) \quad (2.21)$$

where

q_t = amount of solute adsorbed at any time (mg/g)

q_e = amount of solute adsorbed at equilibrium time (mg/g)

k_1 = Lagergren pseudo first order rate constant (min^{-1})

When integrated within the boundary conditions $q_e = 0$ at $t = 0$ and $q_e = q_t$ at $t = t$, equation (2.21) becomes,

$$\log \left[\frac{q_e}{q_e - q_t} \right] = k_1 t \quad (2.22)$$

The linearized form of the Lagergren equation is [113]

$$\log(q_e - q_t) = \log(q_e) - \frac{k_1 t}{2.303} \quad (2.23)$$

If the experimental data fits into Lagergren pseudo first order rate equation, the plot of $\log(q_e - q_t)$ versus time (t) should be linear. k_1 and q_e can be calculated from the slope and intercept of the plot of $\log(q_e - q_t)$ versus t .

2.6.3 Ho pseudo second order rate equation

Ho pseudo second order rate equation can be used to analyze experimental data to derive the kinetic model. The Ho pseudo second order rate equation is given by [114].

$$\frac{dq_e}{dq_t} = k_2 (q_e - q_t)^2 \quad (2.24)$$

where

q_t = amount of solute adsorbed at any time (mg/g)

q_e = amount of solute adsorbed at equilibrium time (mg/g)

k_2 = Ho Pseudo second order rate constant (g/mg.min)

The separation of the variables in equation (2.24) yields

$$\frac{dq_e}{(q_e - q_t)^2} = k_2 dt \quad (2.25)$$

When integrated for the boundary conditions $t = 0$ to $t = t$ and $q_e = 0$ and $q_e = q_t$, equation (2.25) becomes

$$\frac{t}{q_t} = \frac{1}{k_2 q_e^2} + \frac{t}{q_e} \quad (2.26)$$

Equation (2.26) represents the linear form of Ho second order equation. If the experimental data fits into Ho pseudo second order rate equation, a plot of t/q_t versus t should be linear. q_e and k_2 can be calculated from the slope and intercept of the plot of t/q_t versus t .

2.6.4 Intra-particle diffusion

One of the important models to understand the movement of solutes from one area to another in the presence of adsorbent is intra-particle diffusion. Intra-particle diffusion is a transport process which involves movement of species from the bulk of the solution to the solid phase. The linear form of intra-particle diffusion model is, given by the equation [113].

$$q_t = k_{id} t^{0.5} + C_i \quad (2.27)$$

where

q_t = Amount of metal adsorbed at any time (mg/g),

k_{id} = Intra-particle diffusion rate constant $(\text{mg}(\text{min})^{0.5}/\text{g})$,

C_i = Gives information about the boundary layer thickness (mg/g)

Experimental data fitted into Weber and Morris intra-particle diffusion equation should fulfill three important factors which are [115] :

- (i) High R^2 values to ascertain applicability
- (ii) Straight line which passes through the origin for the plot area q_t vs. $t^{0.5}$.
- (iii) Intercept $C_i < 0$.

If the linear portion of the plot is extrapolated back to the axis, it provides intercept (C_i) which is proportional to the degree of the boundary layer thickness i.e, the larger the intercept, the greater the boundary layer effect. However, it has been reported that the boundary layer thickness retards intra-particle diffusion [116]. Therefore negative values of the intercept favor intra-particle diffusion. If the plot did not pass through the origin, it implies there is some degree of boundary layer control which further indicates that intra-particle diffusion is not the only rate-limiting step but there are other kinetic models which may control the rate of adsorption, working together simultaneously [117].

2.6.5 Elovich model

The linearized form of Elovich equation is shown below [118, 119].

$$q_t = \frac{1}{\beta} \ln(\alpha\beta) + \frac{1}{\beta} \ln t \quad (2.28)$$

where

α = initial adsorption rate (mg/g.min)

β = desorption constant (g/mg) during any experiment.

A plot of q_t versus $\ln(t)$ should be linear with a slope of $(1/\beta)$ and an intercept of $(1/\beta) \ln(\alpha\beta)$. The Elovich model is not used to predict any definite mechanism but it is effective in defining predominantly, chemical adsorption on highly heterogenous adsorbents [120-121]. Elovich model has been reported to exhibit essentially identical behavior with pseudo second order kinetic [122]. However, it gives more information of a chemisorption process from the values of the initial adsorption and desorption constant.

2.7 Adsorption Isotherm

When a definite quantity of an adsorbent interacts with a liquid containing a given volume of absorbable solute, adsorption occurs until equilibrium is attained. The equilibrium state is a point of no significant reaction with a certain solute concentration on the adsorbent (q_e) and a corresponding final solute concentration in the liquid phase (C_e). A wide range of data can be obtained from the reaction between the initial solute concentration in the liquid and the adsorbents. The data can further be analyzed with isotherm equations so that the relationship between q_e and C_e can be expressed in mathematical form. The two common isotherm equations that is widely used to analyze adsorption data is Langmuir and Freundlich equations. The popular choice of these two isotherm equations includes their simplicity and ease of interpretation. However, linear regression has also been frequently used to evaluate these models [123]. I

2.7.1 Freundlich adsorption isotherm

The Freundlich adsorption isotherm is among the earliest known relationship which describes the adsorption system. The Freundlich isotherm takes into account the surface heterogeneity of the adsorbent. According to *Davis et al.* [124], Freundlich isotherm assumes that stronger binding sites are occupied first and that the binding strength decreases with increase in site occupation. According to the Freundlich isotherm, the absorbed mass per mass of adsorbent can be deduced from the following equation

$$q_e = K_F C_e^{1/n} \quad (2.29)$$

where

K_F = Freundlich constant related with adsorption capacity (mg/g),

n = heterogeneity coefficient (dimensionless).

The linear form of the equation is presented in the logarithmic form as shown below

$$\log q_e = \log K_F + (1/n) \log C_e \quad (2.30)$$

If the data fits into Freundlich isotherm, a plot of $\log q_e$ versus $\log C_e$ should be linear. $1/n$ is calculated from the slope while K_F is calculated from the intercept.

2.7.2 Langmuir adsorption isotherm

Langmuir adsorption isotherm is a well known adsorption isotherm that has been used to explain many adsorption systems. Langmuir adsorption isotherm is based on the principle that adsorption is absolutely limited to monolayer coverage and that all surface sites are alike and can only contain one adsorbed molecule. The intensity of a molecule to be adsorbed on a given site is independent of the occupants of a nearby site and the adsorbed molecule cannot move across the surface or interact with neighbouring molecules. The equation is applicable to mainly homogenous adsorption with adsorption process having equal activation energy according to the following assumptions :

- i. Molecules are adsorbed at a fixed number of well-defined localized sites,
- ii. One adsorbate molecule is held on each site,
- iii. The energy of all sites are the same,
- iv. Molecules adsorbed on any site do not interact with molecules on another site.

The linear form of the Langmuir is defined as [125].

$$\frac{C_e}{q_e} = \frac{1}{Q_o b} + \frac{C_e}{Q_o} \quad (2.31)$$

Where

Q_o = Langmuir constant related to the monolayer capacity (mg/g)

b = Binding energy constant

When C_e/q_e versus C_e graph is plotted, the slope is equal to $1/Q_o$ and the intercept is equal to $1/Q_o b$ [123].

2.7.3 Thermodynamics

Adsorption thermodynamics study gives information about the mechanism of adsorption. The thermodynamic parameters which include free energy change (ΔG°),

standard enthalpy of reaction (ΔH°) and entropy change (ΔS°) can be used to deduce the reaction mechanism. The thermodynamic parameters can be calculated from equations (2.32) and (2.33) [126].

$$\Delta G^\circ = -RT \ln K_c \quad (2.32)$$

$$\ln K = \frac{\Delta S^\circ}{R} - \frac{\Delta H^\circ}{RT} \quad (2.33)$$

where

K_c = distribution coefficient,

R = thermodynamic gas constant (8.314 J/mol.K),

T = temperature (K).

The standard enthalpy change (ΔH°) and entropy of the process (ΔS°) can be calculated from the slope and intercept of the plot of $\ln K_c$ against $1/T$.

2.7.4 Kinetic model test

The suitability of both pseudo first order and pseudo second order kinetic models can also be evaluated using the chi-square (χ^2) represented as [127].

$$\chi^2 = \frac{(q_e^{(exp)} - q_e^{(cal)})^2}{(q_e^{(cal)})} \quad (2.34)$$

where

$q_e^{(exp)}$ = experimental adsorption capacity at equilibrium (mg/g),

$q_e^{(cal)}$ = calculated adsorption capacity at equilibrium (mg/g).

The chi-square test is mainly the sum of the squares of the difference between the experimental equilibrium adsorption data and the calculated equilibrium adsorption data. The chi-square (χ^2) for the applicable model should be very low. A good correlation coefficient and a low chi-square (χ^2) indicate that the model is applicable.

CHAPTER 3

METHODOLOGY

3.1 Chapter overview

This chapter describes the procedures for analysis, the equipment used, the mode of experiments and the methods for preparation of samples. Boron removal efficiency was investigated in both batch and continuous mode. A preliminary study was conducted with synthetic wastewater to obtain the optimal operating parameters. The obtained optimum parameter/conditions were subsequently applied to produced water.

3.2 Electrode type

Aluminum plate electrodes and iron plate electrodes were used for this study. The size of the electrodes was 10 cm x 1 cm x 0.3 cm.

3.2.1 Operating parameters

Several operating parameters were investigated in this study. They were pH, current density, boron concentration, treatment time, inter-electrode spacing, temperature, flowrate and retention time. The range of the operating parameters is shown in Table 3.1

3.2.2 Synthetic wastewater preparation

2g of boric acid was dissolved in 1 liter distilled water. Different concentration of boron was made from the prepared stock solution according to the experimental plan.

Table 3.1: Range of parameters

S/n	Operating parameters	Units	Range
Batch mode			
1	pH		3, 4, 5, 6, 7, 8, 9, 10, 11
2	Current density	mA/cm ²	6.25, 12.5, 18.75
3	Concentration	mg/L	10, 20, 30
4	Treatment time	Minutes	15, 30, 45, 60, 75, 90
5	Inter-electrode spacing	cm	0.5, 1.0, 1.5
6.	Voltage	V	2.4,6
Continuous mode			
1	Flowrate	mL/min	20, 25, 30
2	Retention time	Minutes	20, 40, 60, 80, 100, 120, 140
3	Concentration	mg/L	5, 10, 15
Adsorption kinetics			
1	Temperature	K	298, 308, 318, 328
2	Concentration	mg/L	10, 20, 30

3.2.3 Produced water sampling

The produced water used in this study was collected from the onshore site of a local Crude Oil Terminal in Malaysia. The sample was collected on 19th November, 2011 and was transported to Universiti Teknologi PETRONAS Environmental Engineering Laboratory where it was stored in a cold room at 4°C. The characteristics of the sample were analyzed with atomic absorption spectrometry (AAS) and ion exchange

chromatography (IC) and results tabulated in Table 3.2. The experimental work was carried out at the environmental engineering laboratory of Universiti Teknologi PETRONAS (UTP) Malaysia.

Table 3.2: Characteristics of produced water

Parameters (mg/L)	Value	Parameters	Value
Boron	15	pH	7.84
Oil and grease	67	Turbidity (NTU)	72
Bromine	31.2	Temperature (°C)	24
Total phosphate	12	Conductivity (μS/cm)	30,000
Phenol	15	Hardness (mg/L)	957
TSS	136	Lead (mg/L)	0.185
TDS	15,829	Total chromium (mg/L)	0.07
COD	1560	Zinc (mg/L)	0.0441
BOD	883	Fluoride (mg/L)	0.61
Nitrite	0.028	Free chlorine (mg/L)	0.30
Iron	1.66	Cyanide (mg/L)	0.086
Copper	2.98	Magnesium (mg/L)	600
Ammonia Nitrogen	16.5	Calcium (mg/L)	357
Total Kjeldahl Nitrogen	60.71	Sodium (mg/L)	3,952
Sulphate	168	Total alkalinity (mg/L)	1, 546
Chloride	7,546	Potassium (mg/L)	284
Nitrate	1.9	Aluminum (mg/L)	0.65
Sulfide	0.213		

3.3 Electrochemical Set-up

The electrochemical treatment was carried out in batch and continuous mode.

3.3.1 Batch study

The batch study was conducted with a 500 mL beaker. Separate experiments were conducted for aluminum and iron electrodes. In each experiment, six electrodes (three anodes and three cathodes) were arranged vertically in the beaker at a pre-selected separation distance from each other. The electrodes were connected to a digital DC supply characterized by the ranges of 0-3A for current and 0-30V for voltage. The voltage was regulated between 2-6 V to give the desired current according to the experimental plan. The electrode surface area is 60 cm². A digital ammeter-voltmeter was used to regulate the current and voltage respectively. A pH meter (Hach Sension2 pH meter) was used to measure pH of the samples. The conductivity of the samples was measured using a conductivity meter (Myron L conductivity meter) while the turbidity of the samples was measured using a turbidimeter (2100P portable turbidimeter). 1M NaOH and H₂SO₄ were used to adjust the pH of the samples. The treatment time for the samples was varied from 15-90 minutes. After each run of the experiment, the supernatant was collected and analyzed. After each experiment, the iron electrodes were dipped in dilute HCl for 5 minutes. They were then washed with acetone and rinsed with deionized water to remove surface grease and impurities and dried at 105 °C for 10 minutes before being reused. The aluminum electrodes were similarly washed with acetone and rinsed with deionized water before drying at 105 °C. Boron concentration after treatment was analyzed with carmine method using DR 2800 spectrophotometer. All chemicals and reagents used for this study were analytical grade (Merck). The parameters investigated in the batch study were (i) pH (ii) initial concentration (iii) current density (iv) treatment time (v) inter-electrode spacing. All results were triplicates of experimental runs. Experimental setup for batch study is shown in Figure 3.1.

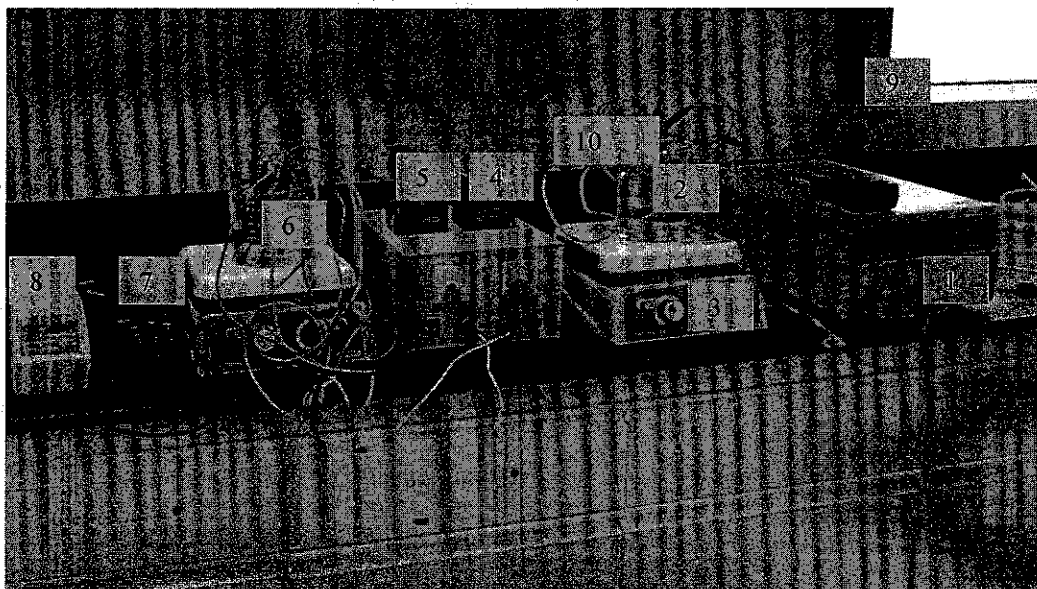


Figure 3.1: Experimental setup for batch study

(1) DC Power supply (2) Aluminum electrode (3) Magnetic stirrer (4) Digital Ammeter (5) Digital Voltmeter (6) Iron electrode (7) pH meter (8) Turbidimeter (9) AC power supply (10) Beaker

3.3.2 Continuous Mode Study

A continuous mode study was conducted for the treatment of produced water. This study was necessary to investigate the applicability of the method in a water treatment plant. An electrocoagulation reactor with the dimension of 18 cm height x 10 cm width x 8 cm length with 0.9L volume was used. The optimal conditions obtained from the batch study were used for the continuous mode study in addition to other parameters. The parameters varied in the continuous mode study are (i) flowrate (ii) concentration (iii) retention time. The flow-rate was maintained with a peristaltic pump. The electrodes were arranged in a monopolar pattern on a perforated plexiglas support. The DC supply which supplies the current was switched on when the samples reached near the exit point of the effluent with about 80% of the electrode surface area submerged in the sample. The retention time was set and supernatant was collected for analysis. The range of the parameters that were varied and investigated in the continuous mode study are (i) flowrate (20-30) mL/min, (ii) boron concentration (5-15 mg/L), retention time (20-140 minutes). All results were

triplicates of experimental runs. Experimental setup for continuous mode study is shown in Figure 3.2.



Figure 3.2: Electrochemical setup for continuous mode study

- (1) DC Power supply (2) Magnetic stirrer (3) Aluminum electrode (4) Digital Ammeter (5) Digital Voltmeter (6) Iron electrode (7) pH Meter (8) Peristaltic pump (9) EC reactor (10) AC power supply (11) Influent (12) Effluent [Iron] (13) Effluent [Aluminum].

3.3.3 Determination of boron in aqueous solution

Boron concentration in the sample was determined using the standard method (Carminie method) for water and wastewater. DR 2800 spectrophotometer was used to read the boron concentration after each treatment time. The percent removal efficiency was calculated using the following equation

$$\frac{C_o - C_t}{C_o} \times 100 \quad (3.1)$$

where

C_o = initial concentration (mg/L)

C_t = concentration at time t (mg/L)

3.3.4 Collection of EC flocs from the reactor

The flocs produced during the electrocoagulation treatment were collected after settling. The suspended flocs were transferred into an evaporating dish and were placed in the oven at room temperature for 24 hours to dry. The low temperature drying of the EC floc is to prevent it from crystallizing at high temperature. The dried flocs were subsequently transferred to the dessicator to cool for 20 minutes. The chemical composition of the flocs were analyzed with X-ray fluorescence (XRF).

3.3.5 Hydrothermal mineralization of EC flocs

The dried EC flocs were grounded and 2 g of EC flocs were accurately weighed to recover boron according to the method described by *Boncukcuoglu et al.* [107]. 10 mL solution of 3M HNO₃ was used to dissolve the flocs. The solution was placed in an orbital shaker for one hour at 150 rpm to enable complete dissolution. Calcium hydroxide Ca(OH)₂ was used as the mineralizer. The recovery study was conducted with 40 mL solution containing 2g of the EC floc in a pressure vessel lined with a glass lid according to the method described by *Itakura et al* [110]. The pH of the solution was 9.1 and 9.9 for aluminum and iron EC floc; respectively and was adjusted to pH 10 with 1M NaOH. The boron concentration in the EC floc measured by colorimetric method was 12.87 mg/L and 12.24 mg/L for aluminum and iron flocs, respectively. 0.3 g of Calcium hydroxide Ca(OH)₂ was used for the experiment. The hydrothermal mineralization study was conducted with a conventional oven. The hydrothermal temperature was kept at 120 °C and the hydrothermal treatment time was kept as 2 hours. After 2 hours of treatment time, the pressure vessel was removed from the oven. The remaining solvent in the pressure vessel was collected to

investigate the final boron concentration while the precipitates in the pressure vessel were kept in the dessicator to cool. The final boron concentration was calculated using equation 3.1. The dried precipitates were then collected and analyzed with scanning electron microscope (SEM) and X-ray diffraction (XRD). Using simens diffractometer (Model D5000) with graphite monochromated Cu K α source operated at 40 kV and 40 mA, the XRD spectrum was obtained at scanning angles ($2^\circ\Theta$) ranging from 5° to 150° and at scanning speed of 0.04° per second. Experimental setup for hydrothermal mineralization study is shown in Figure 3.3 and Figure 3.4. The general experimental flow plan with a schematic diagram showing the experimental processes and parameters is depicted in Figure 3.5

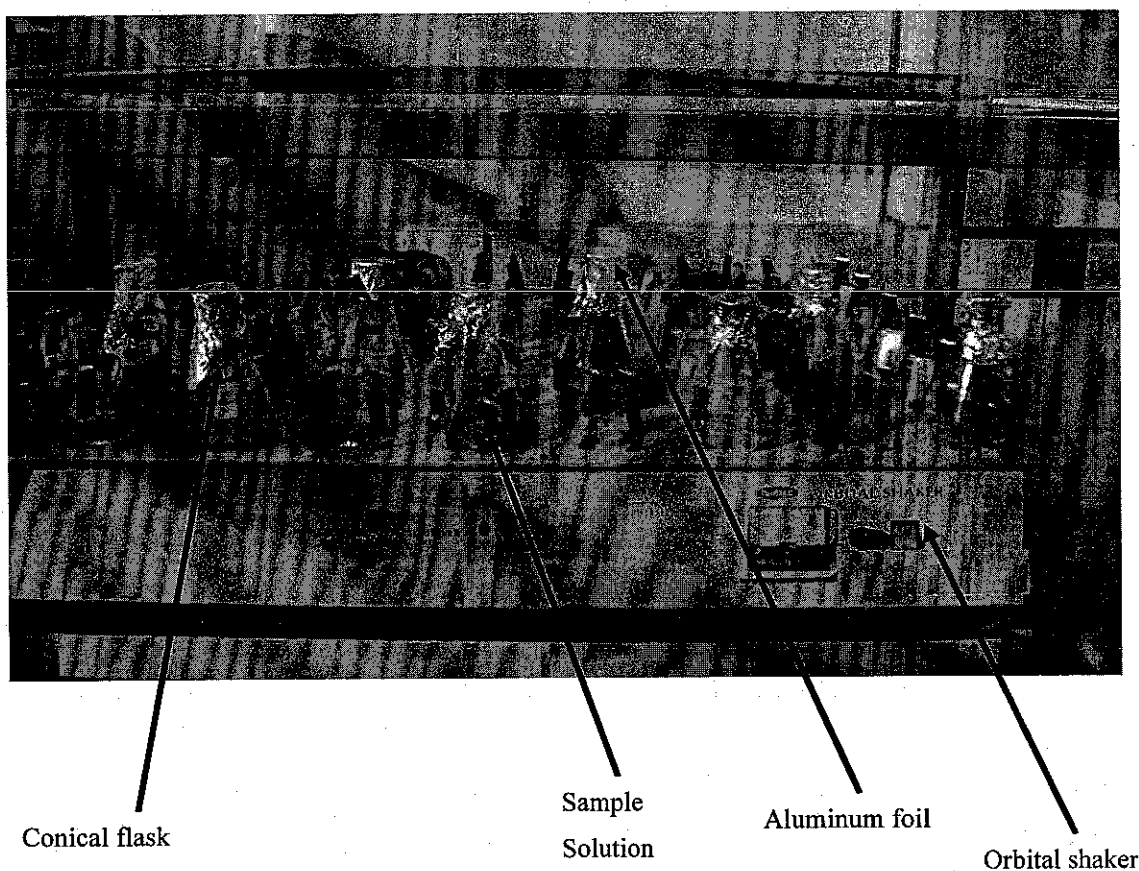


Figure 3.3: Experimental setup for dissolution of EC floc

3.3.6 Apparatus used for both Batch and Continuous mode study

- i. DC power supply: A digital DC power supply (Zhaoxin 303D) in the range of (3A-30V) was used to supply current for the experimental study.
- ii. Digital Ammeter: A digital ammeter was used to regulate the amount of current passing through the electrode during the study.
- iii. Digital Volt Meter: A digital voltmeter was used to measure the operational voltage during the experiment.

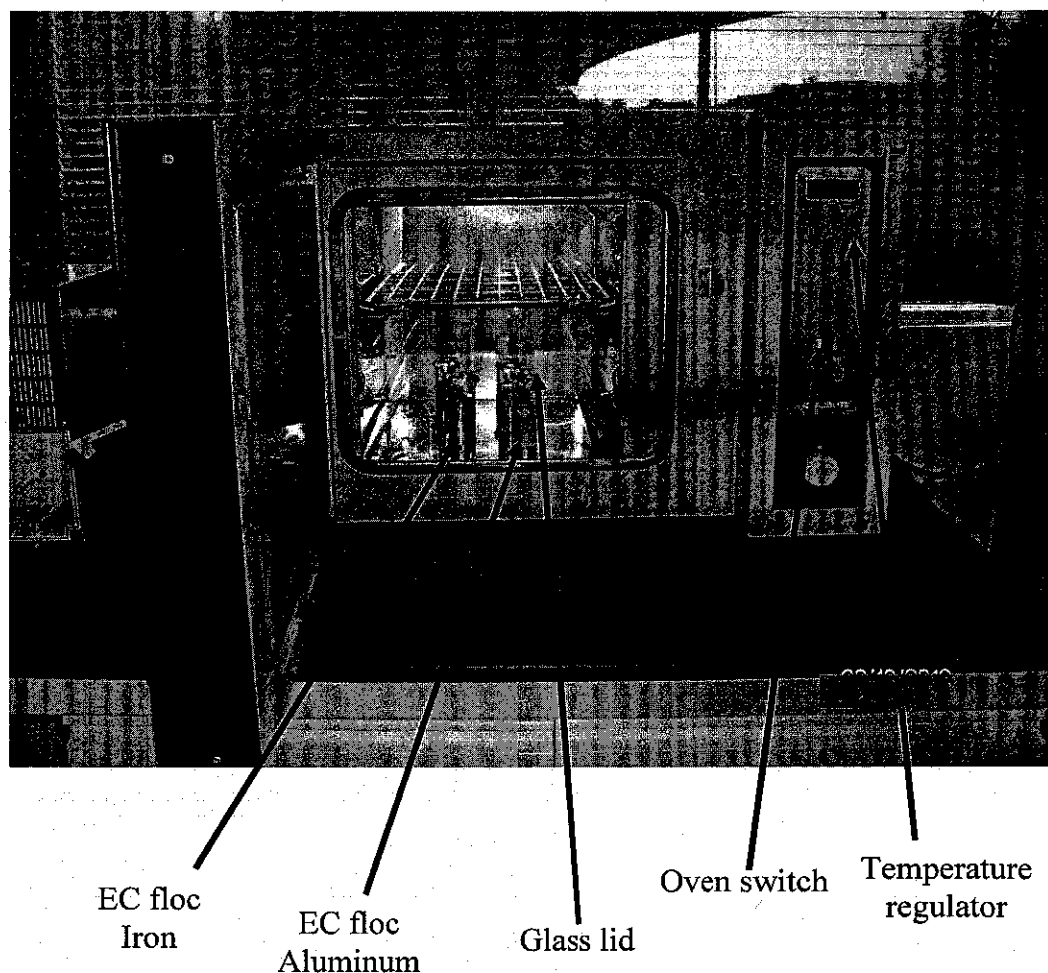


Figure 3.4: Experimental setup for hydrothermal mineralization process with EC floc

- iv. pH Meter: A pH meter (Hach Sension2 pH meter) was used to read and control the pH of the sample.
- v. Conductivity Meter: A conductivity meter (Myron L conductivity meter) was used to measure the conductivity of the sample.

- vi. Turbidimeter: A turbidimeter (2100P Portable turbidimeter) was used to measure the turbidity of the sample.
- vii. Magnetic bar and stirrer: A magnetic bar and stirrer in the range of 0-1000 rpm was used to provide mixing for the sample during the experiment.
- viii. Peristaltic pump: A Peristaltic pump with the flow rate range of 5-50 mL/min was used to control flowrate during the experimental study.
- ix. Thermometer: A thermometer was used to measure and regulate the temperature of the sample.
- x. Water bath: A water bath with the temperature range of 0-180°C was used to control the temperature of the sample.
- xi. Glasswares: Some glasswares such as pipets, burettes, beakers, conical flasks, volumetric flasks, vials, porcelain dish and others were used in this study.
- xii. Perforated plexiglass: Different plexiglass perforated with vertical turrette milling machine with an inter-electrode distance of 0.5 cm, 1.0 cm and 1.5 cm was used to hold the electrodes at their right position.
- xiii. Dessicator: A dessicator was used to cool the petridish containing the dried EC flocs after hydrothermal mineralization.
- xiv. Atomic absorption spectrometer: Atomic absorption spectrometer (AAS) was used to measure the characteristics of the sample
- xv. Ion Chromatography: Ion Chromatography (IC) was also used to measure the concentration of anions and cations in the sample.
- xvi. Electrocoagulation Cell: A 500 mL beaker was used for the batch study while a 0.9 L reactor was used for the continuous mode study.

3.3.7 Materials used for batch and continuous mode study

The following materials were used during the experimental study for the removal of boron.

- i. Boric acid (H_3BO_3) with a purity upto 99%, product of Fisher Chemicals, USA.
- ii. Sulfuric acid
- iii. Hydrochloric acid

- iv. Sodium hydroxide
- v. Buffer solutions for pH calibration (4,7,10)
- vi. Distilled water
- vii. Acetone
- viii. Ultra pure water
- ix. Aluminum and iron electrode
- x. Carmine reagent powder pillow

3.3.8 Materials used for hydrothermal mineralization

- i. Nitric acid (70%)
- ii. Calcium hydroxide $\text{Ca}(\text{OH})_2$
- iii. Whatman coarse filter paper (110 mm). Schleicher & Schuell.
- iv. Distilled water
- v. NaOH

3.4 Adsorption study

Adsorption kinetics was conducted to understand the rate limiting step in the removal of boron using electrocoagulation. Boron concentration for the adsorption study was varied in the range 10-30 mg/L using a 500 mL beaker. The following parameters were kept constant; current density 12.5 mA/cm^2 , pH 7, temperature 308K, and inter-electrode spacing 0.5 cm. Boron concentrations and treatment time were varied while other parameters were kept constant. The treatment time was varied in the range of 15-90 minutes. At the end of the adsorption process, supernatant was collected and analyzed against each treatment. The amount of boron adsorbed at equilibrium (q_e) was calculated using the following equation;

$$q_e = (C_o - C_e) \frac{v}{w} \quad (3.2)$$

where

C_o = initial concentration of contaminant (mg/L)

C_e = equilibrium concentration (mg/L)

V = volume of sample (L)

W = mass of adsorbent (g)

The amount of boron adsorbed at any time (q_t) was obtained using the equation below

$$q_t = (C_o - C_t) \frac{v}{w} \quad (3.3)$$

where

C_t = concentration at any time t (mg/L)

The equilibrium concentration (C_e) was obtained using the equation below

$$C_e = C_o - \frac{(q_e w)}{v} \quad (3.4)$$

3.5 Thermodynamic study

The thermodynamic study for the removal of boron was conducted at four different temperatures ranging from 298K to 328K. Four different temperature ranges were controlled using a polyscience thermostatic warm water bath. Boron concentration for the thermodynamic study was kept constant at 20 mg/L in a 500 mL beaker. The following parameters were kept constant; current density 12.5 mA/cm², pH 7 and inter-electrode spacing 0.5 cm while temperature and treatment time were varied to obtain the thermodynamic constants.

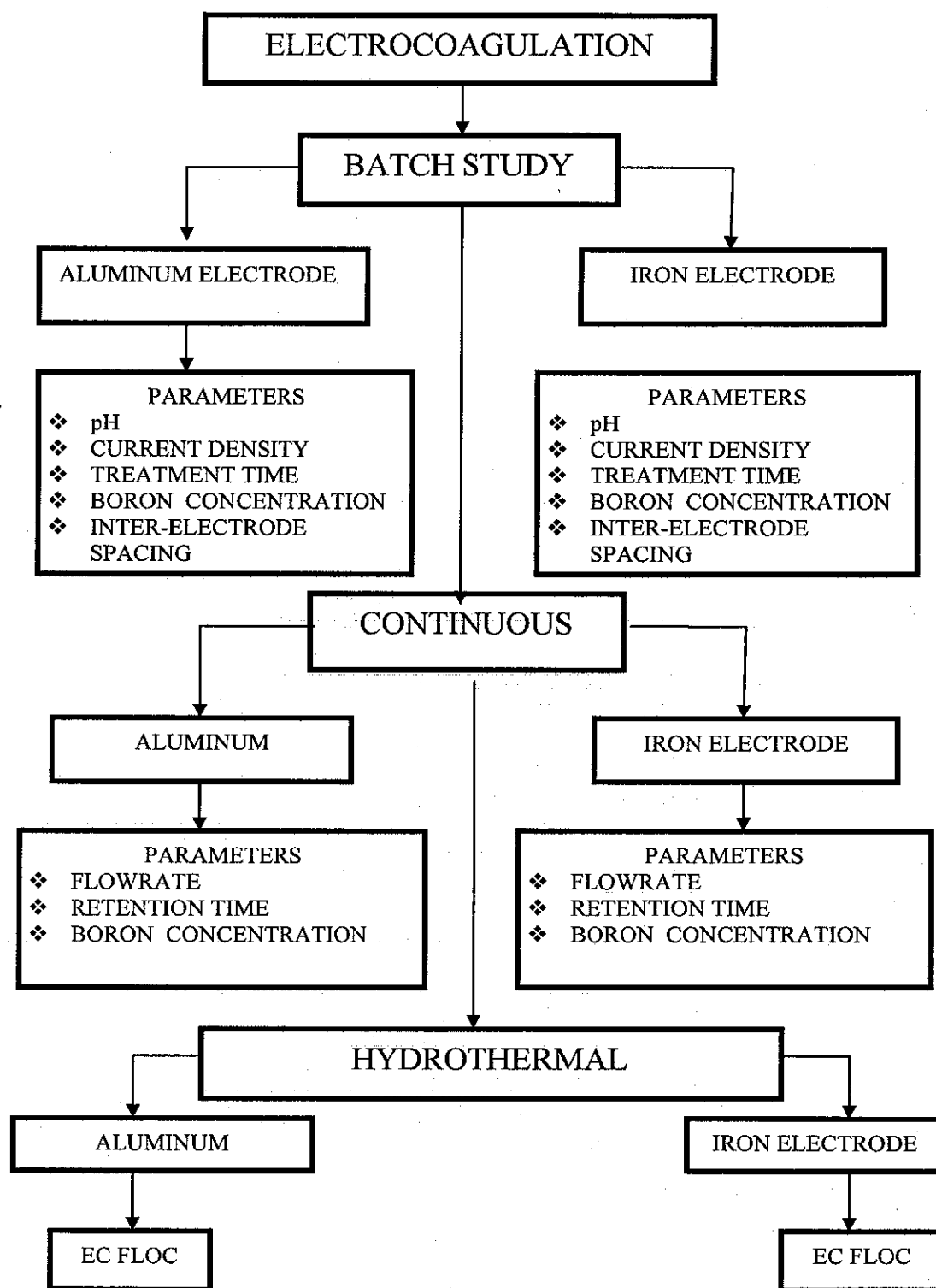


Figure 3.5: Experimental Flow chart

CHAPTER 4

RESULTS AND DISCUSSION

4.1 Chapter overview

In this chapter, the various results obtained from this study and the effects of operating parameters which were found to affect the efficiency of electrocoagulation process are presented and discussed. The kinetics and thermodynamics of boron adsorption on $\text{Al}(\text{OH})_3$ and $\text{Fe}(\text{OH})_3$ are investigated and reported. The possibility of recovering boron as a recyclable precipitate was also investigated.

4.1.1 Justification of parameters

Boron removal and final solution pH was monitored during the experimental process. However, total suspended solids (TSS), calcium, magnesium and phenol were also measured at the end of the experiment. It was important to monitor the final solution pH so as to verify if it falls within the normal pH range for potable water. Final solution pH indicates if the sample is fit for use without the addition of chemicals. Investigating the calcium and magnesium concentration after the experiment was important because these compounds are responsible for hardness of water and produced water contains high concentration of the hardness ions. Hardness ions form scales and deposits that can clog installations and lead to serious failure. Total suspended solids (TSS) and phenol was also measured at the end of the experiment. This was carried out to know the amount suspended solids left in the sample after treatment. Phenols concentration after the experiment was measured because phenols are considered as priority contaminants since at low concentration, they are harmful to organisms and pose a potential danger to human health [128].

4.2 Synthetic wastewater batch study result

After several experiment with synthetic wastewater, the optimal operating conditions were obtained. The effects of the parameters are discussed below.

4.2.1 Effect of initial solution pH

pH has been confirmed to be an important parameter in electrocoagulation. pH controls metal hydroxide formation and the removal mechanism of ions and pollutants. On the other hand, the formation of H_2 at the cathode and the aggregation of hydroxide ions in the solution are controlled by pH of the sample [98]. However, pH has been observed to change during electrocoagulation. This change depends mainly on the type of electrode material [129]. To investigate the effect of pH, experiments with different initial pH values were carried out. The experimental conditions are shown in Table 3.1. The experiments were conducted with synthetic wastewater to obtain the optimal parameters for produced water treatment. Aluminum and iron electrodes showed near similar effect with pH variation and their respective results are discussed below.

4.2.1.1 Aluminum electrodes

pH showed a significant effect on boron removal using aluminum electrodes. The results obtained (Figure 4.1) from the experiments conducted showed that removal efficiency increased when initial solution pH was increased from 3-7 and remained constant at pH 8. The experimental result is tabulated in Table A.1 (Appendix A). From initial solution pH 9, the removal efficiency decreased significantly. It was reported that boron exists in water as boric acid (H_3BO_3) at low pH and from pH 10, the borate anion $[B(OH)_4]^-$ predominate.

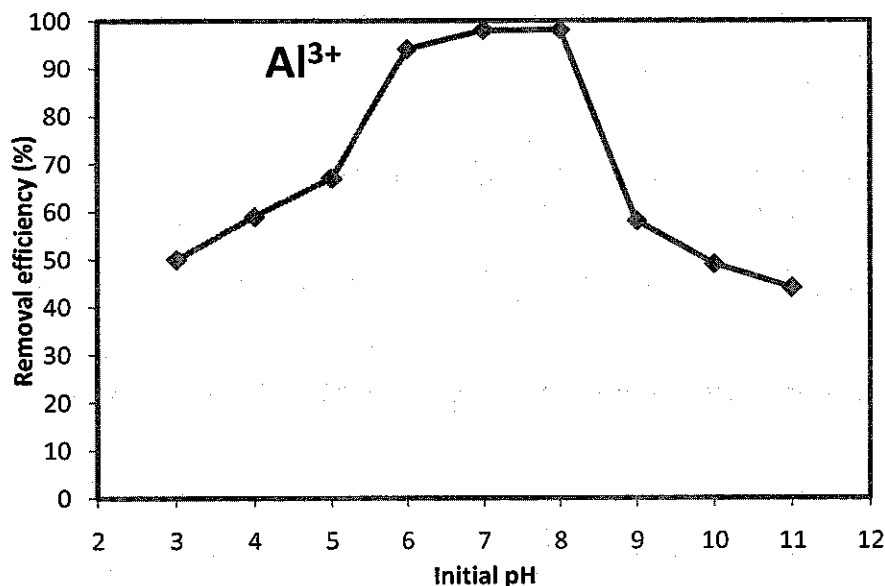


Figure 4.1: Effect of initial pH on boron removal, concentration 10 mg/L, current density 12.5 mA/cm², time 90 minutes, inter-electrode spacing 0.5cm.

From about pH 11, highly water soluble polyborate ions such as $B_3O_3(OH)_4^-$, $B_4O_5(OH)_4^-$ and $B_5O_6(OH)_4^-$ are formed [11 25]. This result can be explained that between initial solution pH 4-9, Al^{3+} and OH^- generated by the electrodes react to form various monomeric and polymeric species that finally transform into insoluble amorphous $Al(OH)_3(s)$ through complex polymerization. The insoluble amorphous aluminum species have large surface area for adsorption and trapping of colloidal particles. Above pH 10, the highly soluble monomeric $Al(OH)_4^-$ anion concentration increases at the expense of $Al(OH)_3(s)$ [130]. The removal efficiency of boron was highest between initial solution pH 6-8. The removal efficiency of boron at initial solution pH 7 was 98% after 90 minutes as shown in Figure 4.2 and the experimental result tabulated in Table A.2 (Appendix A). The lowest removal efficiency of 45% was observed at initial solution pH 11. The optimal time for this study was observed to be 75 minutes. This is concluded because at 75 minutes, a removal efficiency of 96% was observed and meets the WHO permissible limit of boron in potable water. Above 75 minutes, removal efficiency was slow and neared the point of equilibrium. Further increase in treatment time will increase the energy consumption which will also increase cost. It was observed during this study that electrocoagulation exhibited some buffering capacity at alkaline pH. From initial solution pH 9 – pH 11, final solution pH was observed to be lower than initial solution pH. However, from initial

solution pH 3-8, final solution pH was observed to be higher than initial solution pH. The final solution pH after treatment at initial solution pH 7 is 7.28. High removal efficiency at initial solution pH 7 indicates that the highest amount of coagulant was released at this condition. This could be so because the solubility of aluminum hydroxide is less between initial solution pH 6-8 [15]. In this study, initial solution pH 7 is used as the optimum pH. This is because further increase in initial pH requires the addition of chemicals and did not improve removal efficiency.

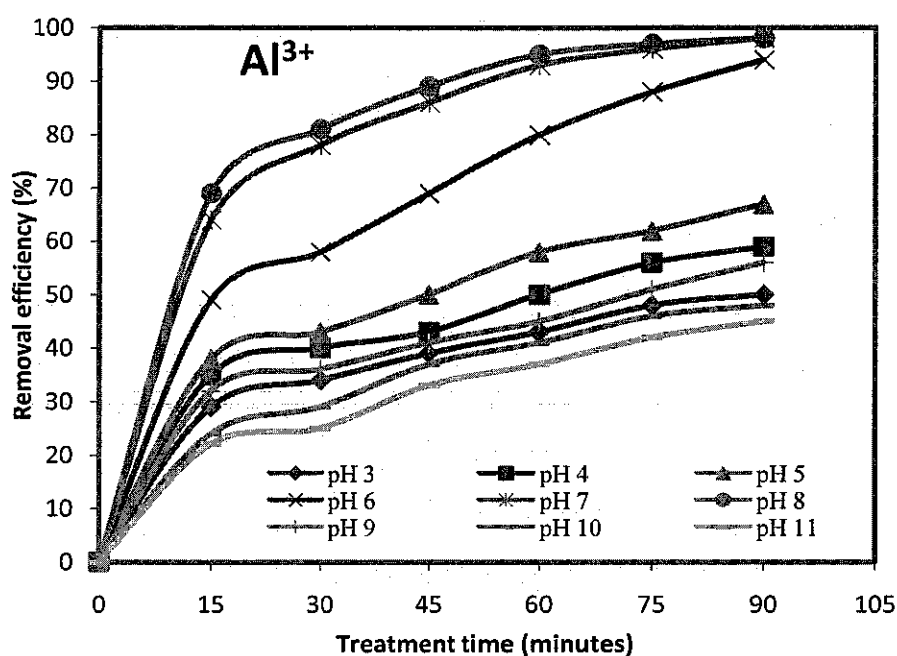


Figure 4.2: Boron removal efficiency at different initial pH values; concentration 10 mg/L, current density 12.5 mA/cm², inter-electrode spacing 0.5cm.

Similar results were obtained by *Vasudevan et al.* [131] in their study of electrochemical coagulation for chromium removal from water using magnesium as the anode and galvanized iron as the cathode. They observed 98.6% chromium removal efficiency at initial solution pH 7.

Few literature are of contrasting views on why the final solution pH at acidic condition is high but lower than initial solution pH at alkaline condition. While *Vik et al.* [132] is of the opinion that it is caused by the evolution of hydrogen at the cathode, *Chen et al.* [94] is of the opinion that it involves a series of mechanisms. Firstly, CO₂ could be released from wastewater due to hydrogen bubble disturbance at acidic

condition which causes an increase of final solution pH. Secondly, some anions present in wastewater such as Cl^- , SO_4^{2-} , HCO_3^- , HSiO_4^- , NO_3^- can exchange partly with the OH^- of $\text{Al}(\text{OH})_3$ which results in an increase in final solution pH. However, at high initial solution pH (alkaline), Ca^{2+} and Mg^{2+} present in wastewater can co-precipitate with $\text{Al}(\text{OH})_3$ in the form of hydroxides which results in a decrease of final solution pH. Due to the amphoteric nature of $\text{Al}(\text{OH})_3$, more reactions can take place which can cause a decrease in final solution pH such as shown in equation 4.1.



These monomeric form of aluminum ($\text{Al}(\text{OH})_4^-$) are called alkalinity consumers [133].

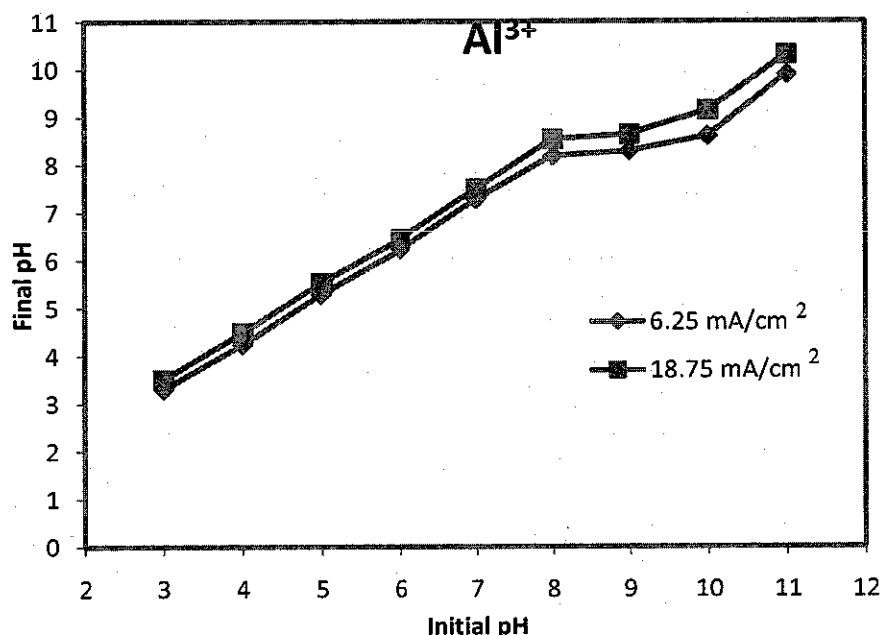


Figure 4.3: Plot of final pH vs initial pH at different current densities. Concentration 10 mg/L, inter-electrode spacing 0.5 cm, time 90 minutes.

Some literature has made similar observations [134-136]. However, final solution pH spontaneously increased as current density is increased in this study. This could be attributed to more electrolysis as the current is increased [137]. The plot of final solution pH against initial solution pH at various current densities is depicted in Figure 4.3 and the experimental data tabulated in Table A.3 (Appendix A).

4.2.1.2 Iron electrodes

To investigate the effect of initial solution pH on boron removal, the initial solution pH range was selected from pH 3-11. After several experiments with different concentration and current density, the result shows that the removal efficiency increased when initial solution pH was increased from 3-8 and decreased from initial solution pH 9-11. At initial solution pH 7, a removal efficiency of 97% was observed as shown in Figure 4.4 and tabulated in Table A.4 (Appendix A). At initial solution pH 11, the lowest removal efficiency of 41% was observed. It has been reported that from initial solution pH 4-9, highly insoluble coagulants are released by iron electrode [138]. These highly insoluble coagulants interact with particles in suspension through surface complexation or electrostatic attraction. Above initial solution pH 9, highly soluble monomeric $\text{Fe}(\text{OH})_4^-$ anion concentration increases at the expense of $\text{Fe}(\text{OH})_3$ [138]. At about initial solution pH 10, the cathode is exposed to risk of being attacked by OH^- ions generated with H_2 [139]. The obtained results depicted in Figure 4.5 and tabulated in Table A.5 (Appendix A) for all initial solution pH values investigated indicate that highest amount of coagulants was released between initial solution pH 7 and 8 as shown by their respective removal efficiency. pH 7 is therefore considered as the optimal pH since the permeate boron at this condition meets the 0.5 mg/L as stipulated by WHO. The optimal treatment time was 75 minutes. At 75 minutes, a removal efficiency of 95% was observed. Above 75 minutes, removal efficiency was slow and close to equilibrium. Further increase in time will result to increase in cost due to waste of energy.

The pH of the medium has been reported to change during electrocoagulation, however this change has been found to depend on the nature of the electrode material and the initial solution pH [129]. The plot of final solution pH against initial solution pH at various current densities is depicted in Figure 4.6 and the experimental data tabulated in Table A.6 (Appendix A). Figure 4.6 shows that the final solution pH at all pH values was higher than the initial solution pH. This observation is well documented in literature [134].

This result can be compared with the results of *El-Nass et al.* [140] who investigated the use of electrocoagulation in the treatment of refinery wastewater

using aluminum, iron and stainless steel electrodes. They observed that the removal efficiency of sulfate and COD was best at initial solution pH 8.

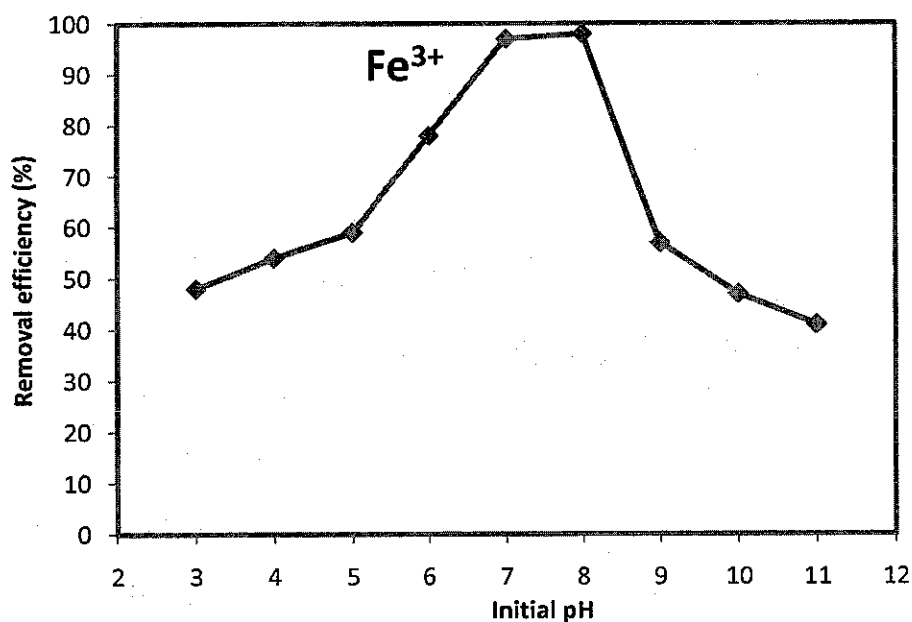


Figure 4.4: Effect of initial pH on boron removal, concentration 10 mg/L, current density 12.5 mA/cm², inter-electrode spacing 0.5cm.

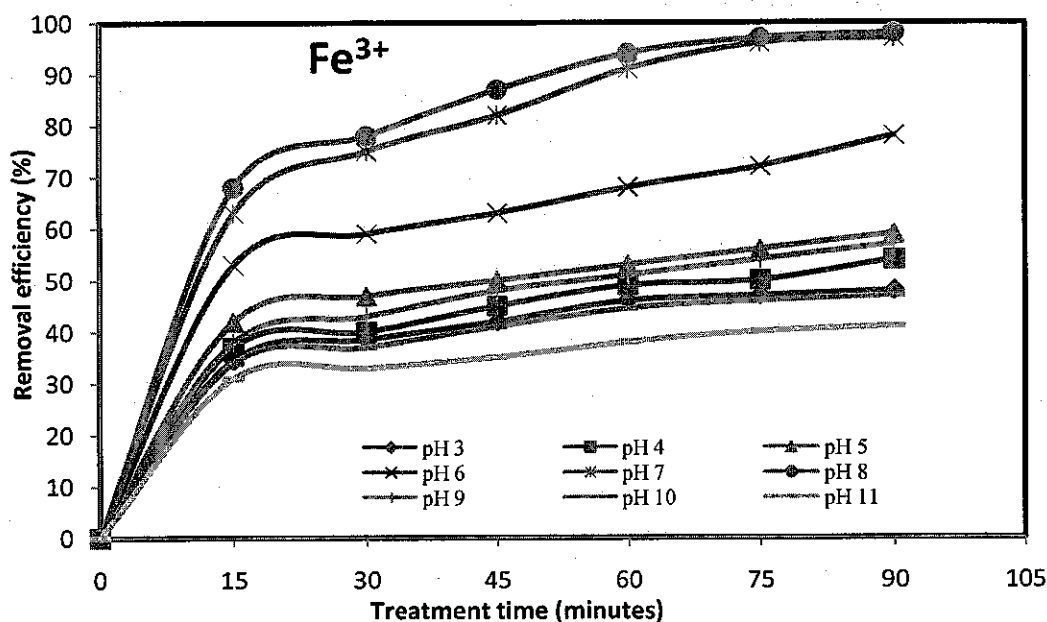


Figure 4.5: Boron removal efficiency at different initial pH values; concentration 10 mg/L, current density 12.5 mA/cm² and inter-electrode spacing 0.5cm.

The spontaneous increase in final solution pH of water sample treated with iron electrode especially in alkaline conditions may be attributed to several intermediate

reactions and non generation of chemical species which are alkalinity consumers. In addition, the possible formation of Fe(VI) anions can increase the final solution pH of effluent sample upto 10 [136].

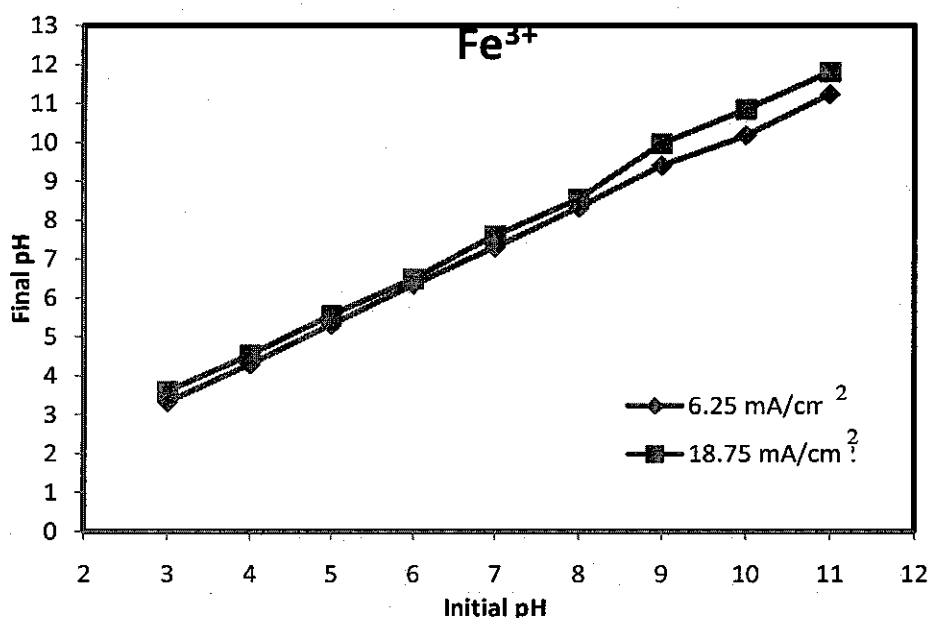


Figure 4.6: Plot of final pH vs initial pH at different current densities. Concentration 10 mg/L, inter-electrode spacing 0.5 cm, electrode area 60 cm² and time 90 minutes.

4.2.2 Effect of current density

Current density is an important parameter in electrocoagulation. It controls the amount of metal ions released from the respective electrodes. Current density generally affects the overall reaction process during electrocoagulation and reduces treatment cost [141]. The collision between particles, the rate of floc growth, release of coagulants and effective interaction and trapping of colloidal materials are controlled by the current. When different electrodes are used in electrocoagulation, different metal ions are released. To investigate the effect of current density, experiments were conducted with different current densities. The experimental conditions are shown in Table 3.1.

4.2.2.1 Aluminum electrodes

The effect of current density on boron removal by electrocoagulation was significant. The amount of metal ions released from aluminum electrode determines the coagulating efficiency. The amount of metal ions released from aluminum electrode was calculated using equation 2.16 in subsection 2.3.6 and shown in Figure 4.7.

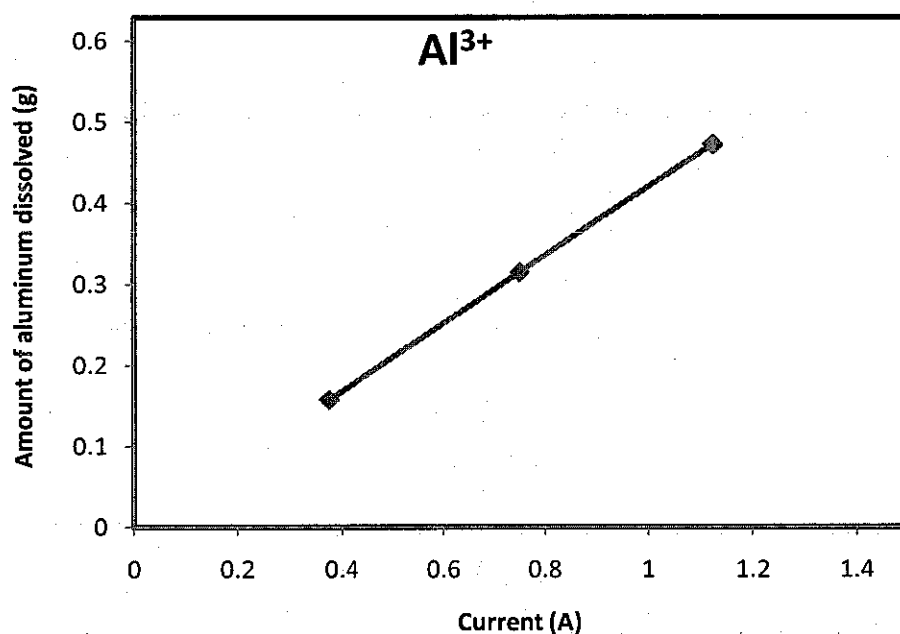


Figure 4.7: Amount of aluminum dissolved (g) at different current; Time 90 minutes.

From Figure 4.7, it can be clearly seen that the metal ions released at high current is higher than the metal ions released at low current. This observation has two implications in electrocoagulation. Firstly, when current is high, high amount of metal ions are released from the electrode and effective coagulation takes place. Secondly, at high current, treatment time reduces because the release of metal ions is rapid while at low current, the release of metal ions is slow.

The effect of current density on boron removal was observed to improve removal efficiency. From the obtained results, it was observed that increase in current density resulted in increase in removal efficiency and a corresponding decrease in treatment time. This is so because an increase in current density increases the amount of metal ions released at the sacrificial anode. A removal efficiency of 64%, 86.5% and 94% was observed at current densities of 6.25 mA/cm², 12.5 mA/cm² and 18.75 mA/cm²

respectively after 90 minutes treatment time with an initial boron concentration of 20 mg/L at pH 7 as shown in Figure 4.8. However, the use of current density should be done with care considering the energy consumption and cost. When the energy consumption is put into consideration, using very high current density may not be feasible.

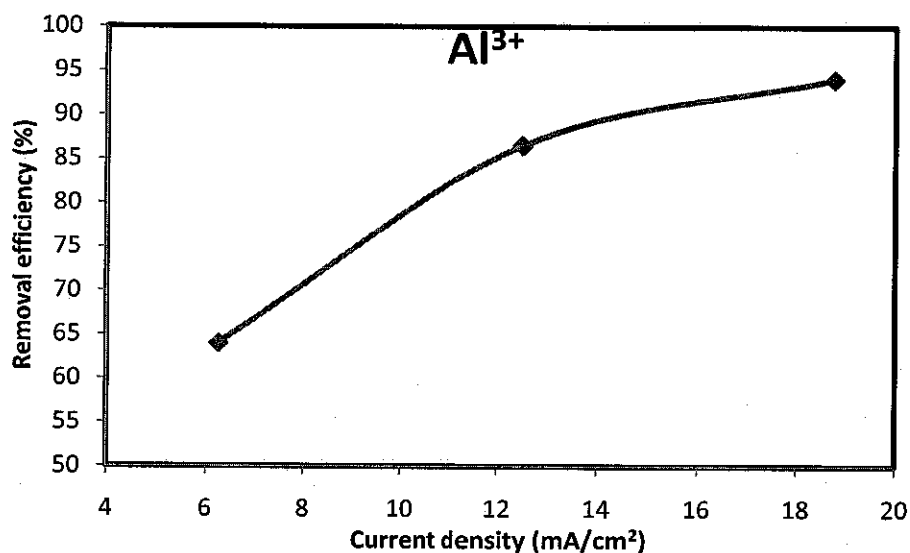


Figure 4.8: Effect of current density on boron removal, time 90 minutes, concentration 20 mg/L, initial pH 7, inter-electrode spacing 0.5cm.

The optimal current density in this study was 12.5 mA/cm². This is because removal efficiency at 12.5 mA/cm² meets the objective of this study and above 12.5 mA/cm², the temperature of the effluent increased due to ohmic heating. This results to waste of energy and at the same time, increase cost.

The energy consumption in this study was calculated using equation 2.19 in subsection 2.3.6 and shown in Table 4.1. From Table 4.1, the energy consumption at 18.75 mA/cm² was the highest compared to other current densities based on the time to reach equilibrium.

The removal efficiency of boron for different current densities is shown in Figure 4.9 and the experimental results tabulated in Table A.7 (Appendix A). From Figure 4.9, the removal efficiency reached equilibrium at different treatment times for the three current densities investigated.

Table 4.1: Energy consumption at different current densities; concentration 10 mg/L, pH 7, inter-electrode spacing 0.5 cm and electrode area 60 cm²

Current density (mA/cm ²)	Energy consumption (kWh/m ³)
6.25	2.25
12.5	3.75
18.75	4.5

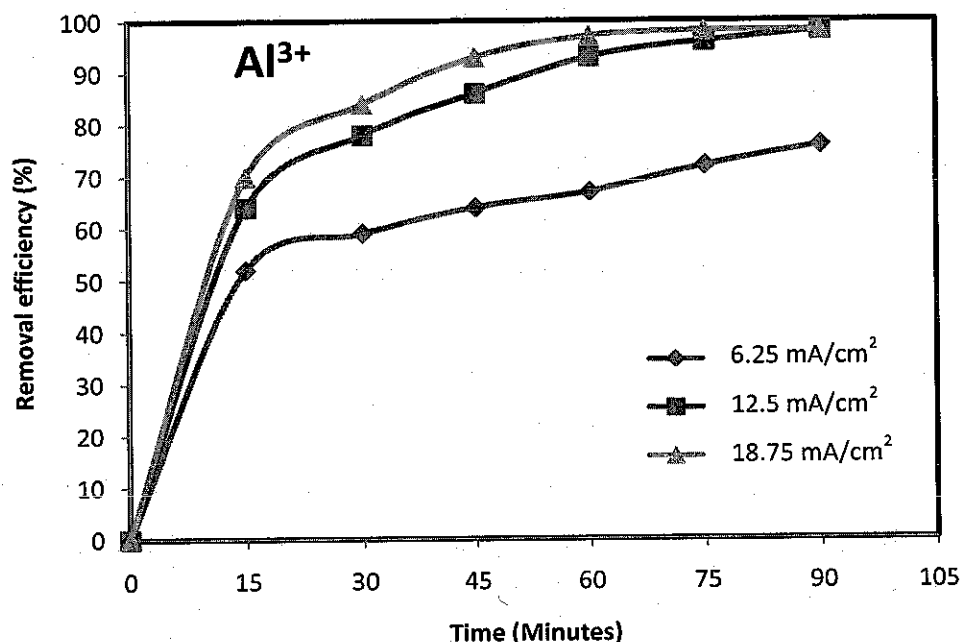


Figure 4.9: Boron removal efficiency at different current densities: Concentration 10 mg/L, initial pH 7, Inter-electrode spacing 0.5 cm.

For 18.75 mA/cm², equilibrium was attained within 60 minutes while at 12.5 mA/cm², equilibrium was attained at 75 minutes. 6.25 mA/cm² required longer treatment time, more than 90 minutes to attain equilibrium. From these results, 12.5 mA/cm² can be referred as the optimum current density and was used in this study.

The obtained results is similar with the findings of Yetilmezsoy et al. [141] in their study of color and COD reduction of UASB pretreated poultry manure wastewater by electrocoagulation. They observed that increase in current density resulted in increase in COD and color removal and the treatment time was reduced significantly. They reported a COD removal efficiency of 80.8% at current density of 5 mA/cm² in 30 minutes. When the current density was increased to 10 mA/cm² and 15 mA/cm², the

removal efficiencies increased to 81%, and 82% and the treatment time reduced to 20 minutes and 10 minutes respectively. Further increase in current density to 25 mA/cm² resulted in a removal efficiency of 80% at 5 minutes treatment time. Similar results were also obtained for color removal. Color removal efficiency of 69%, 70% and 69% was obtained with current density of 5 mA/cm², 10 mA/cm² and 25 mA/cm² at 30 minutes, 15 minutes and 5 minutes treatment time respectively.

4.2.2.2 Iron electrodes

The amount of metal ions released from the iron electrodes increases with increase in current as shown in Figure 4.10. There was effective coagulation at high current density and reduction of treatment time. Figure 4.10 shows that at high current, the amount of metal ions released from the electrode is higher than the metal ions released at low current.

The removal efficiency of boron increased when current was increased from 6.25 mA/cm² to 12.5 mA/cm² and subsequently to 18.75 mA/cm². A removal efficiency of 59% at 6.25 mA/cm², 81% at 12.5 mA/cm² and 87% at 18.75 mA/cm² was obtained after 90 minutes with an initial boron concentration of 20 mg/L at pH 7 as shown in Figure 4.11. However, it was observed during the experiment that the rate of oxidation of Fe²⁺ to Fe³⁺ was more rapid at high current density. During the experiment, the water sample was initially green in colour and later changed to yellow and finally became turbid. The green colour suggests the formation of Fe²⁺ ions and the yellow colour is due to the formation of Fe³⁺. Fe²⁺ ions are formed at the dissolved electrodes and are easily oxidized to Fe³⁺ by dissolved oxygen in water.

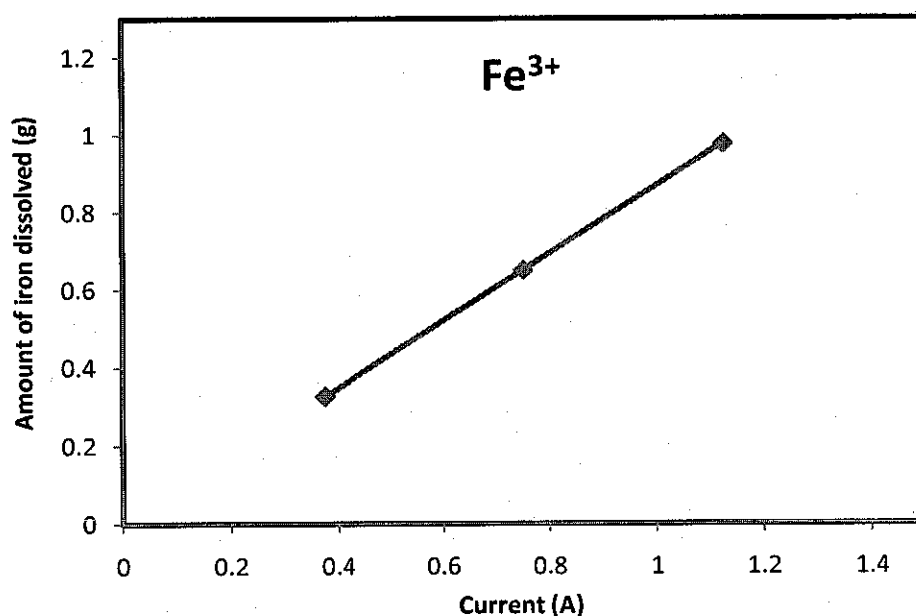


Figure 4.10: Amount of iron dissolved (g) at different current, time 90 minutes.

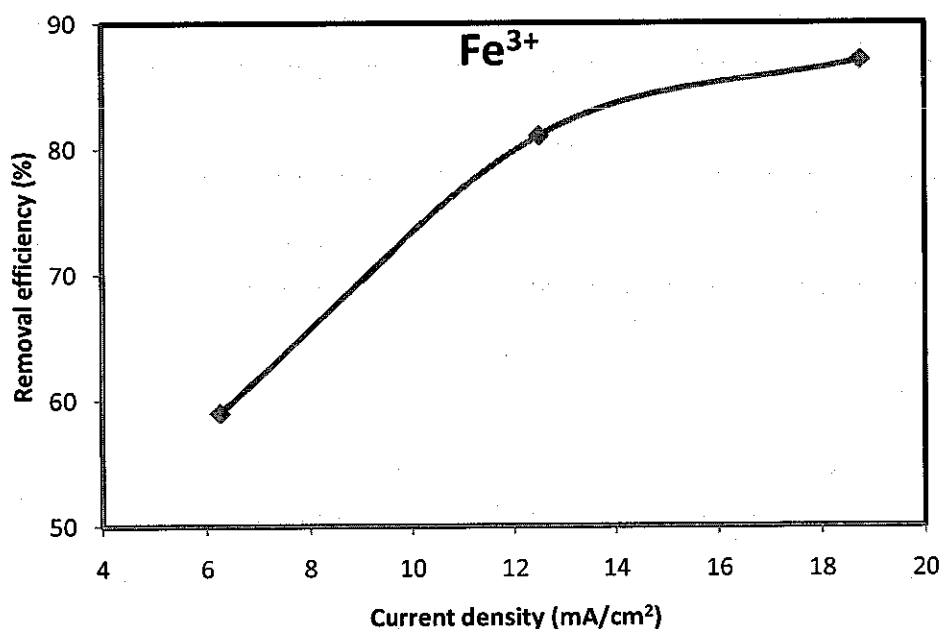


Figure 4.11: Effect of current density on boron removal, treatment time 90 minutes, concentration 20 mg/L, pH 7, inter-electrode spacing 0.5cm.

The various energy consumption for iron electrode at different current densities is shown in Table 4.2 based on the time to reach equilibrium. The removal efficiency of boron at different current densities using iron electrode is shown in Figure 4.12. From Figure 4.12, it is clearly seen that removal efficiency increases when current density is increased. However, considering the energy consumption and cost, very high current

density may not be feasible for this study. In addition, ohmic heating which resulted to increase in temperature of the effluent was observed when current density was increased above 12.5 mA/cm^2 . Therefore 12.5 mA/cm^2 was selected as the optimum current density and used in this study. The experimental result for boron removal at different current densities is tabulated in Table A.7 (Appendix A).

Similar observation was made by *Othman et al.* [142]. They investigated COD and suspended solids removal to improve wastewater quality. They observed that the water sample was initially greenish in colour and later changed yellow. They suggest that the formation of Fe^{2+} and subsequent oxidation to Fe^{3+} may be responsible for the green and yellow colours.

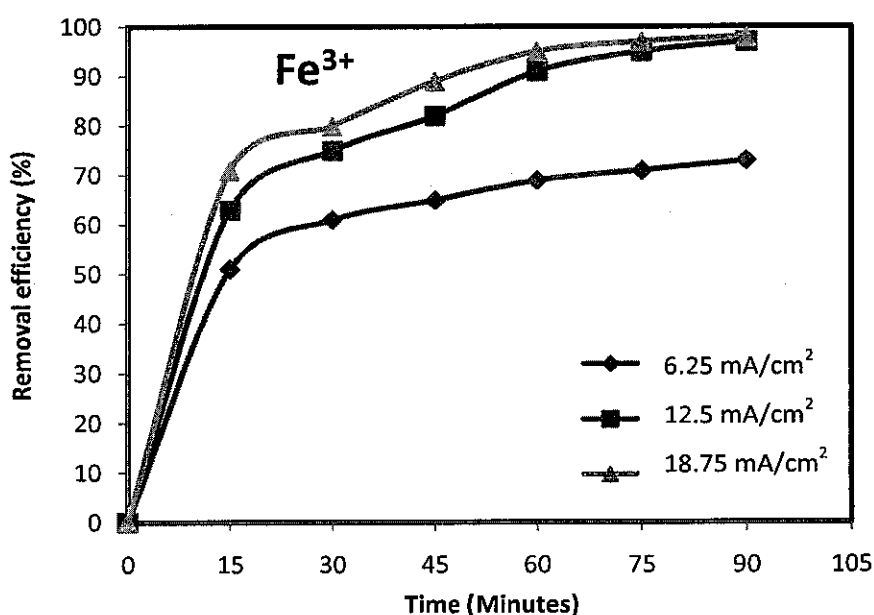


Figure 4.12: Boron removal efficiency at different current densities: Concentration 10 mg/L, initial pH 7, Inter-electrode spacing 0.5 cm.

Table 4.2: Energy consumption at different current densities; concentration 10 mg/L, pH 7, inter-electrode spacing 0.5 cm and electrode area 60 cm^2

Current density (mA/cm^2)	Energy consumption (kWh/m^3)
6.25	2.25
12.5	3.75
18.75	4.86

4.2.3 Effect of Initial Boron Concentration

The effect of initial boron concentration was investigated with aluminum and iron electrodes. The initial boron concentration was examined in the range of 10-30 mg/L. The range of concentration was selected in accordance with the objective of this study and with knowledge of the concentration of boron in the produced water sample to be treated. The experimental operating conditions are shown in Table 3.1.

4.2.3.1 Aluminum electrodes

After series of experiments with aluminum electrodes, it was observed from the results that when concentration was increased, removal efficiency decreased. This can be attributed to the fact that the amount of metal ions generated at the same current density for a low boron concentration was insufficient for solutions of higher boron concentration. At initial boron concentrations of 10 mg/L, 20 mg/L and 30 mg/L, removal efficiencies of 98%, 86.5% and 82.7% was obtained respectively at current density of 12.5 mA/cm^2 . The removal efficiency of boron at different initial boron concentrations is shown in Figure 4.13 and tabulated in Table A.8 (Appendix A).

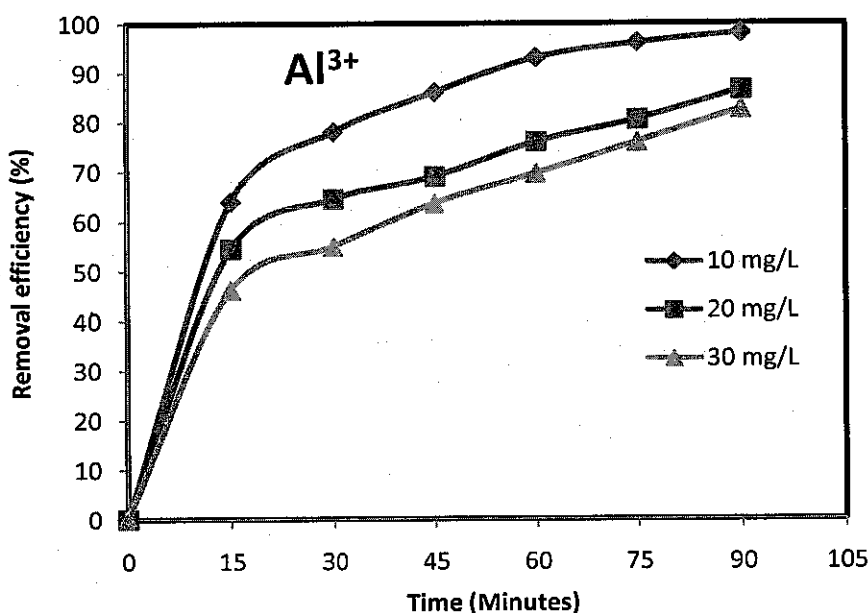


Figure 4.13: Boron removal efficiency at different initial boron concentration: initial pH 7, current density 12.5 mA/cm^2 , inter-electrode spacing 0.5 cm.

4.2.3.2 Iron electrodes

Increase in initial boron concentration was found to decrease removal efficiency. This phenomenon may be explained thus: although the same amount of Fe^{3+} was released into the solution at the same current density for all boron concentration, these metal ions were insufficient for solutions of higher boron concentration. Hence, when boron concentration was increased, removal efficiency decreased. A removal efficiency of 97% was observed at current density of 12.5 mA/cm^2 at initial boron concentration of 10 mg/L. Subsequent increase of initial boron concentration to 20 mg/L and 30 mg/L yielded a removal efficiency of 81% and 72.2% respectively. The removal efficiency at different initial boron concentrations is depicted in Figure 4.14 and tabulated in Table A.8 (Appendix A).

These results can be compared with the results of *Demirçivi and Nasün-Saygılı* [143] in their study of removal of boron from wastewaters by ion-exchange in a batch system. They used different boron concentrations of 20, 40 and 60 mg/L. They observed that removal efficiency decreased with increase in boron concentration. *Yan et al.* [144] also investigated the removal of boron from brine using selective ion exchange resins. Their results show that increase in initial boron concentration resulted in decrease in removal efficiency. Initial boron concentrations of 40, 50 and 100 mg/L. Their results showed that high boron concentration was not favorable to the removal of boron. They suggested that the active sites on the resins might not be enough to absorb so much boron with high initial concentrations.

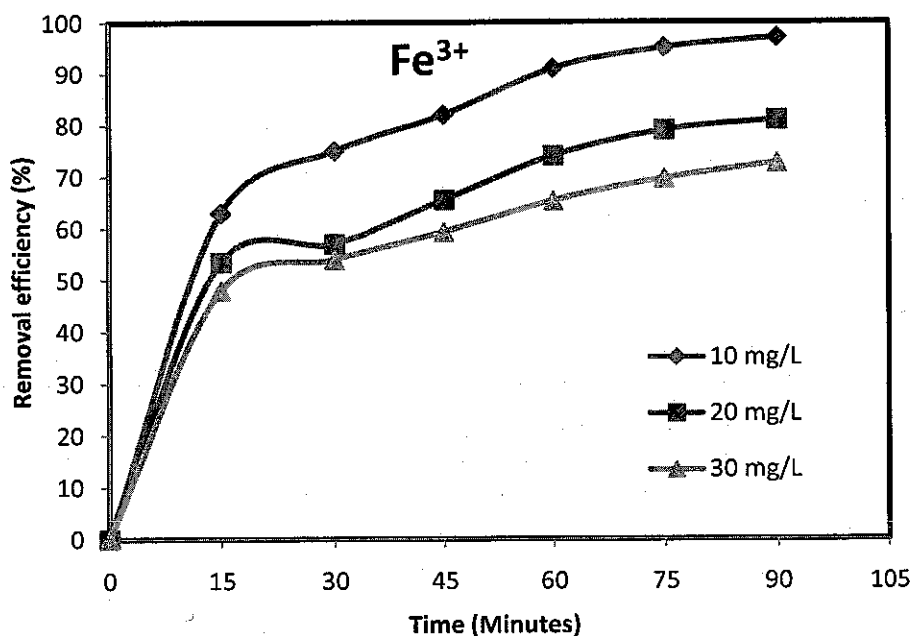


Figure 4.14: Boron removal efficiency at different initial boron concentration: initial pH 7, current density 12.5 mA/cm², inter-electrode spacing 0.5 cm.

4.2.4 Effect of Treatment time

Electrolysis time is an essential parameter in electrocoagulation. Electrolysis time determines the duration for metal ions release from the electrode. To investigate the effect of electrolysis time, supernatant was collected at different times in the range of 15-90 minutes. The experimental conditions for electrolysis time are shown in Table 3.1. The optimum treatment was observed as the point at which removal efficiency meets the WHO boron permissible limit in potable water.

4.2.4.1 Aluminum electrodes

The effect of electrolysis time on boron removal efficiency using aluminum electrodes was investigated in the range of 15-90 minutes. It was observed during the experiment that increase in electrolysis time resulted in an upward trend in removal efficiency. However, boron removal efficiency was rapid at the initial stage but was slow as the experiment proceeded. This observation may suggest that after the initial stage of the experiment, the boron concentration in the sample reduced. This may

have reduced the contact between boron and the coagulants at the later stage of the experiment. At 75 minutes of electrolysis time, the obtained removal efficiency was high and below 0.5 mg/L and represent the optimum treatment time. The effects of electrolysis time on removal efficiency is shown in Figure 4.15 and tabulated in Table A.9 (Appendix A).

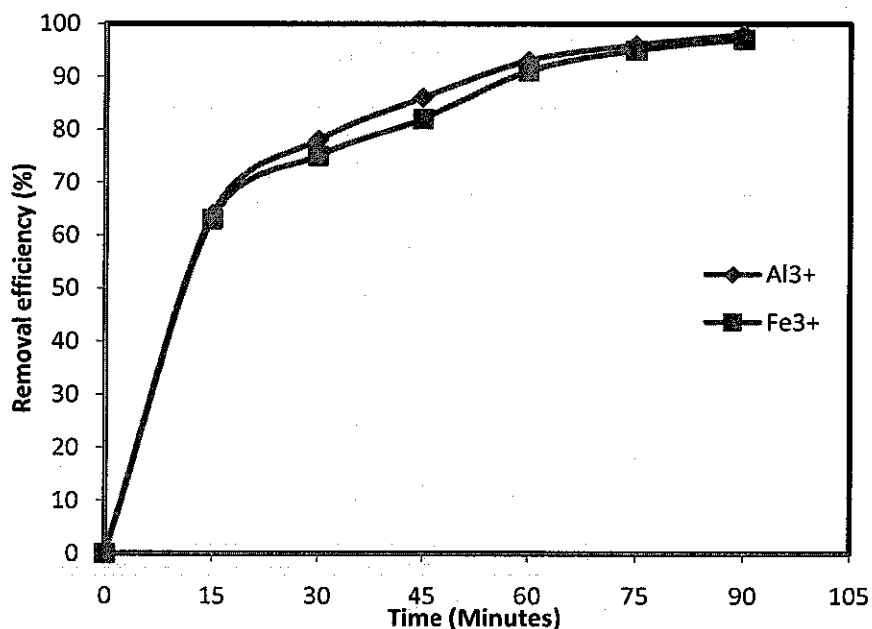


Figure 4.15: Effect of electrolysis time on boron removal: initial pH 7, conc. 10 mg/L, current density 12.5 mA/cm², inter-electrode spacing 0.5 cm.

4.2.4.2 Iron electrodes

Similar observation was made for iron electrodes. Increase in treatment time was spontaneous with increase in removal efficiency. Removal efficiency was also rapid in the initial stage of the experiment but became slow as the experiment proceeded. This could be because of reduced concentration after the initial stage of the experiment. The effect of electrolysis time on removal efficiency is shown in Figure 4.15 and tabulated in Table A.9 (Appendix A).

4.3 Produced water batch study result

The characteristics of the produced water are tabulated in Table 3.2. After several experiments with the synthetic wastewater, the optimal parameters were obtained. The optimal parameters for boron removal was obtained as pH 7 and current density 12.5 mA/cm² for both aluminum and iron electrodes. The optimal parameters were then applied to produced water treatment. The boron concentration in produced water is 15 mg/L. The current density and pH was kept constant for both aluminum and iron electrodes. However, inter-electrode spacing was varied to investigate the effect of inter-electrode spacing in boron removal. The operating condition for inter-electrode spacing is tabulated in Table 3.1. The experimental results for the removal of boron at different inter-electrode spacing for both aluminum and iron electrodes are tabulated in Table A.10. (Appendix A)

4.3.1 Effect of Inter-electrode spacing

Inter-electrode spacing is an important parameter in electrocoagulation. The drop in ohmic potential of a cell is proportional to the inter-electrode spacing. The distance between electrodes also affect the electrolysis energy consumption especially when the conductivity is low [145]. Additionally, the strength of the electric field and the electrical resistance between electrodes is also affected by inter-electrode spacing. Some authors have reported the effect of inter-electrode spacing on removal efficiency of pollutants [146-147]. It can be concluded from their work that the effect of inter-electrode spacing depends on the nature of pollutant, setup of electrode and some process hydrodynamic conditions. To investigate the effect of inter-electrode spacing, three values in the range of 0.5, 1.0 and 1.5 cm were selected. This range was selected according to the size of the batch reactor (500 mL beaker). However, fixing the electrode to this pre-selected spacing was among the biggest difficulty encountered in this study.

4.3.1.1 Aluminum electrodes

After several experiments with different inter-electrode spacing, the results as represented in Figure 4.16 show that boron removal efficiency decreased as inter-electrode spacing was increased. This could be attributed to rapid generation of coagulant and increase in electric field strength when electrodes are kept close to each other. It has also been observed that when the inter-electrode spacing is increased, interaction of ions with hydroxyl polymers is reduced. Increase in inter-electrode spacing also decreases electrostatic attraction between particles in suspension [145]. The removal efficiency at inter electrode spacing of 0.5 cm, 1.0 cm and 1.5 cm were 98%, 90.6% and 84% respectively after 90 minutes. The optimum inter-electrode spacing was 0.5 cm and was used in this study.

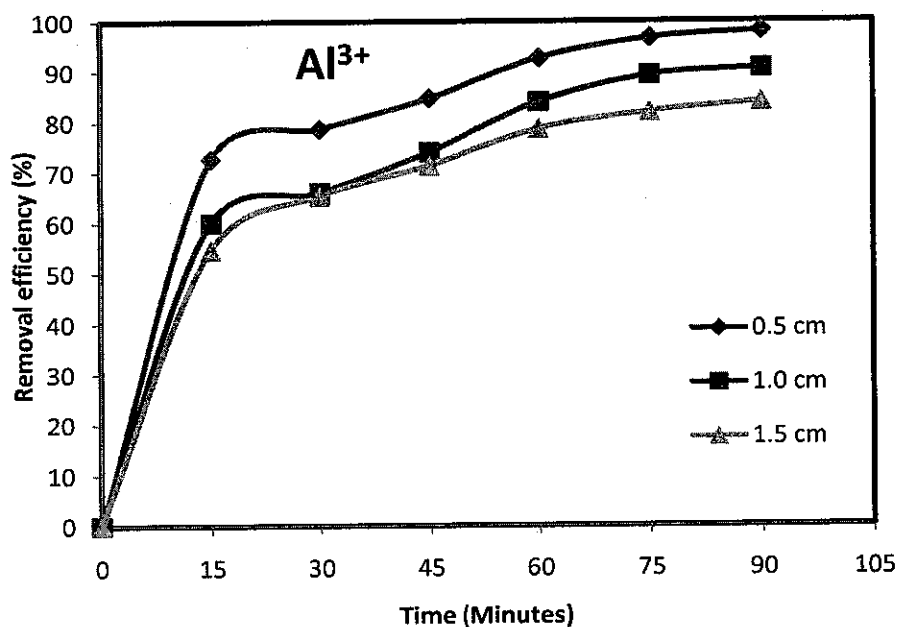


Figure 4.16: Effect of inter-electrode spacing on boron removal from produced water: initial pH 7, Conc. 15 mg/L, Current density 12.5 mA/cm².

4.3.1.2 Iron electrodes

Similar observation was also made for iron electrodes. After several experimental work, the results as depicted in Figure 4.17 shows that increase in inter-electrode spacing decreased boron removal efficiency. A removal efficiency of 97% at 0.5cm,

89.3% at 1.0 cm and 82.7% at 1.5 cm inter-electrode spacing was observed after 90 minutes. This can be explained that when the electrodes were kept close to each other, the electric field strength increased and coagulant generation was accelerated.

This result can be compared with the result of *Drouichea et al.* [145, 146] in their study of flouride removal from pretreated photovoltaic wastewater by electrocoagulation. They observed that increase in inter-electrode spacing resulted in decrease in removal efficiency of flouride and removal efficiency favored lower inter-electrode spacing. *Daneshvar et al.* [146] also investigated the effect of inter-electrode spacing in decolorization of orange II using electrocoagulation. They observed a 5.61% reduction in removal efficiency when the inter-electrode spacing was increased from 1 to 4 cm. Therefore, 0.5 cm inter-electrode spacing is the optimum spacing for this study.

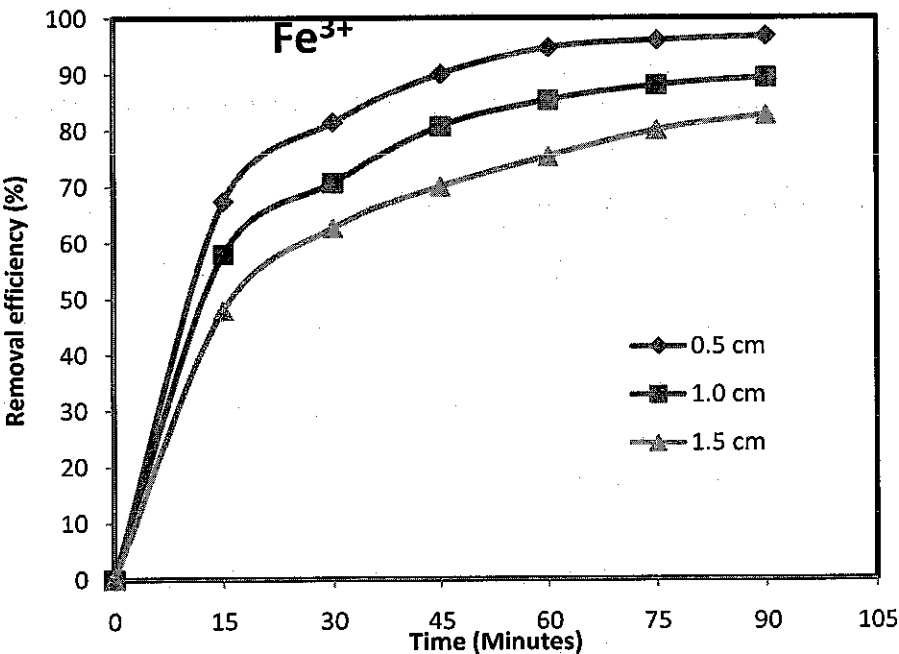


Figure 4.17: Effect of inter-electrode spacing on boron removal from produced water: initial pH 7, Concentration 15 mg/L, Current density 12.5 mA/cm².

Aluminum and iron electrodes were effective in removing boron from both synthetic wastewater and produced water. The optimal parameters were investigated and effects of each parameter discussed. As can be seen from Figure 4.16 and 4.17 above, the removal of boron by both aluminum and iron electrodes were rapid at the initial stage and then followed a slow process afterwards.

4.4 Continuous Mode Study

The use of continuous mode in this study was necessary to investigate the applicability of electrocoagulation in the industry. The optimal parameters obtained from the batch study were kept constant during the continuous mode study; current density 12.5 mA/cm^2 , inter-electrode spacing of 0.5 cm and initial solution pH 7. Retention time was further increased to cater for effect of flow, such as short circuiting on boron removal. The produced water was diluted to vary its concentration according to the experimental plan. The experimental conditions for the continuous mode study are outlined in Table 3.1 The three major parameters of interest are flowrate, Retention time, and concentration.

4.4.1 Effect of Flowrate

The flow of sample into the reactor is an important parameter in treatment processes. It controls the amount of sample which flows into the reactor per minute. The study of the flowrate is important because the amount of metal ions released from the electrodes should be sufficient enough to treat the volume of sample in the reactor at a particular retention time. To investigate the effect of flowrate, three flowrate values were selected in the range of 20 mL/min, 25 mL/min and 30 mL/min. The size of the electrocoagulation reactor was 0.9L. The range of the flowrate was selected based on the size of the reactor. The experimental result for effect of flowrate is tabulated in Table B.1 (Appendix B) for aluminum and iron electrodes.

4.4.1.1 Aluminum electrodes

The removal efficiency of boron using aluminum electrodes as a function of flowrate at the optimum conditions was investigated. Flowrate determines the amount of sample that flows into the electrocoagulation reactor at a specific time. To investigate the effect of flowrate on removal efficiency, three flowrate values was selected in the range of 20-30 mL/min. The current density, pH and inter-electrode spacing were kept constant. The results as depicted in Figure 4.18 show that when the flowrate is

increased, removal efficiency decreased. This implies that removal efficiency favors low flowrate.

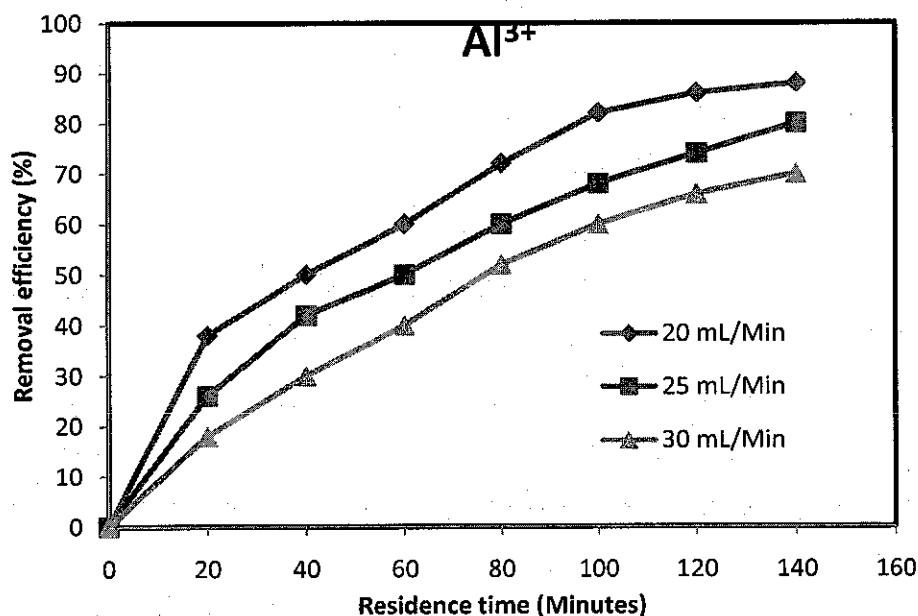


Figure 4.18: Effect of flowrate: initial pH 7, concentration 5 mg/L, inter-electrode spacing 0.5 cm, current density 12.5 mA/cm².

Removal efficiency was observed to reach more than 80% for aluminum electrodes within 20-25 mL/min but decreased to about 70% when the flowrate was increased to 30 mL/min. This phenomenon of decrease in removal efficiency as the flowrate is increased is rather expected since at low flowrate, the sample has higher retention time to react with the released metal ions from the sacrificial anode than at high flowrate. At low flowrate, the influent sample remains in the electrocoagulation reactor for longer time during reaction while at high flowrate, the influent sample does not have enough time to react with the released metal ions before flowing out of the electrocoagulation reactor. At low flowrate, the coagulants generated by the electrochemical oxidation of the sacrificial anode and the boron molecules mix properly which enhances the rate of coagulation. At higher flowrate, the retention time is lowered in the electrochemical reactor which in turn reduces the rate of coagulation. The optimum flowrate was observed at 20 mL/min since the highest removal efficiency was obtained in this condition.

However, it was observed during the experiment that the amount of sludge produced from the electrocoagulation reactor reduced with increasing flowrate. At high flowrate, the volume of sludge formed was small compared to the volume of sludge formed at low flowrate. This observation is quite understandable since at low flowrate, the influent sample is retained in the compartment of the electrocoagulation reactor for a higher retention time and reactions are more prolonged than at high flowrate.

4.4.1.2 Iron electrodes

Increase in flowrate resulted in decrease in removal efficiency. A removal efficiency of about 70%-78% was observed between 25 and 20 mL/min flowrates. This removal efficiency subsequently dropped to 62% when the flowrate was increased to 30 mL/min. Figure 4.19 shows the effect of flowrate in removal efficiency of boron using iron electrode. Therefore, 20 ml/min is the optimum flowrate because it had the highest removal efficiency.

These results can be compared with the result of *Mollah et al.* [148] and *Kobyas et al.* [149] in their respective studies. *Mollah et al.* [148] investigated the treatment of orange II azo-dye by electrocoagulation (EC) technique in a continuous flow cell using sacrificial iron electrodes while *Kobyas et al.* [149] studied the treatment of rinse water from zinc phosphate coating by batch and continuous electrocoagulation processes. Both authors observed that increase in flowrate reduced the removal efficiency of azo dye and zinc-phosphate respectively.

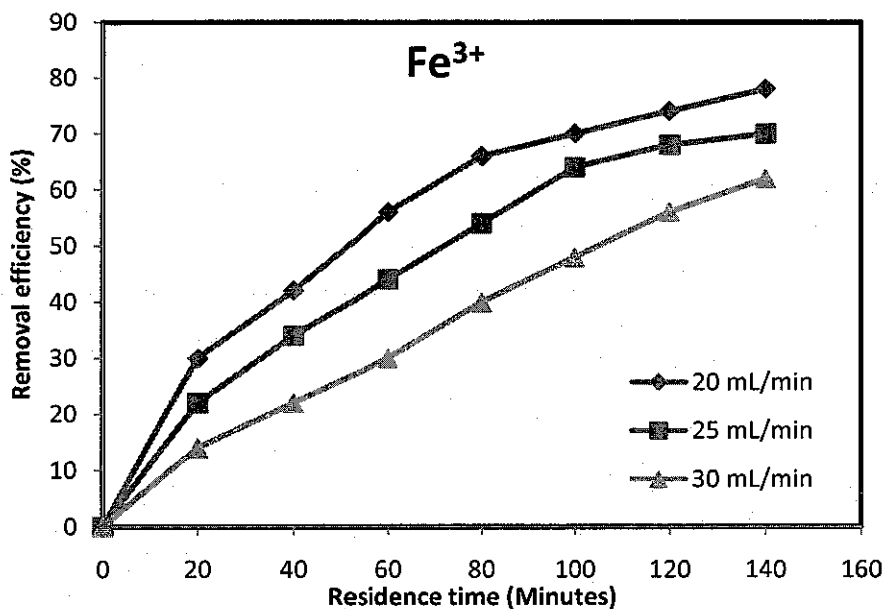


Figure 4.19: Effect of flowrate: initial pH 7, inter-electrode spacing 0.5 cm, current density 12.5 mA/cm², electrode area 60 cm².

4.4.2 Effect of Concentration

The effect of concentration in the continuous mode study was investigated with different boron concentrations of 5, 10 and 15 mg/L respectively. The experimental conditions for concentration are outlined in Table 3.1 and the obtained experimental results tabulated in Table B.2 (Appendix B). The optimal parameters obtained from the synthetic wastewater study were all kept constant.

4.4.2.1 Aluminum electrodes

After several experiments, the obtained results were analyzed and shown in Figure 4.20. The results show that when concentration is increased, removal efficiency decreases. This effect was also observed in the batch study and discussed in section 4.2.3.1.

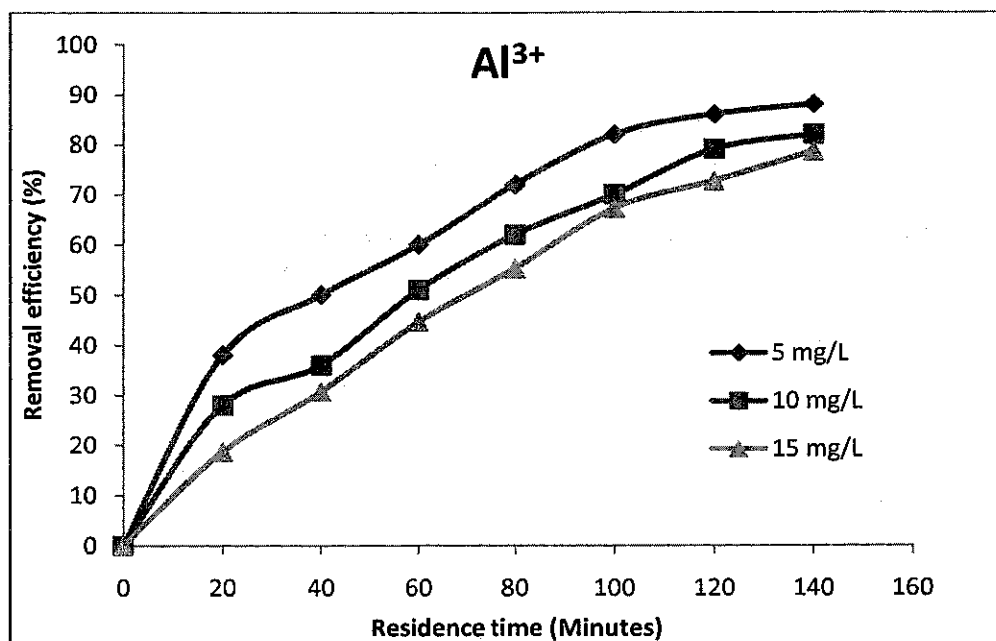


Figure 4.20: Effect of concentration: pH 7, flowrate 20 ml/min, current density 12.5 mA/cm², inter-electrode spacing 0.5 cm.

4.4.2.2 Iron electrodes

Similar results were obtained for iron electrode at the same experimental condition. When concentration is increased, removal efficiency decreases. The removal efficiency of boron after 140 minutes retention time for 5, 10 and 15 mg/L was 78%, 71% and 67.3% respectively at 20 mL/min flowrate. Figure 4.21 shows the effect of concentration on boron removal.

These findings corroborate the findings of *Emamjomeh and Sivakumar* [15] in their study of fluoride removal by a continuous flow electrocoagulation reactor. They observed that increase in fluoride concentration from 5 mg/L to 15 mg/L resulted in increase in residual fluoride concentration at a constant current density. They concluded that increase in concentration reduces the fluoride removal efficiency.

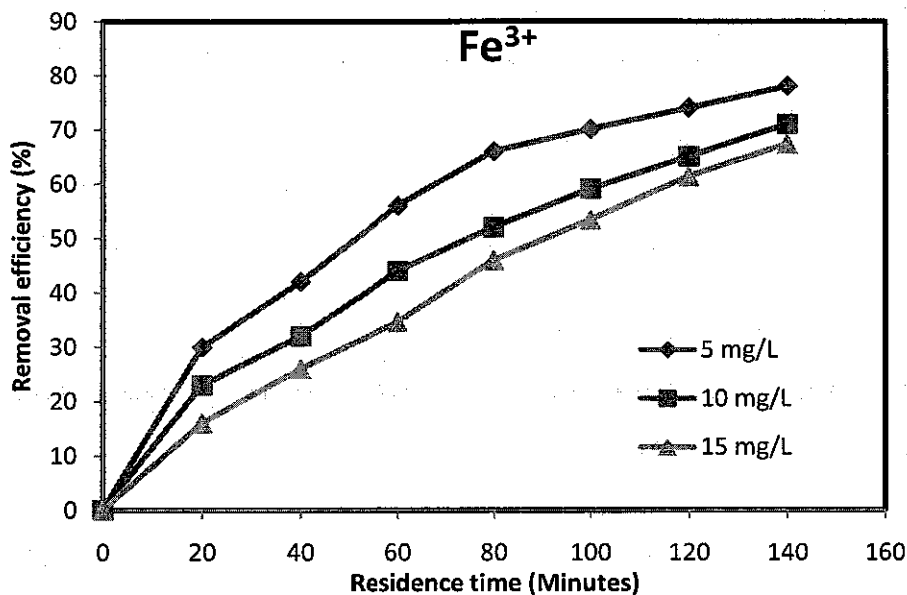


Figure 4.21: Effect of concentration: pH 7, Flowrate 20 ml/min, current density 12.5 mA/cm², inter-electrode spacing 0.5 cm.

4.4.3 Effect of Retention time

Retention time is an important parameter in an electrochemical setup. In electrocoagulation, retention time and current density are conventionally related and work simultaneously. Whereas current density determines the amount of metal ions released from the sacrificial anode, retention time determines the duration at which metal ions are released at a specific current density. This relationship is explained better with the Faraday's law. In other words, when the retention time is increased, the amount of metal ions generated at a specific current density increases. The Effect of retention time is similar to the effects observed during the batch study and discussed in section 4.2.4 for aluminum and iron electrodes.

4.4.4 Residue concentration of electrode materials

Investigation of the residue concentration after the treatment process is important. Although aluminum electrode was efficient throughout the treatment process, its

residue concentration was higher than the initial concentration. A residue concentration of 2.86 mg/L was observed from an initial concentration of 0.65 mg/L. The WHO standard for drinking water quality is set at 0.2 mg/L for aluminum ions [150]. This suggests that aluminum can be used as a pre-treatment process when the objective is to produce quality drinking water. However, the effluent is still useful in irrigation, livestock and other related activities. The standard limit for aluminum in irrigation water is 5 mg/L [151] and the obtained residue concentration is far below the irrigation and discharge limit. The increase in concentration of aluminum during the reaction process may be attributed to rate of oxidation of the sacrificial anode which is related to current.

On the contrary, the residue concentration of iron was 0.12 mg/L which is far below the WHO standard of 0.3 mg/L [82]. This implies that precipitation of iron effectively occurred during the reaction process. The initial concentration of iron in the influent was 1.66 mg/L.

4.5 Adsorption Kinetics

The kinetics of boron adsorption using aluminum and iron electrodes were analyzed respectively using Lagergren Pseudo first order rate equation, Ho pseudo second order rate equation, Weber and Morris intra-particle diffusion model and Elovich model. Aluminum and iron electrode exhibited almost similar behavior for the adsorption of boron. Kinetic parameters for the adsorption of boron onto $\text{Al}(\text{OH})_3$ and $\text{Fe}(\text{OH})_3$ were evaluated by means of its linearity, correlation coefficient (R^2), the calculated q_e and the chi-square (χ^2). The statistical parameters used to compare the goodness fit of the kinetic models are correlation coefficient (R^2), chi-square (χ^2) and equilibrium theoretical adsorption capacity (q_e^{cal}). The best kinetic model should have the highest correlation coefficient (R^2) and the lowest chi-square (χ^2) [152-154]. The equilibrium theoretical adsorption capacity (q_e^{cal}) should also correspond with the equilibrium experimental adsorption capacity (q_e^{cal}).

Three important observations were made during the adsorption process.

a) Adsorption of boron onto $\text{Fe}(\text{OH})_3$ and $\text{Al}(\text{OH})_3$ was rapid at the initial stage

This can be attributed to high boron concentration at the initial stage. At high boron concentration, the contact between the coagulants and boron is faster. The concentration gradient after the initial stage affects the adsorption of boron onto the adsorbents which results in a slow adsorption at later stages.

b) There was increase in uptake rate of boron when concentration was increased

This can be attributed to the rate of mass transfer as a result of high driving force which is related to higher concentration difference. Therefore at high concentration, large volume of the sorbate reacts with the absorbent materials which accounts for the increase in uptake as concentration increases.

c) Removal efficiency decreased when boron concentration was increased

This can be explained that the amount of generated coagulants released at low concentration was not sufficient enough to completely remove boron of higher concentration.

Similar observations was made by *Gupta and Babu*, [155], and *Bansal et al.* [156] in their study of chromium (VI) removal from aqueous solution using waste products and hexavalent chromium removal from aqueous solution by agriculture wastes carbon, respectively.

4.5.1 Lagergren pseudo first order kinetics

Lagergren pseudo first order kinetics was tested with the data obtained from the adsorption study. Lagergren Pseudo First Order Kinetics is shown in equation 2.22. If the data fits into Lagergren pseudo first order kinetics, the plot of $\log (q_e - q_t)$ against

time should be linear. The correlation coefficient should be higher than any other kinetic model and the calculated equilibrium adsorption capacity (q_e^{cal}) should be in agreement with the experimental equilibrium adsorption capacity (q_e^{exp}). The chi square (χ^2) should be the lowest when compared with another kinetic model.

4.5.1.1 Aluminum electrodes

When data was fitted into the Lagergen equation, the plot of $\log (q_e - q_t)$ as shown in Figure 4.22 was near linear with a high correlation coefficient for different concentrations as shown in Table 4.3. The k_1 and the calculated equilibrium adsorption capacity (q_e^{cal}) were obtained from the intercept and slope of plot of $\log (q_e - q_t)$ versus (t) respectively. However, the calculated equilibrium adsorption capacity (q_e^{cal}) deviated from the experimental equilibrium adsorption capacity (q_e^{exp}) and the chi-square (χ^2) was high. This could imply that the adsorption kinetic did not follow the pseudo first order kinetic completely. The experimental data obtained from the adsorption study is tabulated in Table C.1 (Appendix C).

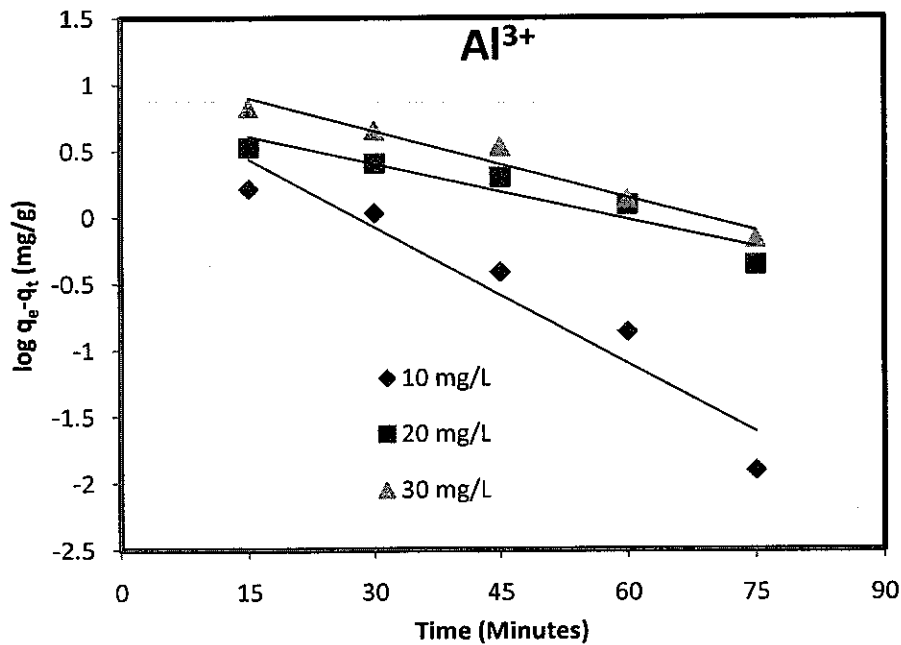


Figure 4.22: First order plot of different concentrations. Conditions: initial pH 7, current density 12.5 mA/cm², inter-electrode spacing 0.5cm, temperature 308K.

Table 4.3: Lagergren pseudo first order adsorption kinetic constants

Aluminum					
C_o (mg/L)	q_e^{exp} (mg/g)	Pseudo-First Order			
		K_1 (min ⁻¹)	q_e^{cal} (mg/g)	R^2	(χ^2)
10	6.09	0.08	4.45	0.92	0.62
20	11.22	0.03	6.56	0.89	3.31
30	16.68	0.04	14.06	0.96	0.49

4.5.1.2 Iron electrodes

The experimental data obtained from the adsorption study using iron electrode was fitted into Lagergren pseudo first order kinetics. The plot of $\log (q_e - q_t)$ against time (t) was more linear than that of aluminum electrode. The calculated equilibrium adsorption capacity (q_e^{cal}) did not correspond with the experimental equilibrium adsorption capacity (q_e^{exp}) as calculated from the slope of plot of $\log (q_e - q_t)$. The k_1 was calculated from the intercept of the plot. The chi-square (χ^2) was also high. This could suggest that the adsorption of boron onto $Fe(OH)_3$ did not follow completely the pseudo first order kinetics despite the linearity of the plot. The plot of $\log (q_e - q_t)$ against time (t) is depicted in Figure 4.23 for different concentrations and the adsorption experimental data is tabulated in Table C.2 (Appendix C). The adsorption constant for Lagergren pseudo first order kinetics using iron electrode is shown in Table 4.4.

Some authors [120-121] have reported that good linearity of the Lagergren pseudo first order kinetics does not imply that the adsorption process is applicable to the kinetic order. However, consideration is given more to the comparison between the experimental equilibrium adsorption capacity (q_e^{exp}) and the calculated equilibrium adsorption capacity (q_e^{cal}), the correlation coefficient (R^2) and the chi-square (χ^2). In addition, the values of the theoretical equilibrium adsorption capacity (q_e^{cal}) should be very close to the experimental equilibrium adsorption capacity (q_e^{exp}). This is because the pseudo first order kinetic is used to evaluate experimental data when the concentration gradient of the external mass transfer is generated as a result of a driving force [157].

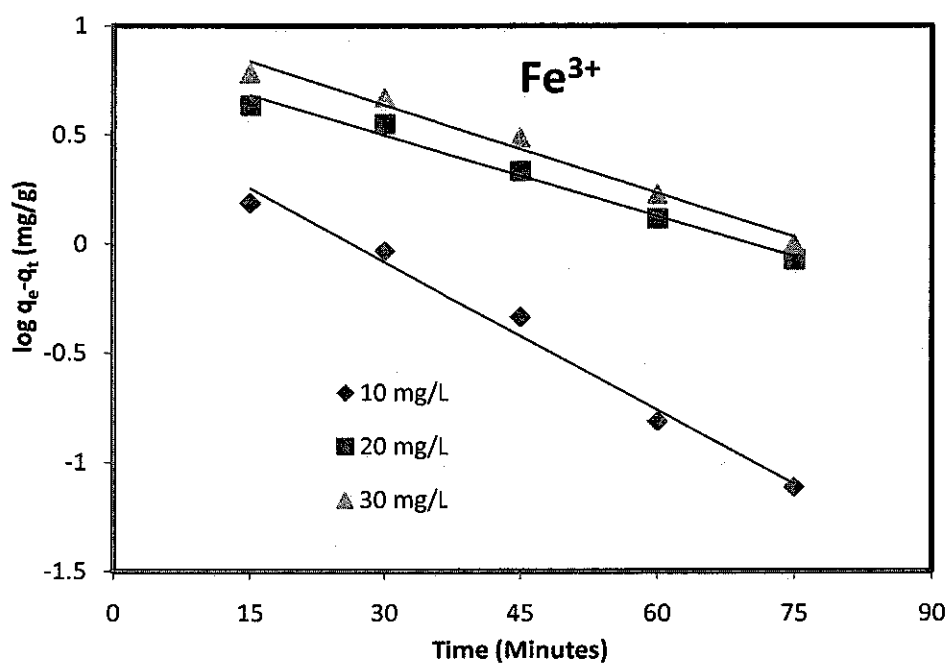


Figure 4.23: First order plot of different concentrations. Conditions initial pH 7, current density 12.5 mA/cm², inter-electrode spacing 0.5cm, temperature 308K.

Table 4.4: Lagergren pseudo first order adsorption kinetic constants

Iron					
C ₀ (mg/L)	q _e ^{exp} (mg.g)	Pseudo-First Order			
		K ₁ (min ⁻¹)	q _e ^{Cal.} (mg/g)	R ²	(χ ²)
10	7.54	0.05	3.89	0.96	3.4
20	13.46	0.03	7.33	0.98	5.13
30	20.30	0.03	10.89	0.98	8.14

4.5.2 Ho Pseudo Second Order Kinetic

The adsorption kinetics was also evaluated with Ho pseudo second order kinetic as shown in equation 2.25. If the experimental data fits into Ho equation, the plot of t/q_t versus time should be linear. The correlation coefficient should be high, the experimental equilibrium adsorption capacity (q_e^{exp}) and the calculated equilibrium

adsorption capacity (q_e^{cal}) should be in agreement while the chi-square (χ^2) should be low. The calculated equilibrium adsorption capacity (q_e^{cal}) and k_2 was calculated from the slope and intercept of the plot of t/q_t versus time.

4.5.2.1 Aluminum electrodes

The experimental data obtained from the adsorption study using aluminum electrodes was fitted into equation 2.25. The plot of t/q_t versus time showed good linearity with high correlation coefficient. In addition, the calculated equilibrium adsorption capacity (q_e^{cal}) and the experimental equilibrium adsorption capacity (q_e^{exp}) were in good agreement and chi square was low. Figure 4.24 depicts the plot of t/q_t versus time for different concentrations.

The adsorption constants for second order kinetics study using aluminum electrodes are shown in Table 4.5 and the experimental data obtained from the adsorption study is shown in Table C.3 (Appendix C). From the obtained graph, the pseudo second order kinetics is in more agreement with the experimental data and describes the kinetic process better.

Table 4.5: Ho pseudo second order adsorption kinetic constants

Aluminum					
C _o (mg/L)	q _e ^{exp} (mg/g)	Pseudo-Second Order			(χ ²)
		K ₂ (g/mg.min)	q _e ^{Cal} (mg.g)	R ²	
10	6.09	0.02	6.80	0.99	0.08
20	11.22	0.08	11.90	0.99	0.04
30	16.68	0.04	17.86	0.99	0.08

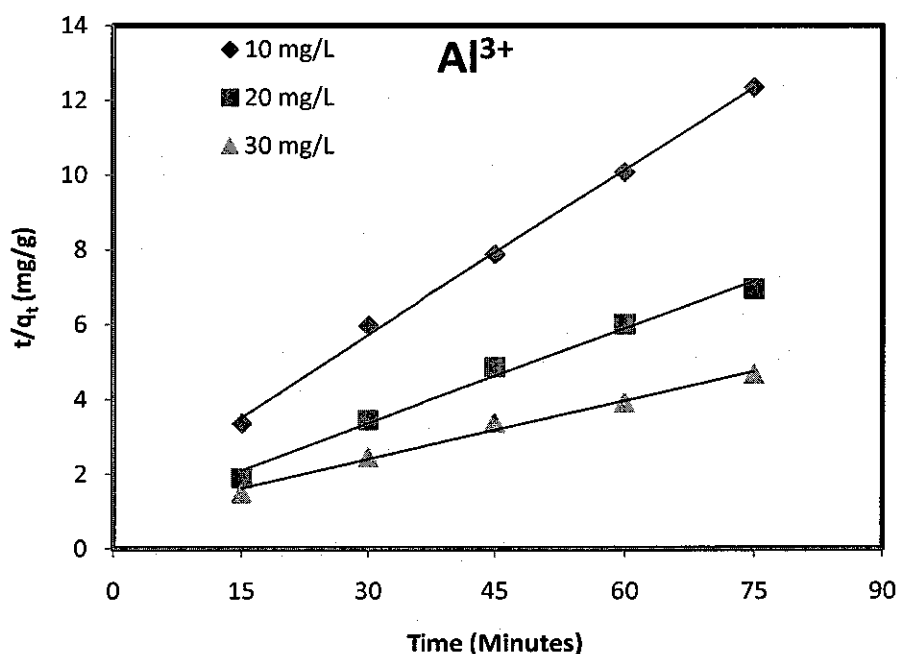


Figure 4.24: Second order plot of different concentrations. Conditions: initial pH 7, current density 12.5 mA/cm², inter-electrode spacing 0.5cm, temperature.

4.5.2.2 Iron electrodes

The adsorption of boron onto Fe(OH)₃ was also evaluated with second order kinetic equation. From the adsorption experiment data, the plot of t/q_t versus time was found to be linear with high correlation coefficient. The equilibrium experimental adsorption capacity (q_e^{exp}) was in agreement with the equilibrium calculated adsorption capacity (q_e^{cal}) in all the concentrations investigated. The chi-square (χ^2) was also very low. Figure 4.25 depicts the plot of t/q_t versus time. The adsorption kinetic constants are shown in Table 4.6 while the adsorption experimental data are tabulated in Table C.4 (Appendix C). From the plot of t/q_t versus time (t), it can be seen that the adsorption kinetics of boron onto Fe(OH)₃ were in better agreement with second order kinetics than with the first order kinetics and describes the kinetic process better.

Table 4.6: Ho pseudo second order adsorption kinetic constants

Iron					
C_0 (mg/L)	q_e^{exp} (mg.g)	Pseudo-Second Order			(χ^2)
		K_2 (g/mg.min)	$q_e^{cal.}$ (mg/g)	R^2	
10	7.54	0.02	8.07	0.99	0.03
20	13.46	0.07	14.29	0.99	0.05
30	20.30	0.05	21.74	0.99	0.09

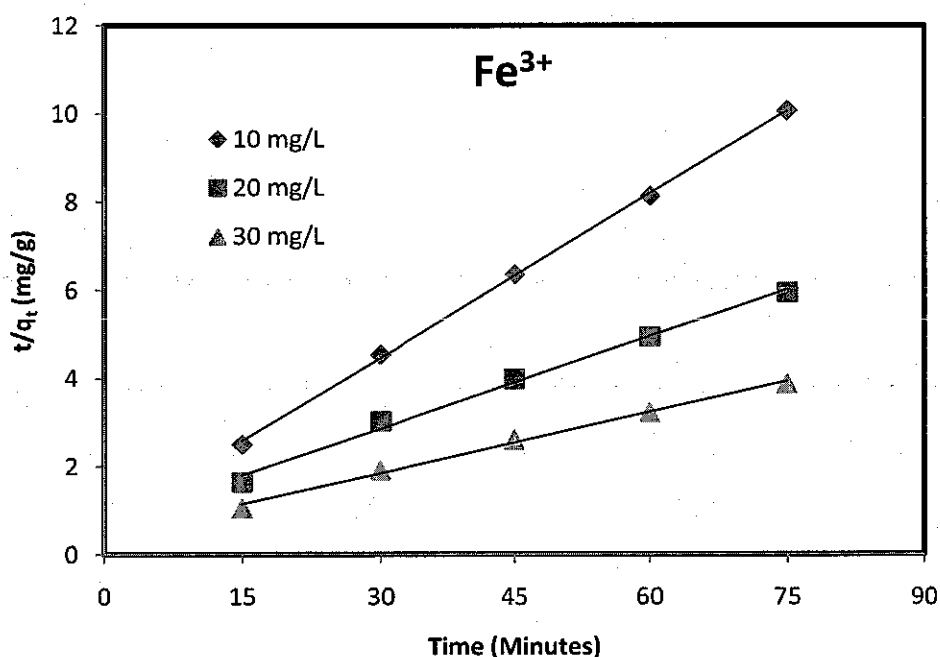


Figure 4.25: Second order plot of different concentrations. Conditions: Initial pH 7, current density 12.5 mA/cm², inter-electrode spacing 0.5cm, temperature 308K.

4.5.3 Intra-particle diffusion

Intra-particle diffusion was further used to evaluate the adsorption kinetics of boron (boric acid) onto both Al(OH)₃ and Fe(OH)₃. Intra-particle diffusion controls the movement of species from the bulk of the solution to the solid phase. The linear form of intra-particle diffusion is shown in equation 2.26. A plot of q_t versus the square root of time ($t^{0.5}$) should be linear with high correlation coefficient if the adsorption

kinetics followed intra-particle diffusion. Despite the linearity of the intra-particle diffusion plot, there are other conditions that the plot of q_t versus $t^{0.5}$ should meet. Intra-particle diffusion becomes the rate-limiting step if the following conditions are met.

- i. High correlation coefficient
- ii. A linear plot passing through the origin of the plot of q_t vs $t^{0.5}$
- iii. The intercept C_i should be less than zero ($C_i < 0$)

An observation which deviates from conditions (ii) and (iii) implies that the mode of transport is influenced by more than one process [158].

4.5.3.1 Aluminum electrodes

The adsorption data obtained with aluminum electrode was fitted into intra-particle diffusion equation. The plot of q_t versus $t^{0.5}$ as depicted in Figure 4.26 shows linearized straight lines in all concentration with high correlation coefficient. However, the C_i which is proportional to the thickness of the boundary layer is greater than zero ($C_i > 0$) and the straight line plots of q_t versus $t^{0.5}$ did not pass through the origin. Therefore it can be concluded that intra-particle diffusion may be involved in the transport process of boron species but the overall transport process is influenced by more than one mechanism. The intra-particle diffusion constants are shown in Table 4.7 while the adsorption experimental data are tabulated in Table C.5 (Appendix C).

Table 4.7: Adsorption rate constants for Intra-Particle Diffusion

Aluminum			
C_0 (mg/L)	Intra-Particle Diffusion		
	K_{id} (mg/g.min ^{0.5})	C_i (mg/g)	R^2
10	0.36	3.13	0.96
20	0.59	4.81	0.98
30	1.28	5.02	0.98

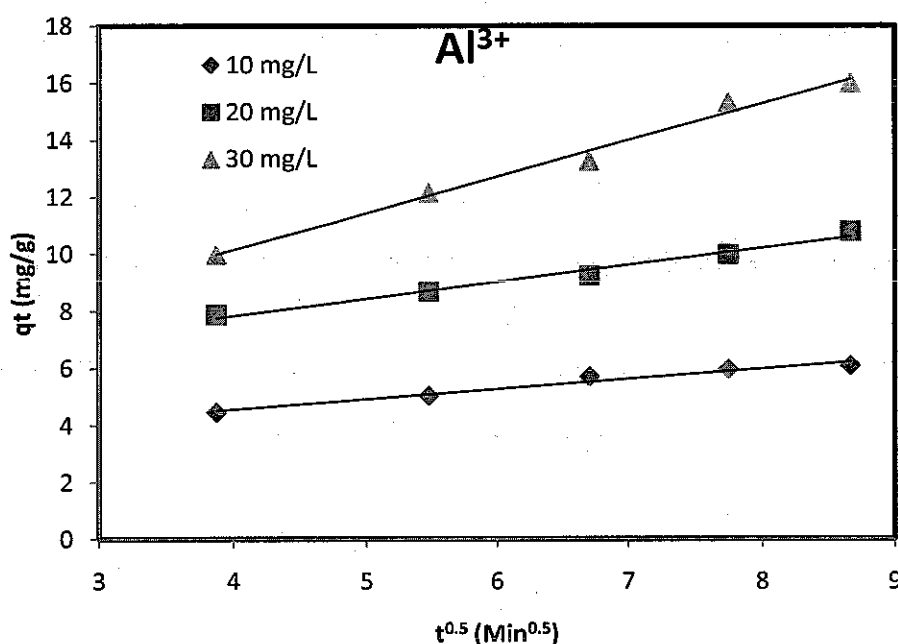


Figure 4.26: Intra particle diffusion plot: initial pH 7, current density 12.5 mA/cm², temperature 308K, inter-electrode spacing 0.5cm, Time 75 minutes.

4.5.3.2 Iron electrodes

The adsorption data fitted into the intra-particle diffusion equation as depicted in Figure 4.27 showed linear straight lines at all concentrations investigated with high correlation coefficient. However, the straight lines of the plot of q_t versus $t^{0.5}$ did not pass through the origin and the C_i is greater than zero ($C_i > 0$). This also suggests that

intra-particle diffusion may not be the only transport mechanism but more than one transport mechanism was involved. The intra-particle diffusion constants are shown in Table 4.8 and the adsorption experimental data are tabulated in Table C.6 (Appendix C).

Table 4.8: Adsorption rate constants for Intra-Particle Diffusion

Iron			
C _o (mg/L)	Intra-Particle Diffusion		
	K _{id} (mg/g.min ^{0.5})	C _i (mg/g)	R ²
10	0.32	4.85	0.97
20	0.77	6.03	0.98
30	1.11	9.81	0.99

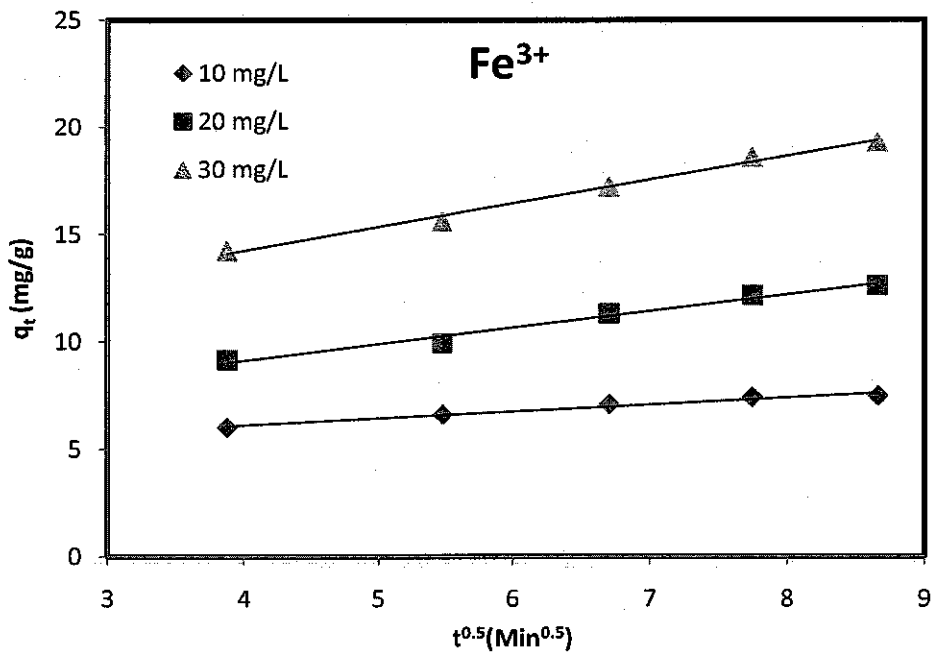


Figure 4.27: Intra-particle diffusion plot: initial pH 7, current density 12.5 mA/cm², temperature 308K, inter-electrode spacing 0.5cm, Time 75 minutes.

The positive values of the rate constant (K_{id}) of the intra-particle diffusion plot of aluminum and iron electrodes suggests that boron may have been predominantly transported onto the solid phase through particle diffusion [159].

4.5.4 Elovich Model

The Elovich model is not used to predict any precise mechanism but it is helpful in explaining predominantly, chemical adsorption on highly heterogenous adsorbents [120]. Elovich model has been reported to exhibit essentially identical behavior with pseudo second order kinetic [122]. However, it gives more information of a chemisorption process from the values of the initial adsorption rate (α) and desorption constant (β). The Elovich model is important for this study since the thermodynamic parameters suggest that boron adsorption onto both $\text{Al}(\text{OH})_3$ and $\text{Fe}(\text{OH})_3$ are through chemisorptive bonds. Initial boron concentration was varied and the adsorption data fitted into equation 2.27. The plot of q_t versus $\ln(t)$ should give a straight line with high correlation coefficient. The adsorption rate (α) and desorption constant (β) are calculated from the slope and intercept of the plot of q_t vs $\ln(t)$.

4.5.4.1 Aluminum electrode

Fitting the data obtained from the adsorption study using aluminum electrodes into the Elovich model equation, a linear straight line plot was obtained with high correlation coefficient as shown in Figure 4.28. It was observed that the adsorption rate constant (α) was increasing and the desorption constant (β) was decreasing as the initial boron concentration was increased from 10-30 mg/L as shown in Table 4.9.

Table 4.9: Adsorption rate constants for Elovich model

Aluminum			
C_o (mg/L)	Elovich Model		
	α (mg/g.min)	β (g/mg)	R^2
10	1.06	1.55	0.98
20	1.72	0.99	0.94
30	3.77	0.49	0.97

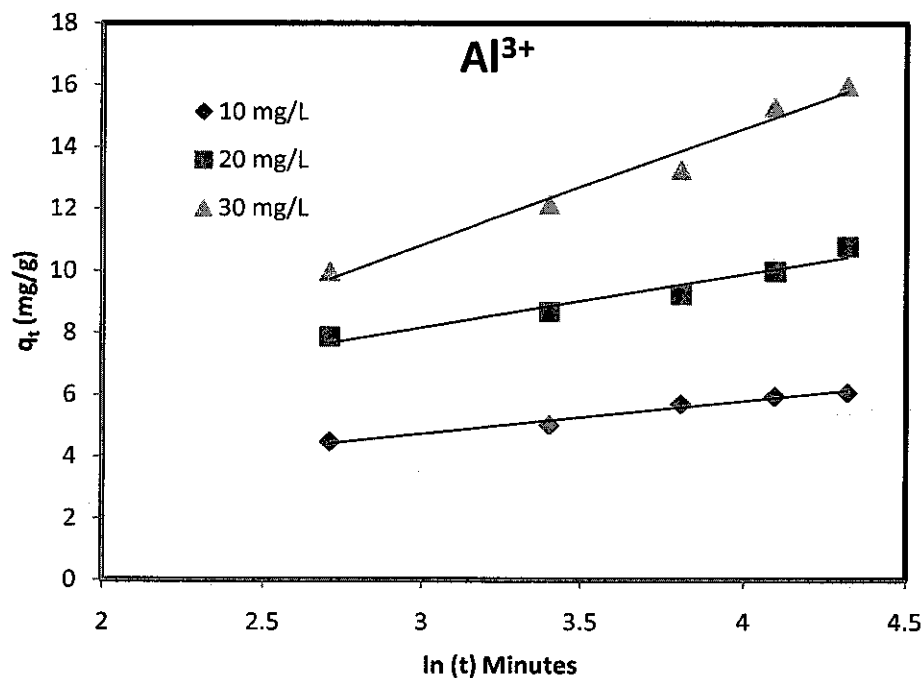


Figure 4.28: Elovich model plot, initial pH 7, current density 12.5 mA/cm², temperature 308K, inter-electrode spacing 0.5cm, Time 75 minutes.

According to *Teng and Hsieh* [160], the constant (α) is related to the rate of chemisorption while (β) is related to the surface coverage. Therefore since (α) represents the initial rate of adsorption, this result suggests that the rate of adsorption of boron onto $\text{Al}(\text{OH})_3$ can be enhanced by increasing the initial boron concentration while the desorption constant reduces. This observed phenomenon is indicative of a chemisorption process. The adsorption experimental data is tabulated in Table C.5 (Appendix C).

4.5.4.2 Iron electrodes

The plot of q_t versus $\ln(t)$ gave linear straight line with high correlation coefficient as shown in Figure 4.29. The adsorption rate constant (α) was increasing and the desorption constant (β) was decreasing as the initial boron concentration was increased from 10-30 mg/L. This observation implies that adsorption of boron onto $\text{Fe}(\text{OH})_3$ may be a chemisorption process. Therefore increasing the boron concentration will enhance the rate of adsorption and reduce the desorption rate. The

adsorption constants for Elovich model are shown in Table 4.10 and the adsorption experimental data tabulated in Table C.6 (Appendix C).

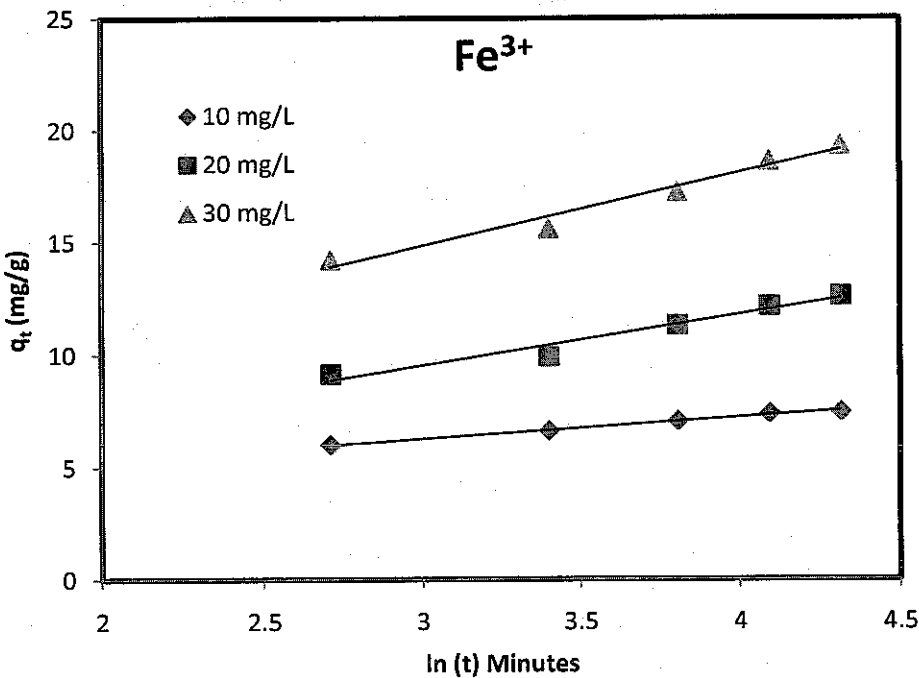


Figure 4.29: Elovich model plot, pH 7, current density 12.5 mA/cm², temperature 308K, inter-electrode spacing 0.5cm, Time 75 minutes.

Table 4.10: Adsorption rate constants for Elovich model (*IRON*)

	Elovich Model		
C_o (mg/L)	α (mg/g·min)	β (g/mg)	R^2
10	0.95	3.42	0.951
20	2.25	2.76	0.955
30	3.25	1.09	0.969

Such observations were also made by *Ho and McKay* [114] in their comparative study of chemisorption kinetic models applied to pollutant removal on various sorbents. In their work, it was reported that the mechanism of sorption of cadmium (II) onto Fe (III) hydroxide may be chemically rate controlling.

4.5.5 Test of Kinetics

The pseudo first order kinetics and pseudo second order kinetics were further evaluated with the test of kinetics using the chi-square (χ^2). As shown in Tables 4.3, 4.4, 4.5 and 4.6, the chi-square (χ^2) for the pseudo second order kinetics was lower than the pseudo first order kinetic. The equilibrium theoretical adsorption capacity (q_e^{cal}) for the pseudo second order kinetics was in agreement with the equilibrium experimental adsorption capacity (q_e^{exp}). The equilibrium theoretical adsorption capacity (q_e^{cal}) for the pseudo first order kinetics deviated from the equilibrium experimental adsorption capacity (q_e^{exp}). This further indicates that the pseudo second order kinetic fits well as the adsorption kinetic model more than pseudo first order kinetic.

The near similar kinetic expression between the pseudo second order and Elovich models for the adsorption of boron (boric acid) onto $Al(OH)_3$ and $Fe(OH)_3$ indicate that the adsorption process is chemical in nature and occurred by internal mechanisms of mass transfer.

In general, the intra-particle diffusion plot of q_t vs $t^{0.5}$ did not pass through the origin and the positive values of the boundary layer imply that the transport of boron did not follow the intra-particle diffusion but rather there were more than one mechanism involved.

In conclusion, the pseudo second order kinetic completely met all the statistical parameters used to evaluate the goodness of fit of the adsorption process. The correlation coefficient for the pseudo second order kinetics was the highest in this study. This implies that the pseudo second order kinetic can account for a higher percentage of the adsorption of boron (boric acid) onto $Al(OH)_3$ and $Fe(OH)_3$ respectively. It is therefore reasonable to conclude that the adsorption kinetics for both $Al(OH)_3$ and $Fe(OH)_3$ followed a the pseudo second order kinetics.

4.6 Adsorption Isotherm

Experimental data for the removal of boron from produced water using aluminum and iron electrode was fitted into Langmuir model and Freundlich model isotherm equations respectively.

4.6.1 Langmuir Isotherm

The goodness of fit for the Langmuir model was evaluated by means of linear regression, adsorption capacity (Q_0) and correction coefficient (R^2).

4.6.1.1 Aluminum electrode

When data was fitted into the Langmuir model, a linear graph was observed. The isotherm constants obtained from the slope and intercept of the plot of C_e/q_e vs C_e showed that the correlation coefficient was high (0.99). The adsorption capacity (Q_0) was also high (15.63) implying that that adsorption of boron onto aluminum electrode was favorable. The binding energy constant ($b = 0.83$) was less than one. It is expected that the binding energy constant should be lower than one. The Langmuir adsorption plot is depicted in Figure while the adsorption isotherm constant is tabulated in Table 4.11. The experimental data for the Langmuir isotherm is tabulated in Table D.1 (Appendix D). The plot of the Langmuir isotherm is depicted in Figure 4. 30.

Table 4.11: Langmuir Isotherm Constants

Aluminum		
Langmuir Isotherm		
Q_0 (mg/g)	b (L/mg)	R^2
15.63	0.83	0.99

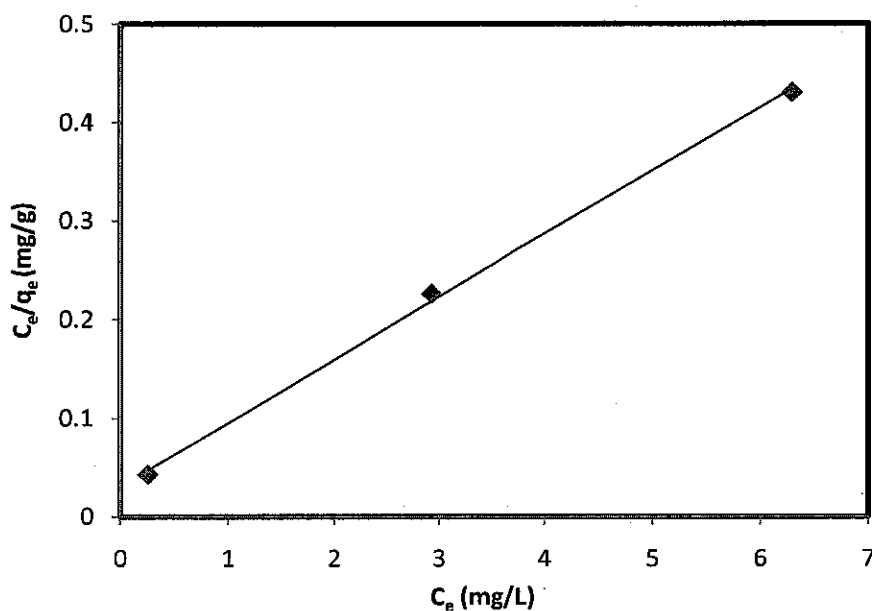


Figure 4.30: Langmuir plot for aluminum electrode: initial pH 7, current density 12.5 mA/cm², Inter-electrode spacing 0.5 cm, Time 75 minutes.

4.6.1.2 Iron electrode

The Langmuir isotherm plot obtained from the data with iron electrode is depicted in Figure 4.31. The Langmuir isotherm constants are tabulated in Table 4.12 while the experimental data is tabulated in Table D.2 (Appendix D). The Langmuir plot for iron electrode has high correlation coefficient (0.96) but lower than aluminum electrode. The Langmuir adsorption capacity (Q_0) was high (24.4) while the binding energy (b) is less than one (0.64). A high correlation coefficient and high adsorption capacity indicates that experimental data fits well into Langmuir isotherm.

Table 4.12: Langmuir Isotherm constants

Langmuir isotherm		
Q_0 (mg/g)	b (L/mg)	R^2
24.4	0.64	0.962

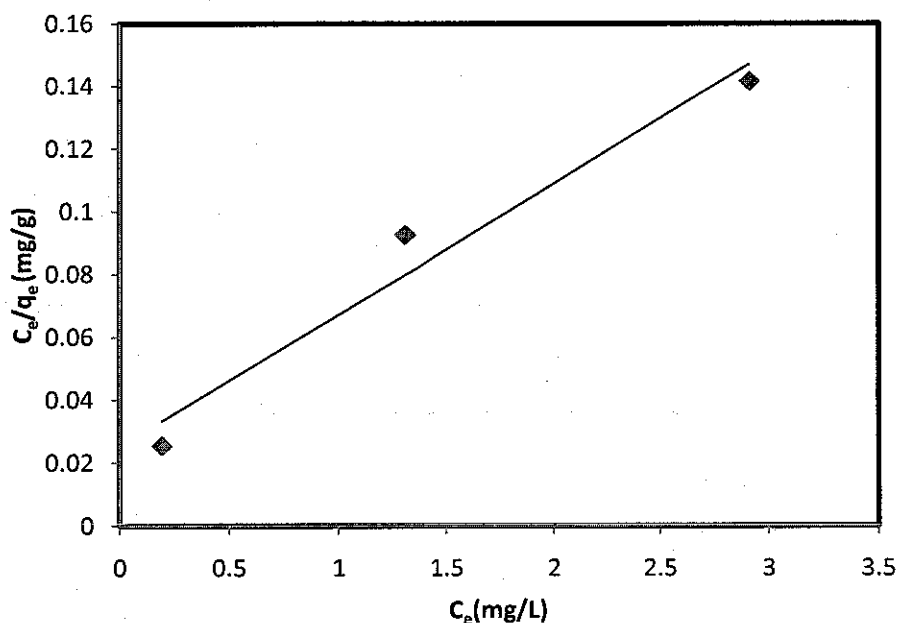


Figure 4.31: Langmuir plot for iron electrode: initial pH 7, current density 12.5 mA/cm², Inter-electrode spacing 0.5 cm, Time 75 minutes.

4.6.2 Freundlich Isotherm

The goodness of fit for the Freundlich model was evaluated by means of linear regression, adsorption capacity (K_F) and correction coefficient (R^2). The magnitude of the exponent (n) gives an indication if adsorption is favorable. Values of (n) between 1-2 represent moderately difficult adsorption, 2-10 represent good adsorption while less than 1 represent poor adsorption characteristics [161].

4.6.2.1 Aluminum electrode

The experimental data from aluminum electrode fitted into Freundlich Isotherm equation is shown in Figure 4.32. The Freundlich isotherm constants are depicted in Table 4.13. The experimental data is tabulated in Table D.1 (Appendix D). A high correlation coefficient of (0.98) was observed indicating good linearity. The adsorption capacity (K_F) was also high (8.9) while the magnitude of exponent (n) value of 3.5 indicates favorable adsorption. However, in comparison with the Langmuir isotherm, the adsorption capacity and the correlation coefficient of the

Langmuir isotherm was higher. This implies that the adsorption isotherm was fairly represented by Freundlich isotherm.

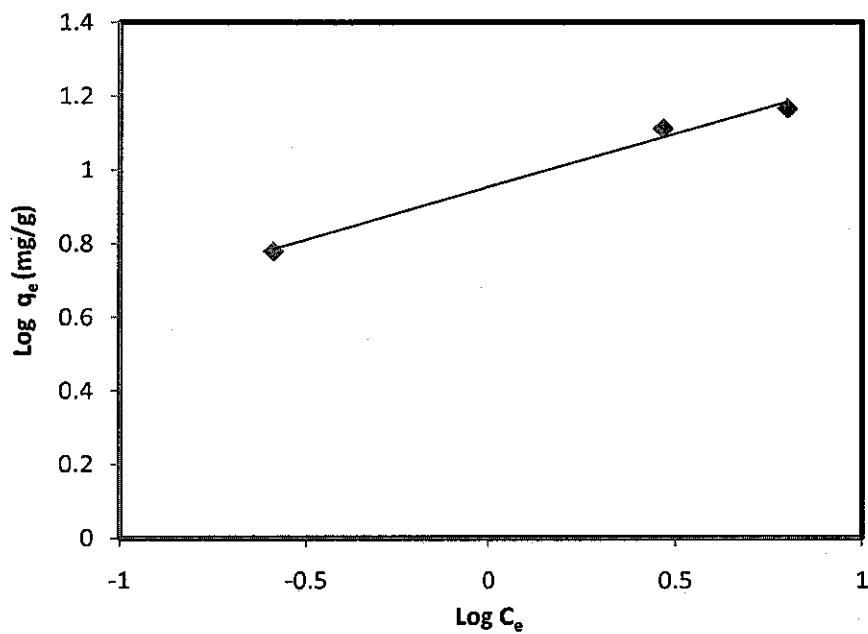


Figure 4.32: Freundlich plot for Aluminum electrode: pH 7, current density 12.5 mA/cm², Inter-electrode spacing 0.5 cm, Time 75 minutes.

Table 4.13: Freundlich Isotherm constants

Freundlich Isotherm		
K _f	n	R ²
8.9	3.5	0.98

4.6.2.2 Iron electrode

The Freundlich plot for iron electrode is depicted in Figure 4.33. The Freundlich isotherm constants are shown in Table 4.14 and the experimental data tabulated in Table D.2 (Appendix D). The correlation coefficient of the Freundlich plot was high (0.96). The adsorption capacity (K_F) was also very high (13.1). The magnitude of exponent (*n*) value of 2.87 indicates favorable adsorption. It can be said that Freundlich isotherm on its own describes the adsorption process. However, when compared with the Langmuir isotherm, the correlation coefficient and the adsorption capacity of the Langmuir isotherm is higher than that of the Freundlich isotherm.

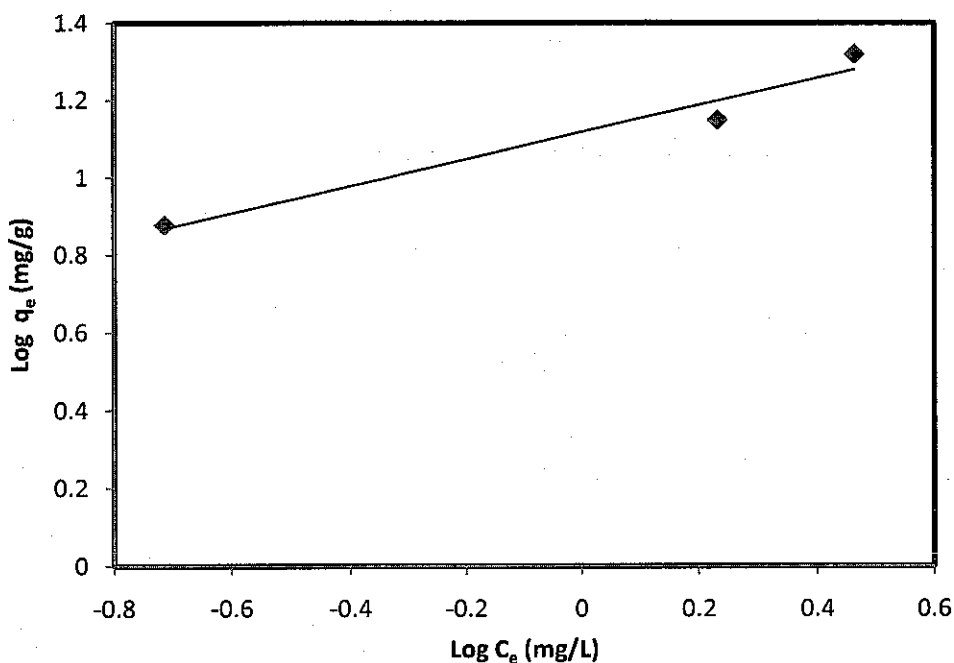


Figure 4.33: Freundlich plot for Iron electrode: pH 7, current density 12.5 mA/cm², Inter-electrode spacing 0.5 cm, Time 75 minutes.

Table 4.14: Freundlich Isotherm constants

Freundlich equation		
K_f	n	R^2
13.1	2.87	0.96

From the obtained results, Langmuir isotherm best described the adsorption process for both aluminum and iron electrode. This was concluded because the correlation coefficient and adsorption capacity of Langmuir isotherm was higher than Freundlich isotherm. Therefore the adsorption isotherm for both electrodes is monolayer coverage and represents a chemisorptions process.

4.7 Thermodynamics

Adsorption thermodynamics was investigated to understand the energy changes during the experiment. The adsorption free energy change (ΔG°), standard enthalpy change (ΔH°) and entropy (ΔS°) of the system were all evaluated by equations 2.28

and 2.29. The enthalpy (ΔH°) and entropy (ΔS°) of the system was calculated from the slope and intercept of Vant Hoff plot of ($\ln K_c$ vs $1/T$ (K)). The temperature range used during the adsorption thermodynamics is shown in Table 3.1.

4.7.1 Aluminum electrodes

After several experiments conducted with aluminum electrodes at various temperatures with initial boron concentration of 20 mg/L, the adsorption thermodynamic constants were obtained. Figure 4.34 shows the linear plot of $\ln K_c$ versus $1/T$. The thermodynamic constants obtained from the plot of $\ln K_c$ against $1/T$ are shown in Table 4.15. As shown in Table 4.15, the free energies were increasingly negative as temperature increases. Negative free energies (ΔG°) indicate that the adsorption process was spontaneous for the temperature range evaluated. The increase in free energies (ΔG°) as temperature increases indicates that high temperatures accelerate the adsorption process [162]. The positive value of the standard enthalpy change (ΔH° 44.8 kJ/mol) implies that the adsorption process is endothermic. Values of enthalpy change less than 40 kJ/mol indicates that the process is physisorption while values above 40 kJ/mol indicate a chemisorption process [163]. A standard enthalpy change value of (ΔH° 44.8 kJ/mol) obtained in this study indicates that the adsorption process is chemisorption. The positive value of entropy change (ΔS° 125.04 J/mol) indicates that there was consistent dispersal of particles during the adsorption process. The thermodynamics adsorption data is tabulated in Table D.3 (Appendix D).

Table 4.15: Thermodynamics Constants for aluminum electrode

Aluminum				
Temp (K)	K_c	ΔG° (kJ/mol)	ΔH° (kJ/mol)	ΔS° (J/mol.K)
298	3.60	-3.18		
308	6.16	-4.66	44.8	125.04
318	8.75	-5.73		
328	12.85	-6.96		

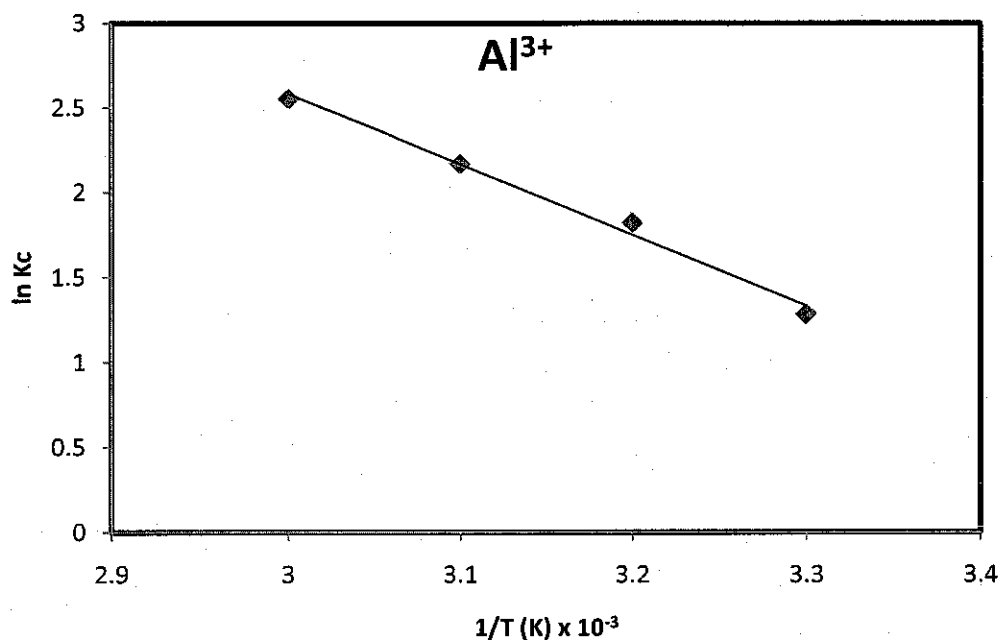


Figure 4.34: Thermodynamic plot of $\ln K_c$ versus $1/T$. initial pH 7, conc. 20 mg/L, current density 12.5 mA/cm², inter-electrode spacing 0.5cm.

4.7.2 Iron electrodes

Adsorption thermodynamics data were fitted into the free energy equation and the linear plot of $\ln K_c$ versus $1/T$ obtained as shown in Figure 4.35. The adsorption thermodynamic constants are shown in Table 4.16 and the adsorption thermodynamics experimental data tabulated in Table D.4 (Appendix D). The enthalpy change (ΔH°) and the entropy of the process (ΔS°) were calculated from the slope and intercept of plot of $\ln K_c$ against $1/T$. From Figure 4.35, the standard enthalpy was positive. A positive standard enthalpy indicates that the process is endothermic [164]. A standard enthalpy value above 40 kJ/mol indicates the adsorption process is chemisorption while enthalpy lower than 40 kJ/mol indicate a physisorption process [163]. A standard enthalpy of 45.8 kJ/mol⁻¹ was obtained from this study and implies the adsorption process was chemisorptions. The positive value of the entropy (ΔS°) (135.5 J/mol) indicates that there was consistent dispersal of particles during the adsorption process. The negative values of the free energy (ΔG°) imply that the adsorption was spontaneous across the temperature range evaluated.

The free energies were observed to increase as temperature increases. It is reported that increase in free energies as temperature is increased implies that temperature facilitates the adsorption process [162].

Table 4.16: Thermodynamics constants for iron electrode

Iron				
Temp (K)	K _c	ΔG° (kJ/mol)	ΔH° (kJ/mol)	ΔS° (J/mol.K)
298	3.27	-2.94		
308	5.37	-4.30	45.8	135.5
318	8.25	-5.58		
328	13.15	-7.02		

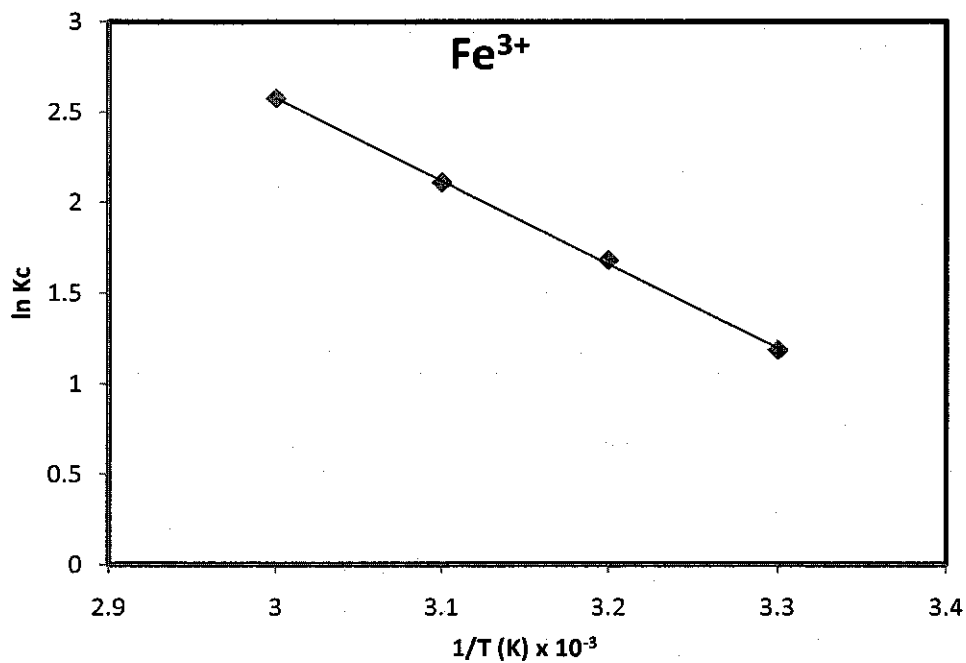


Figure 4.35: Thermodynamics Plot of $\ln K_c$ versus $1/T(K)$. pH 7, conc. 20 mg/L, current density 12.5 mA/cm², inter-electrode spacing 0.5cm.

4.8 Analysis of EC flocs

The electrocoagulation flocs were characterized with X-ray fluorescence (XRF) and analyzed with X-ray diffractogramme (XRD) and Scanning Electron Microscope (SEM) during the recovery of boron as a recyclable precipitate. The chemical composition of the flocs is 2.9% B_2O_3 , 1.3% Al_2O_3 , 1.09% Fe_2O_3 , 14.3% CaO , 19.2% MgO , 28.4% NaO , 6.4% SiO_2 , 2.4% K_2O , 24.01% loss on ignition.

4.8.1 Percent recovery of boron (Aluminum electrode)

After hydrothermal mineralization of electrocoagulation flocs, the results show that about 1.1 mg/L boron remained in the solvent after 2 hours of treatment time. This implies that about 91.4 % of boron was recovered from the electrocoagulation flocs. The precipitates were further sent for XRD and SEM analysis to detect the form in which boron was recovered.

4.8.1.1 XRD and SEM results for aluminum electrodes

The XRD result of EC floc before hydrothermal treatment is shown in Figure 4.36. The XRD result of EC flocs before hydrothermal mineralization showed a bragg reflections possessing broad humps and low intensity which indicates that the analyzed phase is more amorphous and little crystalline. The chemical speciation of this amorphous phase can be aluminum hydroxide or aluminum oxyhydroxide. This is suspected because crystallization of Al hydroxides or oxyhydroxides is a very slow process. It is reported that most Al hydroxides and Al oxyhydroxides are found to be either poorly crystalline or amorphous [165]. The peak at $2\theta^\circ$ 45 represent Aluminum borate $(Al_2O_3)_2 \cdot B_2O_3$ which is the common boron complex from the XRD results in Figure 4.36.

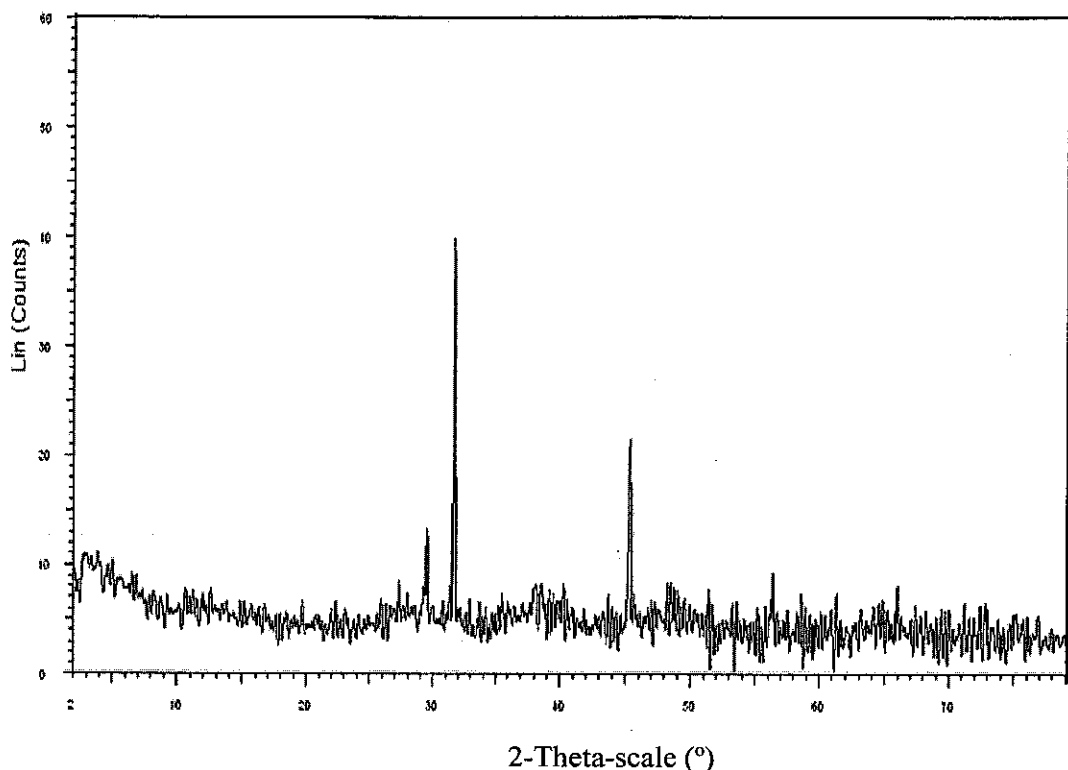


Figure 4.36: XRD pattern of EC floc before hydrothermal mineralization

After hydrothermal mineralization, the obtained precipitates were analyzed with scanning electron microscope (SEM) and XRD. The SEM result as presented in Figure 4.37 shows a fibrous root like structure.

XRD was used to investigate this fibrous root like structure on an irregular beam shape basement. The XRD result is shown in Figure 4.38. The X-ray diffraction result showed broad and diffuse diffraction peaks indicating that the analyzed phase possesses a short-range order i.e amorphous and poorly crystalline in nature. Using Eva Diffra^{Plus} indexing software in combination with ICDD (International Center for Diffraction Data) database, Nifontovite ($\text{Ca}_3\text{B}_6\text{O}_6(\text{OH})_{12} \cdot 2(\text{H}_2\text{O})$), Inyoite ($\text{CaB}_3\text{O}_3(\text{OH})_5 \cdot 4\text{H}_2\text{O}$) and Takedaite ($\text{Ca}_3\text{B}_2\text{O}_6 \cdot 2\text{H}_2\text{O}$) were recognized as the fibrous root like structure from the XRD result.

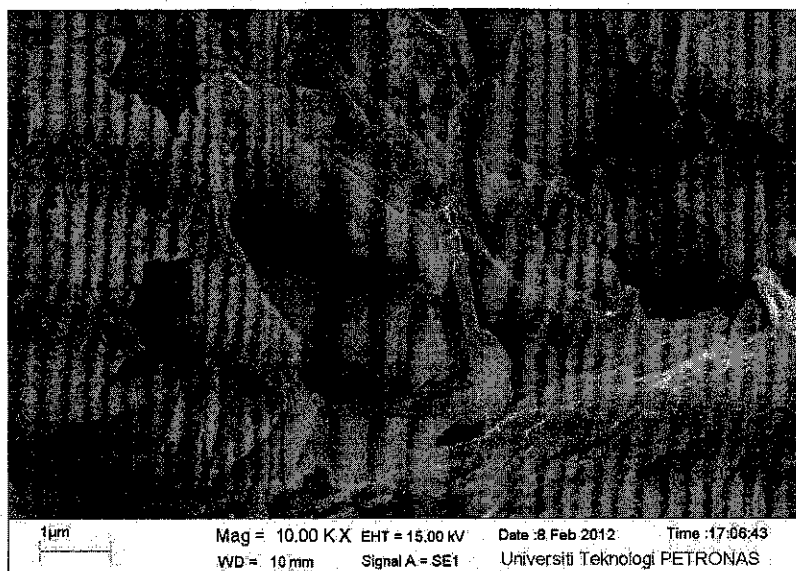


Figure 4.37: SEM result for EC floc after hydrothermal mineralization at 120°C, 2 hours, 0.3g Ca(OH)₂, 2g EC floc, pH 10.

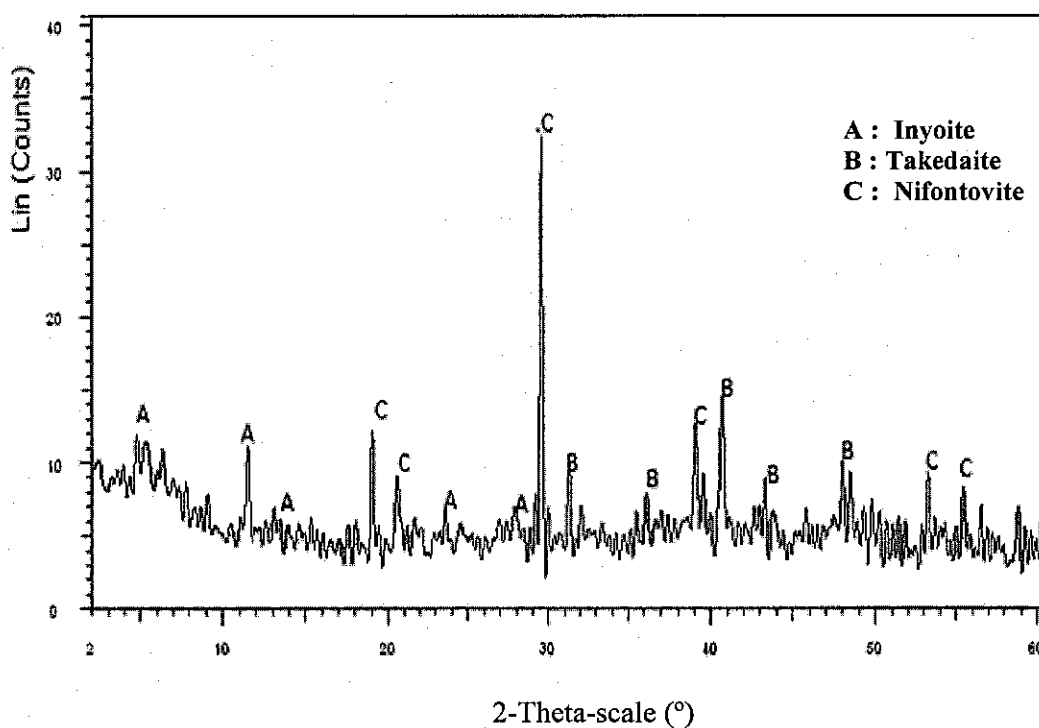


Figure 4.38: XRD pattern after hydrothermal mineralization at 120°C, 2 hours, 0.3g Ca(OH)₂ 2g EC floc, pH 10.

The three identified compounds are rare hydrated calcium borate minerals. The XRD peaks were shallow and tiny. From the XRD, it can be concluded that Nifontovite

could be the fibrous root like structure identified from the SEM result while Inyoite and Takadaite could be the irregular beam shape basement shown in Figure 4.37. The amorphous and poor crystalline nature of aluminum floc has been reported in literature. It is reported that aluminum produces poor crystalline precipitates in the presence of natural organic matter [166]. This could be the reason why the XRD result is more amorphous since produced water contains high concentration of organic compounds.

4.8.2 Percent recovery of boron (Iron electrode)

From the obtained result, about 1.6 mg/L of boron was left in the solvent after 2 hours treatment time. This also implies that about 87% of boron was recovered from the electrocoagulation floc. The precipitates were further sent for XRD and SEM analysis to investigate the recovered boron compounds.

4.8.2.1 XRD and SEM results for Iron electrodes

The EC floc was analyzed with XRD before hydrothermal treatment and the result is presented in Figure 4.39. The XRD result showed bragg reflections possessing very broad humps and low intensity indicating that the analyzed phase is more amorphous and poor crystalline in nature. The poor crystalline phase of iron floc may be due to the presence of iron oxyhydroxides [167]. Iron borate (FeBO_3) was observed as the common boron compounds in the XRD result at 2θ 32.

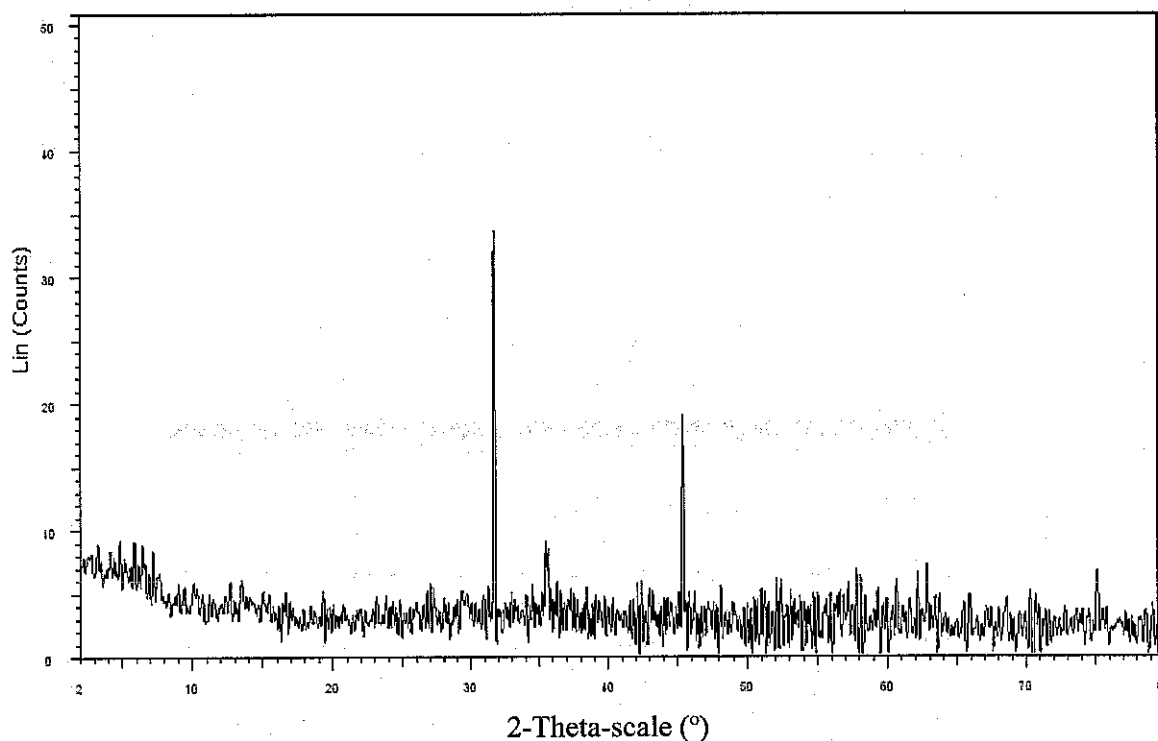


Figure 4.39: XRD pattern of EC floc before hydrothermal mineralization

After hydrothermal mineralization, the obtained precipitates were analyzed with scanning electron microscope (SEM) and XRD. The SEM result as depicted in Figure 4.40 shows a wood stick object on a plate-like structure.

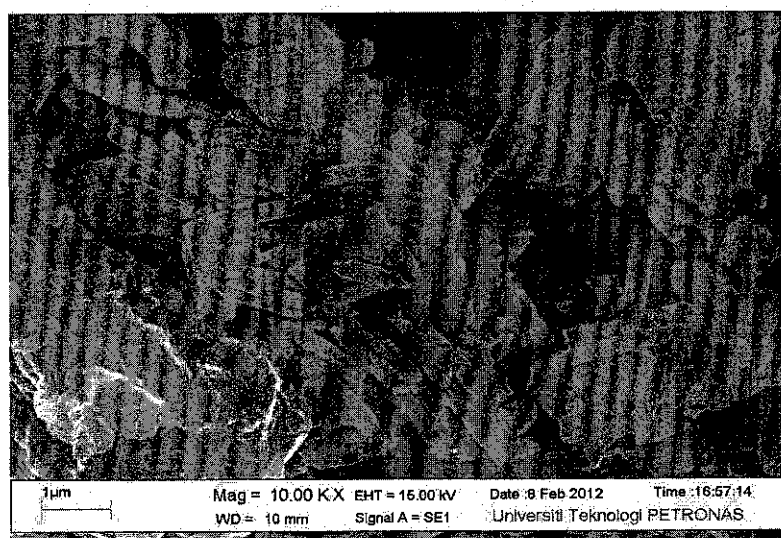


Figure 4.40: SEM result for EC floc after hydrothermal mineralization at 120°C, 2 hours, 0.3g (CaOH), 2g EC floc, pH 10.

Further investigation was done with XRD to discern the wood stick object on a plate like structure. The XRD pattern is shown in Figure 4.41. The XRD result

showed bragg reflections possessing very broad humps and low intensity indicating that the analyzed phase is more amorphous and poorly crystalline in nature. This indicates that the analyzed phase was a short-range order. Using Eva Diffra^{Plus} indexing software in combination with ICDD (International Center for Diffraction Data) database, the presence of Parasirbiskite ($\text{Ca}_2\text{B}_2\text{O}_5 \cdot \text{H}_2\text{O}$), Inyoite ($\text{CaB}_3\text{O}_3(\text{OH})_5 \cdot 4\text{H}_2\text{O}$) and Vimsite ($\text{CaB}_2\text{O}_2(\text{OH})_4$) was identified as the wood stick object on the plate like structure.

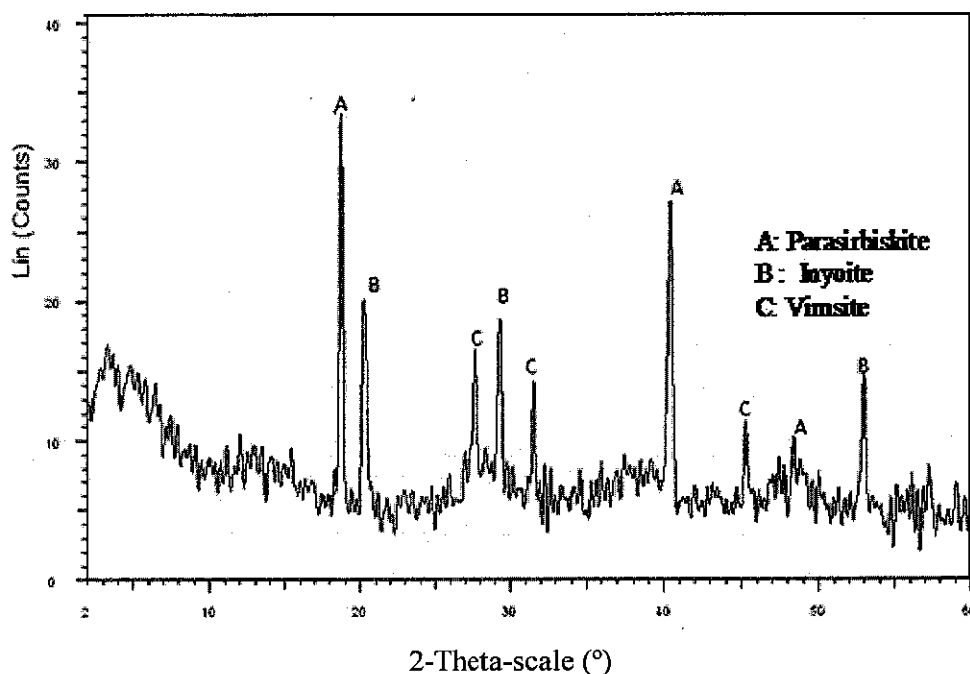


Figure 4.41: XRD pattern after hydrothermal mineralization at 120°C, 2 hours, 0.3g $\text{Ca}(\text{OH})_2$, 2g EC floc, pH 10.

The three identified compounds are rare hydrated calcium borate minerals. From the XRD result, it can be concluded that the wood-stick objects observed from Figure 4.38 could be parasirbiskite while the plate like structure may be inyoite and vimsite.

4.8.3 Produced water as a potential source of hydrated borate minerals

Parasibirskite [168], Inyoite [169], Takedaite [170], Nifontovite [171] and Vimsite are all hydrated borate minerals that have been found at many borate deposits. At Fuka, Okayama Prefecture, Japan, these hydrated borate minerals have been found in large amounts. These hydrated borate minerals occur as monoclinic borate compound

usually found in a vein between gehlenite-spurrite skarns and crystalline limestone. It has been suggested that the abundant formation of these borate minerals occur as a result of alteration of borate minerals [168]. For instance, at Fuka, Okayama Prefecture, Japan, Parasibirskite is a polymorph of Sibirskite. The chemical composition of all the calcium borate reveals the presence of Ca, B and O. More than ten different hydrated borate minerals have been found in Fuka, Okayama Prefecture, Japan. However, Kusachi et al. [170] reported that these hydrated borate minerals are associated with each other. A typical example is the association of Takedaite with Nifontovite, Olshanskyite, Pentahydroborite, Frovolite, Sibirskite, and Calcite [170]. Unlike most hydrated borate compounds, Inyoite is not an alteration product of any borate compound. This is supported by the fact that Inyoite has a unique crystal habit different from other borate compounds and occurs near the surface of borate playas lying below the ulexite bearing bed near one edge of the playa [172]. Inyoite is a transparent borate compound with vitreous luster in hand specimen and colorless in thin section with a structure consisting of two $\text{BO}_2(\text{OH})_2$ tetrahedrons and a BO_2OH triangle linked by calcium and hydroxyl- hydrogen bonds [173].

The occurrence of these borate minerals in produced water is nonetheless, not a surprise because produced water has been in contact with the underground formations for a long period of time. However, it is important to note that the occurrence of these hydrated borate minerals in produced water is independent of electrode material. This is further supported by the appearance of Inyoite in both aluminum and iron electrode flocs. This, however may depend on the crystal formation of the hydrated borate minerals and the linkage between the Ca, B and O complex [174]. The hydrated borate minerals are important raw minerals for borax production. From the results of this study, produced water could be a potential source of hydrated borate minerals.

In a synthetic study conducted by Itakura et al. [110], single crystals of Parasibirskite ($\text{Ca}_2\text{B}_2\text{O}_5 \cdot \text{H}_2\text{O}$) was synthesized from $\text{Ca}(\text{OH})_2$ and Boron oxide (B_2O_3) between 100 and 200 °C. Therefore it can be concluded that the hydrated borate minerals obtained from the hydrothermal mineralization of EC flocs in this study are natural analogue of the synthetic borate minerals.

4.9 Analysis of other parameters

Few other parameters characterized in the produced water were analyzed at the end of the experiment. The parameters include total suspended solids (TSS), Calcium, Magnesium, iron, aluminum and Phenol. The removal efficiencies of these parameters are tabulated in table 4.17 and table 4.18 for aluminum and iron electrode respectively.

Table 4.17: Other parameters analyzed from sample treated with Aluminum electrode

Parameter	Initial conc. (mg/L)	Percent removal (%)	Optimum pH
TSS	136	91.5	7
Calcium	357	79	10
Magnesium	600	95.8	10
phenol	15	94	7

Table 4.18: Other parameters analyzed from sample treated with Iron electrode

Parameter	Initial conc. (mg/L)	Percent removal (%)	Optimal pH
TSS	136	93	8
Calcium	357	83.2	10
Magnesium	600	98.8	10
phenol	15	90	7

CHAPTER 5

CONCLUSIONS AND RECOMMENDATIONS

5.1 Conclusions

In this study, the feasibility of using electrochemical process to remove boron from produced water was investigated. The percentage of boron removal, operating parameters, mode of operation, environmental consequences and recovery of boron as a recyclable precipitate were all considered. Electrochemical process proved to be an efficient way of removing boron from produced water. A summary of the findings obtained from this study is outlined below.

At the end of this study, a removal efficiency of 98% was observed for aluminum electrode. In the case of iron electrode, a removal efficiency of 96.7% was observed. Within 75 minutes, electrocoagulation is able to reduce boron from 15 mg/L to below the World Health Organization guidelines of 0.5 mg/L. for boron in potable drinking water. Aluminum electrode was more efficient in terms of removal efficiency throughout the study. However, residual concentration of aluminum ions (2.89 mg/L) was higher than the residual concentration of iron ion (0.12 mg/L). The overall performance of both aluminum and iron electrode indicate they are effective in boron removal and this meets the first objective of this study.

Different operating parameters were investigated in this study for aluminum and iron electrode respectively. The effects of these parameters were almost near similar for both electrodes except for slight difference in final solution pH. Using iron electrode, the final solution pH for produced water was higher than the initial solution pH. This observation was made in both the acidic and alkaline pH values. Using aluminum electrode, the final solution pH was higher than the initial solution pH at

acidic condition. At alkaline condition, the final solution pH was lower than the initial solution pH. Removal efficiency increased when initial solution pH was increased from pH 3-7 and remained constant at pH 8 using aluminum electrode. For sample treated with iron electrode, removal efficiency increased from initial solution pH 3-8. Above initial solution pH 8, removal efficiency decreased for both electrodes. The removal efficiency of boron was highest between pH 6-8 for aluminum and iron electrodes respectively. Initial solution pH 7 was the optimal pH. Increase in current density resulted in increase in removal efficiency for both electrodes. When boron concentration was increased, removal efficiency decreased. Increase in inter-electrode spacing decreased removal efficiency. These observations meet the second objective of this study.

Removal efficiency was investigated with a continuous flow process. The results show that electrocoagulation can be applied as a continuous flow process in wastewater treatment. The removal efficiency of boron in the continuous mode study was 88% and 78% for aluminum and iron electrodes respectively. Few parameters were investigated in the continuous flow study. Increase in flowrate reduced removal efficiency for both aluminum and iron electrodes. Increase in boron concentration favored a decrease in removal efficiency. From these observations, applicability of electrocoagulation in a continuous flow process is feasible and meets the third objective of this study.

Four kinetic models and two adsorption isotherm models were evaluated to understand the adsorption kinetics and isotherm of boron onto $\text{Al}(\text{OH})_3$ and $\text{Fe}(\text{OH})_3$. The four kinetic models are Pseudo first order kinetics, Pseudo second order kinetics, Intra-particle diffusion and Elovich model. The two adsorption isotherm models are Langmuir isotherm and Freundlich isotherm. The calculated equilibrium adsorption capacity (q_e^{cal}) for boron adsorption onto $\text{Al}(\text{OH})_3$ and $\text{Fe}(\text{OH})_3$ were not in agreement with the experimental equilibrium adsorption capacity (q_e^{exp}) for all the concentrations investigated for the pseudo first order kinetics. The chi-square (χ^2) for both electrodes was also high. The Pseudo second order kinetic was in better agreement with the experimental data. The calculated equilibrium adsorption capacity (q_e^{cal}) for $\text{Al}(\text{OH})_3$ and $\text{Fe}(\text{OH})_3$ were in agreement with the experimental equilibrium adsorption

capacity (q_e^{exp}) for all the concentration investigated. The correlation coefficient (R^2) was higher than all models investigated and the chi square (χ^2) was lower than the pseudo first order kinetic model. Intra-particle diffusion was not the only transport mechanism involved during the study for both electrodes. This was revealed since the intra-particle diffusion plot did not pass through the origin for both electrodes and the C_i was greater than zero. Elovich model showed that the adsorption of boron onto $\text{Al}(\text{OH})_3$ and $\text{Fe}(\text{OH})_3$ was a chemisorption process. The rate of adsorption increased and the desorption rate decreased when concentration was increased. However, the correlation coefficient of Elovich model was lower than that of Pseudo second order kinetics. In general, boron adsorption onto $\text{Al}(\text{OH})_3$ and $\text{Fe}(\text{OH})_3$ was observed to follow the pseudo second order adsorption kinetics. The adsorption isotherm study showed that the adsorption of boron onto $\text{Al}(\text{OH})_3$ and $\text{Fe}(\text{OH})_3$ is a monolayer coverage and was best fitted by the Langmuir isotherm. The correlation coefficient (R^2) for Langmuir isotherm was higher than the Freundlich isotherm. In addition, the adsorption capacity for Langmuir isotherm was also higher than the Freundlich isotherm. By this observation, Langmuir isotherm best describes the adsorption of boron for both electrodes. The thermodynamic investigations showed that the adsorption of boron onto $\text{Al}(\text{OH})_3$ and $\text{Fe}(\text{OH})_3$ was a chemisorption process. The negative values of the free energies for both electrodes indicate that the adsorption of boron was spontaneous. The positive values of the enthalpy for both electrodes indicate that the reaction is endothermic. The positive values of the entropy for both electrodes also indicate that there was good molecular interaction during the reaction. These observations meet the fourth objective of this study.

Rare hydrated calcium borate minerals were observed during the boron recovery studies using hydrothermal mineralization from the EC floc. Parasibirskite, Inyoite, Vimsite, Nifontovite and Takadaite were all present as hydrated borate minerals after the hydrothermal mineralization study with the EC floc. The presence of these hydrated borate minerals in EC floc may be attributed to the composition of produced water as well as the association of produced water with underground formations. These hydrated borate minerals associate with one another. The observation of Inyoite in both aluminum and iron EC flocs indicates that the occurrence of these hydrated borate minerals is independent of electrode material but may depend on the

composition of the sample and the crystal formation. These hydrated borate minerals can be used as starting raw material in borax production. Another advantage of this process is that it reduces the environmental and or health hazards associated with the discharge of boron into the environment. These observations meet the final objective of this study.

5.2 Recommendations for future work

At the end of this study, it was pertinent to indicate few areas that needed further investigations. The recommendations are

- a) Expansion of the continuous flow reactor in a pilot scale
- b) Investigations into the selective recovery of individual boron compounds from EC flocs.
- c) Investigation into the use of bipolar electrode

REFERENCES

- [1] D. W. Woodall, R. P. Gambrell, N. N. Rabalais, and R. D. DeLaune, "Developing a method to track oil and gas produced water discharges in estuarine systems using salinity as a conservative tracer," *Marine pollution bulletin*, vol. 42, pp. 1118-1127, 2001.
- [2] M. Lu, Z. Zhang, W. Yu, and W. Zhu, "Biological treatment of oilfield-produced water: A field pilot study," *International Biodeterioration & Biodegradation*, vol. 63, pp. 316-321, 2009.
- [3] A. Fakhru'l-Razi, A. Pendashteh, L. C. Abdullah, D. R. A. Biak, S. S. Madaeni, and Z. Z. Abidin, "Review of technologies for oil and gas produced water treatment," *Journal of hazardous materials*, vol. 170, pp. 530-551, 2009.
- [4] J. A. Veil, M. G. Puder, D. Elcock, and R. J. Redweik Jr, "A white paper describing produced water from production of crude oil, natural gas, and coal bed methane," *prepared by Argonne National Laboratory for the US Department of Energy, National Energy Technology Laboratory, January. Available at http://www.ead.anl.gov/pub/dsp_detail.cfm*, 2004.
- [5] E. H. Ezechi, M. H. Isa, and S. R. B. M. Kutty, "Boron in Produced Water: Challenges and Improvements: A Comprehensive Review," *Journal of Applied Sciences*, vol. 12, pp. 402-415, 2012.
- [6] A. Glickman, "Produced Water Toxicity: Steps You Can Take to Ensure Permit Compliance," presented at the API Produced Water Management Technical Forum and Exhibition, Lafayette, LA, Nov. 17-18, 1998.
- [7] J. Cline, "Treatment and discharge of produced water for deep offshore disposal," presented at the API Produced Water Management Technical Forum and Exhibition, Lafayette, La, Nov. 17-18, 1998.
- [8] S. Wemede, N. Akani, and C. Eke, "Fungi in an oilfield wastewater in Nigeria," *Asian Journal of Biological Sciences*, vol. 2, pp. 54-57, 2009.
- [9] Y. Puyate and A. Rim-Rukeh, "2D Model for Diffusion of Oxygen with Biochemical Reaction During Biofilm Formation Process in Static Aqueous Medium," *Journal of Applied Sciences*, vol. 8, pp. 1560-1565, 2008.
- [10] P. Dydo, M. Turek, J. Ciba, J. Trojanowska, and J. Kluczka, "Boron removal from landfill leachate by means of nanofiltration and reverse osmosis," *Desalination*, vol. 185, pp. 131-137, 2005.

- [11] M. Bryjak, J. Wolska, and N. Kabay, "Removal of boron from seawater by adsorption-membrane hybrid process: implementation and challenges," *Desalination*, vol. 223, pp. 57-62, 2008.
- [12] H. Liu, X. Ye, Q. Li, T. Kim, B. Qing, M. Guo, *et al.*, "Boron adsorption using a new boron-selective hybrid gel and the commercial resin D564," *Colloids and Surfaces A: Physicochemical and Engineering Aspects*, vol. 341, pp. 118-126, 2009.
- [13] Y. Seki, S. Seyhan, and M. Yurdakoc, "Removal of boron from aqueous solution by adsorption on Al₂O₃ based materials using full factorial design," *Journal of Hazardous Materials*, vol. 138, pp. 60-66, 2006.
- [14] S. Seyhan, Y. Seki, M. Yurdakoc, and M. Merdivan, "Application of iron-rich natural clays in Çamlica, Turkey for boron sorption from water and its determination by fluorimetric-azomethine-H method," *Journal of Hazardous Materials*, vol. 146, pp. 180-185, 2007.
- [15] M. M. Emamjomeh and M. Sivakumar, "Review of pollutants removed by electrocoagulation and electrocoagulation/flotation processes," *Journal of Environmental Management*, vol. 90, pp. 1663-1679, 2009.
- [16] A. Sagiv and R. Semiat, "Analysis of parameters affecting boron permeation through reverse osmosis membranes," *Journal of Membrane Science*, vol. 243, pp. 79-87, 2004.
- [17] K. L. Tu, L. D. Nghiem, and A. R. Chivas, "Boron removal by reverse osmosis membranes in seawater desalination applications," *Separation and Purification Technology*, vol. 75, pp. 87-101, 2010.
- [18] U. C. Gupta, "Boron nutrition of crops," *Adv. Agron*, vol. 31, pp. 273-307, 1979.
- [19] Y. Fujita, T. Hata, M. Nakamaru, T. Iyo, T. Yoshino, and T. Shimamura, "A study of boron adsorption onto activated sludge," *Bioresource Technology*, vol. 96, pp. 1350-1356, 2005.
- [20] M. Özdemir and İ. Kıpçak, "Recovery of boron from borax sludge of boron industry," *Minerals Engineering*, vol. 23, pp. 685-690, 2010.
- [21] P. P. Power and W. G. Woods, "The chemistry of boron and its speciation in plants," *Plant and Soil*, vol. 193, pp. 1-13, 1997.
- [22] D. Lemarchand, J. Gaillardet, C. Göpel, and G. Manhès, "An optimized procedure for boron separation and mass spectrometry analysis for river samples," *Chemical Geology*, vol. 182, pp. 323-334, 2002.
- [23] D. Xue, K. Betzler, H. Hesse, and D. Lammers, "Nonlinear optical properties of borate crystals," *Solid State Communications*, vol. 114, pp. 21-25, 2000.

- [24] M. Fernanda Chillón Arias, D. P. Rico, and P. V. Galvañ, "Kinetic behaviour of sodium and boron in brackish water membranes," *Journal of Membrane Science*, vol. 368, pp. 86-94, 2011.
- [25] W. Bouguerra, A. Mnif, B. Hamrouni, and M. Dhahbi, "Boron removal by adsorption onto activated alumina and by reverse osmosis," *Desalination*, vol. 223, pp. 31-37, 2008.
- [26] J. Redondo, M. Busch, and J. P. De Witte, "Boron removal from seawater using FILMTEC™ high rejection SWRO membranes," *Desalination*, vol. 156, pp. 229-238, 2003.
- [27] A. E. Yilmaz, R. Boncukcuoğlu, and E. Kocadağistan, "An empirical model for kinetics of boron removal from boroncontaining wastewaters by the electrocoagulation method in a batch reactor," *Desalination*, vol. 230, pp. 288-297, 2008.
- [28] Y. Cengeloglu, A. Tor, G. Arslan, M. Ersoz, and S. Gezgin, "Removal of boron from aqueous solution by using neutralized red mud," *Journal of Hazardous Materials*, vol. 142, pp. 412-417, 2007.
- [29] L. Melnyk, V. Goncharuk, I. Butnyk, and E. Tsapiuk, "Boron removal from natural and wastewaters using combined sorption/membrane process," *Desalination*, vol. 185, pp. 147-157, 2005.
- [30] Y. Magara, A. Tabata, M. Kohki, M. Kawasaki, and M. Hirose, "Development of boron reduction system for sea water desalination," *Desalination*, vol. 118, pp. 25-33, 1998.
- [31] A. E. Yilmaz, R. Boncukcuoğlu, M. M. Kocakerim, M. T. Yilmaz, and C. Paluluoglu, "Boron removal from geothermal waters by electrocoagulation," in *Journal of Hazardous Materials* vol. 153, ed, 2008, pp. 146-151.
- [32] World Health Organization (WHO), "Boron," *Environmental Health Criteria*, Vol 204, 1998.
- [33] N. Oztürk and D. Kavak, "Boron removal from aqueous solutions by batch adsorption onto cerium oxide using full factorial design," *Desalination*, vol. 223, pp. 106-112, 2008.
- [34] S. Mondal, C. Hsiao, and S. Ranil Wickramasinghe, "Nanofiltration/reverse osmosis for treatment of coproduced waters," *Environmental Progress*, vol. 27, pp. 173-179, 2008.
- [35] H. Koseoglu, B. Harman, N. Yigit, E. Guler, N. Kabay, and M. Kitis, "The effects of operating conditions on boron removal from geothermal waters by membrane processes," *Desalination*, vol. 258, pp. 72-78, 2010.

- [36] B. M. Smith, P. Todd, and C. N. Bowman, "Boron removal by polymer-assisted ultrafiltration," *Separation Science and Technology*, vol. 30, pp. 3849-3859, 1995.
- [37] C. Murray-Gulde, J. E. Heatley, T. Karanfil, J. H. Rodgers Jr, and J. E. Myers, "Performance of a hybrid reverse osmosis-constructed wetland treatment system for brackish oil field produced water," *Water Research*, vol. 37, pp. 705-713, 2003.
- [38] M. Taniguchi, M. Kurihara, and S. Kimura, "Boron reduction performance of reverse osmosis seawater desalination process," *Journal of Membrane Science*, vol. 183, pp. 259-267, 2001.
- [39] D. Hou, J. Wang, X. Sun, Z. Luan, C. Zhao, and X. Ren, "Boron removal from aqueous solution by direct contact membrane distillation," *Journal of Hazardous Materials*, vol. 177, pp. 613-619, 2010.
- [40] M. Rodríguez Pastor, A. Ferrándiz Ruiz, M. Chillon, and D. Prats Rico, "Influence of pH in the elimination of boron by means of reverse osmosis," *Desalination*, vol. 140, pp. 145-152, 2001.
- [41] H. Koseoglu, N. Kabay, M. Yüksel, S. Sarp, Ö. Arar, and M. Kitis, "Boron removal from seawater using high rejection SWRO membranes—impact of pH, feed concentration, pressure, and cross-flow velocity," *Desalination*, vol. 227, pp. 253-263, 2008.
- [42] Y. Magara, T. Aizawa, S. Kunikane, M. Itoh, M. Kohki, M. Kawasaki, "The behavior of inorganic constituents and disinfection by products in reverse osmosis water desalination process," *Water Science and Technology*, vol. 34, pp. 141-148, 1996.
- [43] V. Bonnelye, M. Sanz, L. Francisci, F. Beltran, G. Cremer, R. Colcuera, "Curacao, Netherlands Antilles: A successful example of boron removal on a seawater desalination plant," *Desalination*, vol. 205, pp. 200-205, 2007.
- [44] E. Güler, N. Kabay, M. Yüksel, E. Yavuz, and Ü. Yüksel, "A comparative study for boron removal from seawater by two types of polyamide thin film composite SWRO membranes," *Desalination*, vol. 273, pp. 81-84, 2011.
- [45] M. H. Oo and L. Song, "Effect of pH and ionic strength on boron removal by RO membranes," *Desalination*, vol. 246, pp. 605-612, 2009.
- [46] A. Bick and G. Oron, "Post-treatment design of seawater reverse osmosis plants: boron removal technology selection for potable water production and environmental control," *Desalination*, vol. 178, pp. 233-246, 2005.
- [47] Z. Yazicigil and Y. Oztekin, "Boron removal by electrodialysis with anion-exchange membranes," *Desalination*, vol. 190, pp. 71-78, 2006.

- [48] B. Bandura-Zalska, P. Dydo, and M. Turek, "Desalination of boron-containing wastewater at no boron transport," *Desalination*, vol. 241, pp. 133-137, 2009.
- [49] N. Kabay, O. Arar, F. Acar, A. Ghazal, U. Yuksel, and M. Yuksel, "Removal of boron from water by electrodialysis: effect of feed characteristics and interfering ions," *Desalination*, vol. 223, pp. 63-72, 2008.
- [50] M. Turek, P. Dydo, J. Ciba, J. Trojanowska, J. Kluczka, and B. Palka-Kupczak, "Electrodialytic treatment of boron-containing wastewater with univalent permselective membranes," *Desalination*, vol. 185, pp. 139-145, 2005.
- [51] L. V. Rajaković and M. D. Ristić, "Sorption of boric acid and borax by activated carbon impregnated with various compounds," *Carbon*, vol. 34, pp. 769-774, 1996.
- [52] Z. C. Çelik, B. Can, and M. M. Kocakerim, "Boron removal from aqueous solutions by activated carbon impregnated with salicylic acid," *Journal of Hazardous Materials*, vol. 152, pp. 415-422, 2008.
- [53] H. Liu, B. Qing, X. Ye, Q. Li, K. Lee, and Z. Wu, "Boron adsorption by composite magnetic particles," *Chemical Engineering Journal*, vol. 151, pp. 235-240, 2009.
- [54] M. del Mar de la Fuente García-Soto and E. M. Camacho, "Boron removal by means of adsorption with magnesium oxide," *Separation and Purification Technology*, vol. 48, pp. 36-44, 2006.
- [55] C. Irawan, J. Liu, and C. C. Wu, "Removal of boron using aluminum-based water treatment residuals (Al-WTRs)," *Desalination*, vol. 276, pp. 322-327, 2011.
- [56] Y. T. Wei, Y. M. Zheng, and J. P. Chen, "Design and fabrication of an innovative and environmental friendly adsorbent for boron removal," *Water Research*, vol. 45, pp. 2297-2305, 2011.
- [57] M. Malakootian and N. Yousefi, "The efficiency of electrocoagulation process using aluminum electrodes in removal of hardness from water," *Iranian Journal of Environmental Health Science & Engineering*, vol. 6, 131-136, 2009.
- [58] N. Kabay, I. Yilmaz, S. Yamac, S. Samatya, M. Yuksel, U. Yuksel, "Removal and recovery of boron from geothermal wastewater by selective ion exchange resins. I. Laboratory tests," *Reactive and Functional Polymers*, vol. 60, pp. 163-170, 2004.
- [59] N. Kabay, S. Sarp, M. Yuksel, M. Kitis, H. Koseoğlu, Ö. Arar, *et al.*, "Removal of boron from SWRO permeate by boron selective ion exchange resins containing N--methyl glucamine groups," *Desalination*, vol. 223, pp. 49-56, 2008.

- [60] C. Jacob, "Seawater desalination: Boron removal by ion exchange technology," *Desalination*, vol. 205, pp. 47-52, 2007.
- [61] S. Şahin, "A mathematical relationship for the explanation of ion exchange for boron adsorption," *Desalination*, vol. 143, pp. 35-43, 2002.
- [62] I. Linares-Hernández, C. Barrera-Díaz, B. Bilyeu, P. Juárez-GarcíaRojas, and E. Campos-Medina, "A combined electrocoagulation–electrooxidation treatment for industrial wastewater," *Journal of Hazardous Materials*, vol. 175, pp. 688-694, 2010.
- [63] H. Stechemesser and B. Dobias, *Coagulation and flocculation, Surfactant Science series, vol 126. 2nd ed.* CRC Press, 2005.
- [64] J. Bratby, *Coagulation and flocculation in water and wastewater treatment: International Water Association (IWA) Publishing, 2nd ed.* 2006.
- [65] F. Renault, B. Sancey, P. M. Badot, and G. Crini, "Chitosan for coagulation/flocculation processes—An eco-friendly approach," *European Polymer Journal*, vol. 45, pp. 1337-1348, 2009.
- [66] J. Ruhsing Pan, C. Huang, S. Chen, and Y. C. Chung, "Evaluation of a modified chitosan biopolymer for coagulation of colloidal particles," *Colloids and Surfaces A: Physicochemical and Engineering Aspects*, vol. 147, pp. 359-364, 1999.
- [67] E. Guibal and J. Roussy, "Coagulation and flocculation of dye-containing solutions using a biopolymer (Chitosan)," *Reactive and Functional Polymers*, vol. 67, pp. 33-42, 2007.
- [68] P. D. Johnson, P. Girinathannair, K. N. Ohlinger, S. Ritchie, L. Teuber, and J. Kirby, "Enhanced removal of heavy metals in primary treatment using coagulation and flocculation," *Water Environment Research*, vol. 80, pp. 472-479, 2008.
- [69] N. Maximova and O. Dahl, "Environmental implications of aggregation phenomena: Current understanding," *Current Opinion in Colloid & Interface Science*, vol. 11, pp. 246-266, 2006.
- [70] S. Deng, G. Yu, and Y. P. Ting, "Production of a bioflocculant by *Aspergillus parasiticus* and its application in dye removal," *Colloids and surfaces B: Biointerfaces*, vol. 44, pp. 179-186, 2005.
- [71] X. Chen, H. Wang, and X. Yang, "Study of Microbial Flocculant and Application Progress [J]," *Journal of Fushun Petroleum Institute*, vol. 4, p. 007, 2002.
- [72] B. Sharma, N. Dhuldhoya, and U. Merchant, "Flocculants- an ecofriendly approach," *Journal of Polymers and the Environment*, vol. 14, pp. 195-202, 2006.

- [73] G. Crini, "Recent developments in polysaccharide-based materials used as adsorbents in wastewater treatment," *Progress in Polymer Science*, vol. 30, pp. 38-70, 2005.
- [74] A. E. Yilmaz, R. Boncukcuoğlu, and M. M. Kocakerim, "A quantitative comparison between electrocoagulation and chemical coagulation for boron removal from boron-containing solution," *Journal of Hazardous Materials*, vol. 149, pp. 475-481, 2007.
- [75] A. K. Golder, V. S. Dhaneesh, A. N. Samanta, and S. Ray, "Removal of Nickel and Boron from Plating Rinse Effluent by Electrochemical and Chemical Techniques," *Chemical Engineering & Technology*, vol. 31, pp. 143-148, 2008.
- [76] M. Schulz, J. Baygents, and J. Farrell, "Laboratory and pilot testing of electrocoagulation for removing scale-forming species from industrial process waters," *International Journal of Environmental Science Technology*, vol. 6, pp. 521-526, 2009.
- [77] G. Chen, "Electrochemical technologies in wastewater treatment," *Separation and Purification Technology*, vol. 38, pp. 11-41, 2004.
- [78] R. R. Babu, N. Bhadrinarayana, K. M. M. S. Begum, and N. Anantharaman, "Treatment of tannery wastewater by electrocoagulation," *Journal of the University of Chemical Technology and Metallurgy*, vol. 42, pp. 201-206, 2007.
- [79] P. K. Holt, "Electrocoagulation: unravelling and synthesising the mechanisms behind a water treatment process," A thesis submitted to the Department of Chemical Engineering, University of Sydney, 2006.
- [80] M. Y. A. Mollah, P. Morkovsky, J. A. G. Gomes, M. Kesmez, J. Parga, and D. L. Cocke, "Fundamentals, present and future perspectives of electrocoagulation," *Journal of hazardous materials*, vol. 114, pp. 199-210, 2004.
- [81] N. Mameri, A. Yeddou, H. Lounici, D. Belhocine, H. Grib, and B. Bariou, "Defluoridation of septentrional Sahara water of North Africa by electrocoagulation process using bipolar aluminium electrodes," *Water Research*, vol. 32, pp. 1604-1612, 1998.
- [82] D. Ghosh, H. Solanki, and M. Purkait, "Removal of Fe (II) from tap water by electrocoagulation technique," *Journal of Hazardous Materials*, vol. 155, pp. 135-143, 2008.
- [83] L. W. Casson and J. W. Bess, "On-Site Sodium Hypochlorite Generation," *Proceedings of the Water Environment Federation*, vol. 2006, pp. 6335-6352, 2006.

- [84] J.-Q. Jiang, N. Graham, C. André, G. H. Kelsall, and N. Brandon, "Laboratory study of electro-coagulation–flotation for water treatment," *Water Research*, vol. 36, pp. 4064-4078, 2002.
- [85] N. Balasubramanian, T. Kojima, and C. Srinivasakannan, "Arsenic removal through electrocoagulation: Kinetic and statistical modeling," *Chemical Engineering Journal*, vol. 155, pp. 76-82, 2009.
- [86] N. Daneshvar, A. Oladegaragoze, and N. Djafarzadeh, "Decolorization of basic dye solutions by electrocoagulation: an investigation of the effect of operational parameters," *Journal of Hazardous Materials*, vol. 129, pp. 116-122, 2006.
- [87] A. A. Bukhari, "Investigation of the electro-coagulation treatment process for the removal of total suspended solids and turbidity from municipal wastewater," *Bioresource Technology*, vol. 99, p. 914-921, 2008.
- [88] B. Merzouk, B. Gourich, A. Sekki, K. Madani, and M. Chibane, "Removal turbidity and separation of heavy metals using electrocoagulation-electroflotation technique: A case study," *J. Hazardous Material*, vol. 164, pp. 215-222, 2009.
- [89] C. P. Nanseu-Njiki, S. R. Tchamango, P. C. Ngom, A. Darchen, and E. Ngameni, "Mercury (II) removal from water by electrocoagulation using aluminium and iron electrodes," *Journal of Hazardous Materials*, vol. 168, pp. 1430-1436, 2009.
- [90] Q. Feng, X. Li, Y. Cheng, L. Meng, and Q. Meng, "Removal of humic acid from groundwater by electrocoagulation," *Journal of China University of Mining and Technology*, vol. 17, pp. 513-520, 2007.
- [91] Y. Cengeloglu, G. Arslan, A. Tor, I. Kocak, and N. Dursun, "Removal of boron from water by using reverse osmosis," *Separation and Purification Technology*, vol. 64, pp. 141-146, 2008.
- [92] M. Busch, W. E. Mickols, S. Jons, J. Redondo, and J. De Witte, "Boron removal in sea water desalination," *International Desalination and Water Reuse Quarterly*, vol. 13, p. 25-41, 2004.
- [93] F. Akbal and S. Camcı, "Copper, chromium and nickel removal from metal plating wastewater by electrocoagulation," *Desalination*, vol. 269, pp. 214-222, 2011.
- [94] X. Chen, G. Chen, and P. L. Yue, "Separation of pollutants from restaurant wastewater by electrocoagulation," *Separation and Purification Technology*, vol. 19, pp. 65-76, 2000.
- [95] G. B. Raju, M. T. Karuppiyah, S. Latha, S. Parvathy, and S. Prabhakar, "Treatment of wastewater from synthetic textile industry by

- electrocoagulation–electrooxidation," *Chemical Engineering Journal*, vol. 144, pp. 51-58, 2008.
- [96] N. Balasubramanian, T. Kojima, C. A. Basha, and C. Srinivasakannan, "Removal of arsenic from aqueous solution using electrocoagulation," *Journal of Hazardous Materials*, vol. 167, pp. 966-969, 2009.
 - [97] M. Bennajah, B. Gourich, A. Essadki, C. Vial, and H. Delmas, "Defluoridation of Morocco drinking water by electrocoagulation/electroflotation in an electrochemical external-loop airlift reactor," *Chemical Engineering Journal*, vol. 148, pp. 122-131, 2009.
 - [98] M. Malakootian, H. Mansoorian, and M. Moosazadeh, "Performance evaluation of electrocoagulation process using iron-rod electrodes for removing hardness from drinking water," *Desalination*, vol. 255, pp. 67-71, 2010.
 - [99] C. Ricordel, A. Darchen, and D. Hadjiev, "Electrocoagulation–electroflotation as a surface water treatment for industrial uses," *Separation and Purification Technology*, vol. 74, pp. 342-347, 2010.
 - [100] M. G. Kılıç, Ç. Hoşten, and Ş. Demirci, "A parametric comparative study of electrocoagulation and coagulation using ultrafine quartz suspensions," *Journal of Hazardous Materials*, vol. 171, pp. 247-252, 2009.
 - [101] M. Solak, M. Kilic, H. Yazici, and A. Sencan, "Removal of suspended solids and turbidity from marble processing wastewaters by electrocoagulation: Comparison of electrode materials and electrode connection systems," *Journal of Hazardous Materials*, vol. 172, pp. 345-352, 2009.
 - [102] Ö. Apaydin, U. Kurt, and M. Gönüllü, "An Investigation on the treatment of tannery wastewater by Electrocoagulation," *Global NEST Journal*, vol. 11, pp. 546-555, 2009.
 - [103] H. Itoh, R. Sasai, T. Itakura, V. Popov, U. Mander, and C. Brebbia, "Consolidation recovery of rare hazardous elements from polluted water by the hydrothermal mineralization process," *Waste Management and the Environment*, vol. 140, p. 369-378, 2010.
 - [104] E. H. Ezechi, M. H. Isa, S. R. Kutty, and N. B. Sapari, "Boron recovery, application and economic significance: A review," in *National Postgraduate Conference (NPC), at Universiti Teknologi PETRONAS, Tronoh, Perak, Malaysia*, 2011.
 - [105] L. Schoderboeck, S. Mühlegger, A. Losert, C. Gausterer, and R. Hornek, "Effects assessment: Boron compounds in the aquatic environment," *Chemosphere*, vol. 82, pp. 483-487, 2011.
 - [106] A. Demirbaş, H. Yüksek, I. Cakmak, M. M. Küçük, M. Cengiz, and M. Alkan, "Recovery of boric acid from boronic wastes by leaching with water, carbon

- dioxide-or sulfur dioxide-saturated water and leaching kinetics," *Resources, Conservation and Recycling*, vol. 28, pp. 135-146, 2000.
- [107] R. Boncukcuoğlu, M. M. Kocakerim, E. Kocadağistan, and M. T. Yilmaz, "Recovery of boron of the sieve reject in the production of borax," *Resources, Conservation and Recycling*, vol. 37, pp. 147-157, 2003.
- [108] M. Yeşilyurt, "Determination of the optimum conditions for the boric acid extraction from colemanite ore in HNO₃ solutions," *Chemical Engineering and Processing: Process Intensification*, vol. 43, pp. 1189-1194, 2004.
- [109] N. Kabay, I. Yilmaz, S. Yamac, M. Yuksel, U. Yuksel, N. Yildirim, "Removal and recovery of boron from geothermal wastewater by selective ion-exchange resins-II. Field tests," *Desalination*, vol. 167, pp. 427-438, 2004.
- [110] T. Itakura, R. Sasai, and H. Itoh, "Precipitation recovery of boron from wastewater by hydrothermal mineralization," *Water Research*, vol. 39, pp. 2543, 2005.
- [111] H. C. Tsai and S. L. Lo, "Boron removal and recovery from concentrated wastewater using a microwave hydrothermal method," *Journal of Hazardous Materials*, vol. 186, pp. 1431-1437, 2011.
- [112] R. E. Treybal, *Mass-transfer operations* vol. 3: McGraw-Hill New York, 1955.
- [113] H. K. Boparai, M. Joseph, and D. M. O'Carroll, "Kinetics and thermodynamics of cadmium ion removal by adsorption onto nano zerovalent iron particles," *Journal of Hazardous Materials*, vol. 186, pp. 458-465, 2011.
- [114] Y. Ho and G. McKay, "A comparison of chemisorption kinetic models applied to pollutant removal on various sorbents," *Process Safety and Environmental Protection: Transactions of the Institution of Chemical Engineers, part B*, vol. 76, pp. 332-340, 1998.
- [115] A. Itodo, F. Abdulrahman, L. Hassan, S. Maigandi, and H. Itodo, "Intraparticle diffusion and intraparticulate diffusivities of herbicide on derived activated carbon," *Researcher*, vol. 2, pp. 74-86, 2010.
- [116] F.-C. Wu, R.-L. Tseng, and R.-S. Juang, "Initial behavior of intraparticle diffusion model used in the description of adsorption kinetics," *Chemical Engineering Journal*, vol. 153, pp. 1-8, 2009.
- [117] A. Özcan, E. M. Öncü, and A. S. Özcan, "Adsorption of Acid Blue 193 from aqueous solutions onto Dedma-sepiolite," *Journal of Hazardous Materials*, vol. 129, pp. 244-252, 2006.
- [118] S. Chien and W. Clayton, "Application of Elovich equation to the kinetics of phosphate release and sorption in soils," *Soil Science Society of America Journal*, vol. 44, pp. 265-268, 1980.

- [119] D. Sparks, "Kinetics of reactions in pure and in mixed systems," *Soil Physical Chemistry*, pp. 83-145, 1986.
- [120] S. S. Gupta and K. G. Bhattacharyya, "Adsorption of Ni (II) on clays," *Journal of Colloid and Interface Science*, vol. 295, pp. 21-32, 2006.
- [121] M. K. Aroua, S. Leong, L. Teo, C. Y. Yin, and W. M. A. W. Daud, "Real-time determination of kinetics of adsorption of lead (II) onto palm shell-based activated carbon using ion selective electrode," *Bioresource Technology*, vol. 99, pp. 5786-5792, 2008.
- [122] W. Rudzinski and W. Plazinski, "On the applicability of the pseudo-second order equation to represent the kinetics of adsorption at solid/solution interfaces: a theoretical analysis based on the statistical rate theory," *Adsorption*, vol. 15, pp. 181-192, 2009.
- [123] S. Basha, Z. Murthy, and B. Jha, "Sorption of Hg (II) from aqueous solutions onto Carica papaya: Application of isotherms," *Industrial & Engineering Chemistry Research*, vol. 47, pp. 980-986, 2008.
- [124] T. A. Davis, B. Volesky, and A. Mucci, "A review of the biochemistry of heavy metal biosorption by brown algae," *Water Research*, vol. 37, pp. 4311-4330, 2003.
- [125] E. Demirbaş, M. Kobya, S. Öncel, and S. Şencan, "Removal of Ni (II) from aqueous solution by adsorption onto hazelnut shell activated carbon: equilibrium studies," *Bioresource Technology*, vol. 84, pp. 291-293, 2002.
- [126] S. Peng, S. Wang, and T. J. S. Chen, "Qing Chengsong (School of Resources and Environment, Hefei University of Technology, Hefei 230009, China); Thermodynamics study of adsorption of water soluble dyestuffs onto purified palygorskite [J]," *Journal of the Chinese Ceramic Society*, vol. 8, pp. 579, 2005.
- [127] C. S. Sundaram, N. Viswanathan, and S. Meenakshi, "Defluoridation chemistry of synthetic hydroxyapatite at nano scale: equilibrium and kinetic studies," *Journal of Hazardous Materials*, vol. 155, pp. 206-215, 2008.
- [128] J. Huang, X. Wang, Q. Jin, Y. Liu, and Y. Wang, "Removal of phenol from aqueous solution by adsorption onto OTMAC-modified attapulgite," *Journal of Environmental Management*, vol. 84, pp. 229-236, 2007.
- [129] S. H. Lin and M. L. Chen, "Treatment of textile wastewater by chemical methods for reuse," *Water Research*, vol. 31, pp. 868-876, 1997.
- [130] M. Bayramoglu, M. Kobya, O. T. Can, and M. Sozbir, "Operating cost analysis of electrocoagulation of textile dye wastewater," *Separation and Purification Technology*, vol. 37, pp. 117-125, 2004.

- [131] S. Vasudevan, J. Lakshmi, and R. Vanathi, "Electrochemical coagulation for chromium removal: process optimization, kinetics, isotherms and sludge characterization," *Clean-Soil, Air, Water*, vol. 38, pp. 9-16, 2010.
- [132] E. A. Vik, D. A. Carlson, A. S. Eikum, and E. T. Gjessing, "Electrocoagulation of potable water," *Water Research*, vol. 18, pp. 1355-1360, 1984.
- [133] G. Mouedhen, M. Feki, M. P. Wery, and H. Ayedi, "Behavior of aluminum electrodes in electrocoagulation process," *Journal of Hazardous Materials*, vol. 150, p. 124, 2008.
- [134] E. Bazrafshan, K. A. Ownagh, and A. H. Mahvi, "Application of electrocoagulation process using Iron and Aluminum electrodes for fluoride removal from aqueous environment," *Journal of Chemistry*, vol. 9, pp. 2297-2308, 2012.
- [135] M. Kobya, O. T. Can, and M. Bayramoglu, "Treatment of textile wastewaters by electrocoagulation using iron and aluminum electrodes," *Journal of Hazardous Materials*, vol. 100, pp. 163-178, 2003.
- [136] M. Chafi, B. Gourich, A. H. Essadki, C. Vial, and A. Fabregat, "Comparison of electrocoagulation using iron and aluminium electrodes with chemical coagulation for the removal of a highly soluble acid dye," *Desalination*, vol. 281, pp. 285-292, 2011.
- [137] M. H. Isa, T. K. Kee, A. A. Zinatizadeh, S. Mohajeri, H. Aziz, and Y. T. Hung, "Electrochemical treatment of semi-aerobic landfill leachate using Response Surface Methodology (RSM)," *International Journal of Environment and Pollution*, vol. 43, pp. 324-338, 2010.
- [138] F. Ozyonar and B. Karagozoglu, "Operating cost analysis and treatment of domestic wastewater by electrocoagulation using aluminum electrodes." *Polish Journal of Environmental Studies*, vol. 20 No. 1 173-179, 2011.
- [139] A. Alinsafi, M. Khemis, M. Pons, J. Leclerc, A. Yaacoubi, A. Benhammou, "Electro-coagulation of reactive textile dyes and textile wastewater," *Chemical Engineering and Processing: Process Intensification*, vol. 44, pp. 461-470, 2005.
- [140] M. H. El-Naas, S. Al-Zuhair, A. Al-Lobaney, and S. Makhoulouf, "Assessment of electrocoagulation for the treatment of petroleum refinery wastewater," *Journal of Environmental Management*, vol. 91, pp. 180-185, 2009.
- [141] K. Yetilmezsoy, F. Ilhan, Z. Sapci-Zengin, S. Sakar, and M. T. Gonullu, "Decolorization and COD reduction of UASB pretreated poultry manure wastewater by electrocoagulation process: A post-treatment study," *Journal of Hazardous Materials*, vol. 162, pp. 120-132, 2009.

- [142] F. Othman, M. Ni'am, J. Sohaili, and Z. Fauzia, "Electrocoagulation technique in enhancing COD and suspended solids removal to improve wastewater quality," *Water Science & Technology*, vol. 56, pp. 47-53, 2007.
- [143] P. Demirçivi and G. Nasün-Saygılı, "Removal of boron from wastewaters by ion-exchange in a batch system," *World Academy of Science, Engineering and Technology*, vol. 47, 2008.
- [144] C. Yan, W. Yi, P. Ma, X. Deng, and F. Li, "Removal of boron from refined brine by using selective ion exchange resins," *Journal of Hazardous Materials*, vol. 154, pp. 564-571, 2008.
- [145] N. Drouichea, S. Aoudja, M. Hecinia, and T. Ouslimanea, "Experimental design for the elimination of fluoride from pretreated photovoltaic wastewater by electrocoagulation," *Chemical Engineering*, vol. 24, 1-6, 2011.
- [146] N. Daneshvar, H. Ashassi-Sorkhabi, and A. Tizpar, "Decolorization of orange II by electrocoagulation method," *Separation and Purification Technology*, vol. 31, pp. 153-162, 2003.
- [147] N. Modirshahla, M. Behnajady, and S. Mohammadi-Aghdam, "Investigation of the effect of different electrodes and their connections on the removal efficiency of 4-nitrophenol from aqueous solution by electrocoagulation," *Journal of Hazardous Materials*, vol. 154, pp. 778-786, 2008.
- [148] M. Y. A. Mollah, S. R. Pathak, P. K. Patil, M. Vayuvegula, T. S. Agrawal, J. A. G. Gomes, *et al.*, "Treatment of orange II azo-dye by electrocoagulation (EC) technique in a continuous flow cell using sacrificial iron electrodes," *Journal of Hazardous Materials*, vol. 109, pp. 165-171, 2004.
- [149] M. Kobya, E. Demirbas, A. Dedeli, and M. Sensoy, "Treatment of rinse water from zinc phosphate coating by batch and continuous electrocoagulation processes," *Journal of Hazardous Materials*, vol. 173, pp. 326-334, 2010.
- [150] M. I. S. Veríssimo and M. Gomes, "The quality of our drinking water: Aluminium determination with an acoustic wave sensor," *Analytica chimica acta*, vol. 617, pp. 162-166, 2008.
- [151] R. S. Ayers and D. W. Westcot, *Water quality for agriculture: Food and Agriculture Organization of the United Nations Rome, Italy*, pp. 1287-1295, 1985.
- [152] M. A. Al- Mahasneh, T. M. Rababah, M. A. Ai- Shbool, and W. Yang, "Thin- layer drying kinetics of sesame hulls under forced convection and open sun drying," *Journal of Food Process Engineering*, vol. 30, pp. 324-337, 2007.
- [153] E. Isik, N. Izli, and B. Akbudak, "Microwave heat treatment of dent corn (*Zea mays* var. *indentata* sturt.): Drying kinetic and physical properties," *African Journal of Biotechnology*, vol. 11, pp. 2740-2751, 2012.

- [154] E. K. Akpinar, "Determination of suitable thin layer drying curve model for some vegetables and fruits," *Journal of Food Engineering*, vol. 73, pp. 75-84, 2006.
- [155] S. Gupta and B. Babu, "Utilization of waste product (tamarind seeds) for the removal of Cr (VI) from aqueous solutions: Equilibrium, kinetics, and regeneration studies," *Journal of Environmental Management*, vol. 90, pp. 3013-3022, 2009.
- [156] M. Bansal, D. Singh, and V. Garg, "A comparative study for the removal of hexavalent chromium from aqueous solution by agriculture wastes' carbons," *Journal of Hazardous Materials*, vol. 171, pp. 83-92, 2009.
- [157] J. Piccin, C. Gomes, L. Feris, and M. Gutterres, "Kinetics and isotherms of leather dyes adsorption by tannery solid waste," *Chemical Engineering Journal*, vol 183, pp 30-38, 2011.
- [158] B. Hameed, "Evaluation of papaya seeds as a novel non-conventional low-cost adsorbent for removal of methylene blue," *Journal of Hazardous Materials*, vol. 162, pp. 939-944, 2009.
- [159] J. Igwe, C. Onyegbado, and A. Abia, "Studies on the kinetics and intraparticle diffusivities of BOD, colour and TSS reduction from palm oil mill effluent (POME) using boiler fly ash," *African Journal of Environmental Science and Technology*, vol. 4, 2010.
- [160] H. Teng and C. T. Hsieh, "Activation energy for oxygen chemisorption on carbon at low temperatures," *Industrial & Engineering Chemistry Research*, vol. 38, pp. 292-297, 1999.
- [161] O. Hamdaoui and E. Naffrechoux, "Modeling of adsorption isotherms of phenol and chlorophenols onto granular activated carbon: Part I. Two-parameter models and equations allowing determination of thermodynamic parameters," *Journal of Hazardous Materials*, vol. 147, pp. 381-394, 2007.
- [162] Q. Li, Q. Y. Yue, Y. Su, B. Y. Gao, and H. J. Sun, "Equilibrium, thermodynamics and process design to minimize adsorbent amount for the adsorption of acid dyes onto cationic polymer-loaded bentonite," *Chemical Engineering Journal*, vol. 158, pp. 489-497, 2010.
- [163] J. Ma, Y. Jia, Y. Jing, Y. Yao, and J. Sun, "Kinetics and thermodynamics of methylene blue adsorption by cobalt-hectorite composite," *Dyes and Pigments*, vol 93, pp 1441-1446, 2011.
- [164] B. Hameed, A. Ahmad, and N. Aziz, "Isotherms, kinetics and thermodynamics of acid dye adsorption on activated palm ash," *Chemical Engineering Journal*, vol. 133, pp. 195-203, 2007.
- [165] J. B. Dixon and S. B. Weed, *Minerals in soil environments*: Soil Science Society of America Inc.(SSSA). 1989.

- [166] A. Masion, J. Bottero, F. Thomas, and D. Tchoubar, "Chemistry and Structure of Al (OH) organics precipitates. A small-angle X-ray scattering study. 2. Speciation and Structure of the Aggregates," *Langmuir*, vol. 10, pp. 4349-4352, 1994.
- [167] J. A. G. Gomes, P. Daida, M. Kesmez, M. Weir, H. Moreno, J. R. Parga, *et al.*, "Arsenic removal by electrocoagulation using combined Al-Fe electrode system and characterization of products," *Journal of Hazardous Materials*, vol. 139, pp. 220-231, 2007.
- [168] I. Kusachi, Y. Takechi, C. Henmi, and S. Kobayashi, "Parasibirskite, a new mineral from Fuka, Okayama Prefecture, Japan," *Mineralogical Magazine*, vol. 62, pp. 521-525, 1998.
- [169] S. A. Kasemann, A. Meixner, J. Erzinger, J. G. Viramonte, R. N. Alonso, and G. Franz, "Boron isotope composition of geothermal fluids and borate minerals from salar deposits (central Andes/NW Argentina)," *Journal of South American Earth Sciences*, vol. 16, pp. 685-697, 2004.
- [170] I. Kusachi, C. Henmi, and S. Kobayashi, "Takedaite, a new mineral from Fuka, Okayama Prefecture, Japan," *Mineralogical Magazine*, vol. 59, pp. 549-552, 1995.
- [171] I. Kusachi and C. Henmi, "Nifontovite and olshanskyite from Fuka, Okayama Prefecture, Japan," *Mineralogical Magazine*, vol. 58, pp. 279-284, 1994.
- [172] S. Muessig, "First known occurrence of inyoite in a playa, at Laguna Salinas," *Peru: The American Mineralogist*, vol. 43, pp. 1144-1147, 1958.
- [173] I. Kusachi, S. Kobayashi, M. Tanabe, S. Kishi, and J. Yamakawa, "Inyoite from Fuka, Okayama Prefecture, Japan," *Journal of Mineralogical and Petrological Sciences*, vol. 99, pp. 67-71, 2004.
- [174] R. Takahashi, I. Kusachi, and H. Miura, "Crystal structure of parasibirskite (CaHBO₃) and polymorphism in sibirskite and parasibirskite," *Journal of Mineralogical and Petrological Sciences*, vol. 105, pp. 70-73, 2010.

APPENDIX A

Table A.1. Experimental data for Effect of pH at final treatment time;
current density 12.5 mA/cm², inter-electrode spacing 0.5cm

Aluminum electrode	
pH	Percent Removal (%)
3	50
4	59
5	67
6	94
7	98
8	98
9	56
10	48
11	45

Table A.2 : Experimental data for effect of pH; current density 12.5 mA/cm², inter-electrode spacing 0.5 cm, electrode area 60 cm².

Aluminum electrode										
Time (Mins)	Conc (mg/L)	pH								
		3	4	5	6	7	8	9	10	11
		Percent Removal (%)								
15	10	29	35	38.0	49.0	64.0	69.0	32	24	22
30	10	34	40	43.0	58.0	78.0	81.0	36	29	25
45	10	39	43	50.0	69.0	86.0	89.0	41	37	33
60	10	43	50	58.0	80.0	93.0	95.0	45	41	37
75	10	48	56	62.0	88.0	96.0	97.0	51	46	42
90	10	50	59	67.0	94.0	98.0	98.0	56	48	45
15	20	27.5	34	35.5	39.5	54.5	56.0	29	22	19
30	20	30.5	37.5	41.0	46.0	64.5	67.0	33	26.5	22
45	20	34	39.5	47.5	54.0	69.0	73.0	37	30	28
60	20	39.5	44	53.0	64.5	76.0	79.0	42	35.5	33
75	20	43.5	48.5	58.5	69.5	80.5	83.5	46	39.5	37
90	20	46	50	60.0	71.5	86.5	87.0	49	44	41
15	30	25.3	34	35.0	37.3	46.3	47.7	28.5	21	17.1
30	30	29.6	36	39.3	43.7	55.0	59.3	31	24.7	20.3
45	30	33.3	38	43.0	52.7	63.7	66.3	35	28.6	26.7
60	30	36.3	42.3	46.3	59.0	69.7	72.3	39	33.6	30
75	30	42	45	53.7	61.7	76.0	77.7	43	37.4	34.8
90	30	45.3	47.3	56.0	65.7	82.7	83.0	47	42.2	39.2

Table A.3: Comparison between initial and final pH at different current densities.
Treatment time 90 minutes, concentration 10 mg/L, inter-electrode spacing 0.5 cm,
electrode area 60 cm².

Final and initial pH for aluminum electrode							
Initial pH	Conc.	Percent Removal (%)			Final pH		
	mg/l	6.25 mA/cm ²	12.5 mA/cm ²	18.75 mA/cm ²	6.25 mA/cm ²	12.5 mA/cm ²	18.75 mA/cm ²
pH 3	10	32	50	52	3.3	3.42	3.51
pH 4	10	35	59	61	4.24	4.38	4.49
pH 5	10	51	67	73	5.29	5.40	5.53
pH 6	10	59	94	95	6.22	6.31	6.45
pH 7	10	76	98	98	7.28	7.39	7.5
pH 8	10	77	98	98	8.19	8.42	8.54
pH 9	10	49	56	71	8.29	8.5	8.64
pH 10	10	26	48	51	8.61	8.8	9.15
pH 11	10	21	45	50	9.9	10.17	10.31

Table A.4. Experimental data for Effect of initial pH at final treatment time; current
density 12.5 mA/cm², inter-electrode spacing 0.5cm.

Iron electrode	
pH	Percent Removal (%)
3	48
4	54
5	59
6	78
7	97
8	98
9	57
10	47
11	41

Table A.5 Experimental data for effect of initial pH; current density 12.5 mA/cm²,
inter-electrode spacing 0.5 cm, electrode area 60 cm².

Iron electrode										
Time (Mins)	Conc (mg/L)	pH								
		3	4	5	6	7	8	9	10	11
		Percent Removal (%)								
15	10	34.5	37	42	53	63	68	38	34	31
30	10	38.5	40	47	59	75	78	43	37	33
45	10	42	45	50	63	82	87	48	41	35
60	10	46	49	53	68	91	94	51	44.5	38
75	10	47	50	56	72	95	97	54	46	40
90	10	48	54	59	78	97	98	57	47	41
15	20	29.7	34	39.5	43	53.5	56.5	34	28	25.5
30	20	32.3	37.8	41.5	45.5	57	60	39	31	28.5
45	20	37	43	45	50.5	65.5	69.5	45	35	31.5
60	20	39.3	46.5	48	54.5	74	75.5	46.8	38.5	34
75	20	38.7	47.5	50	59	79	80.5	49	39	37
90	20	39.7	49.5	52	61.5	81	83.5	51	40	39
15	30	27.7	32.0	33.3	41.0	48.0	50.0	30	27.2	27.0
30	30	30.3	35.0	37.7	44.0	54.0	56.0	35	29.3	28.3
45	30	34.5	39.3	40.7	47.3	59.3	61.3	41.2	32.0	30.
60	30	36.3	42.0	43	49.7	65.3	68.0	43.1	35.0	32.3
75	30	37.7	41.3	45.7	52.0	69.7	71.7	44.8	36	34.7
90	30	38.7	44.9	47.0	57.3	72.7	74.7	46	37	35.9

Table A.6: Comparison between initial and final pH at different current densities. Treatment time 90 minutes, concentration 10 mg/L, inter-electrode spacing 0.5 cm, electrode area 60 cm² (Iron electrode).

Final and initial pH for iron electrode							
Initial pH	Conc.	Percent Removal (%)			Final pH		
	mg/l	6.25 mA/cm ²	12.5 mA/cm ²	18.75 mA/cm ²	6.25 mA/cm ²	12.5 mA/cm ²	18.75 mA/cm ²
3	10	40	48	59	3.32	3.45	3.6
4	10	45	54	60	4.29	4.43	4.54
5	10	52	59	63	5.31	5.42	5.56
6	10	57	78	79	6.34	6.42	6.50
7	10	73	97	98	7.3	7.47	7.61
8	10	75	98	98	8.33	8.43	8.55
9	10	62	57	78	9.41	9.68	9.97
10	10	47	47	57	10.18	10.27	10.85
11	10	40	41	47	11.24	11.48	11.81

Table A.7 Experimental data for effect of current density on boron removal; initial pH 7, inter-electrode spacing 0.5 cm (Aluminum and iron electrode)

Time (Mins)	Conc. (mg/L)	6.25 mA/cm ²		12.5 mA/cm ²		18.75 mA/cm ²	
		Iron	Aluminum	Iron	Aluminum	Iron	Aluminum
15	10	51	52	63	64.0	71	70
30	10	61	59	75	78.0	80	84
45	10	65	64	82	86.0	89	93
60	10	69	67	91	93.0	95	97
75	10	71	72	96	96.0	97	98
90	10	73	76	97	98.0	98	98
15	20	43.5	54.5	53.5	54.5	53.5	55
30	20	49.5	64.5	57	64.5	57	60.5
45	20	54	69	65.5	69.0	65.5	68.5
60	20	58	76	74	76.0	74	77.5
75	20	59	80.5	79	80.5	79	84
90	20	64	86.5	81	86.5	81	87
15	30	38.7	46.3	48.0	46.3	48.0	50.3
30	30	46.3	55.0	54.0	55.0	54.0	56.3
45	30	49.0	63.7	59.3	63.7	59.3	62.7
60	30	52.0	69.7	65.3	69.7	65.3	67.0
75	30	53.0	76.0	69.7	76.0	69.7	73.7
90	30	55.3	82.7	72.7	82.7	72.7	81.0

Table A.8 Experimental data for effect of initial boron concentration; initial pH 7, Current density 12.5 mA/cm², inter-electrode spacing 0.5 cm.

		Aluminum electrode	Iron electrode
Time (Minutes)	Conc. (mg/L)	Percent Removal (%)	Percent Removal (%)
15	10	64.0	63
30	10	78.0	75
45	10	86.0	82
60	10	93.0	91
75	10	96.0	96
90	10	98.0	97
15	20	54.5	53.5
30	20	64.5	57
45	20	69.0	65.5
60	20	76.0	74
75	20	80.5	79
90	20	86.5	81
15	30	46.3	48.0
30	30	55.0	54.0
45	30	63.7	59.3
60	30	69.7	65.3
75	30	76.0	69.7
90	30	82.7	72.7

Table A.9 Effect of electrolysis time on boron removal: initial pH 7, current density 12.5 mA/cm², inter-electrode spacing 0.5 cm

		Aluminum electrode	Iron electrode
Time (Minutes)	Conc. (mg/L)	Percent Removal (%)	Percent Removal (%)
15	10	64	63
30	10	78	75
45	10	86	82
60	10	93	91
75	10	96	96
90	10	98	97

Table A.10 Effect of Inter-electrode spacing on boron removal from produced water. Initial pH 7, Current density 12.5 mA/cm²

		Aluminum electrode			Iron electrode		
Time (Min)	Conc. (mg/L)	Percent Removal (%)			Percent Removal (%)		
		0.5 cm	1.0 cm	1.5 cm	0.5 cm	1.0 cm	1.5 cm
15	15	72.7	60.0	54.7	67.3	58.0	48.0
30	15	78.7	66.0	65.3	81.3	70.7	62.7
45	15	84.7	74.0	71.3	90.0	80.7	70.0
60	15	92.7	84.0	78.7	94.7	85.3	75.3
75	15	96.7	89.3	82.0	96.0	88.0	80.0
90	15	98.0	90.7	84.0	96.7	89.3	82.7

APPENDIX B

Table B.1 Effect of flowrate in boron removal: initial pH 7, current density 12.5 mA/cm², inter-electrode spacing 0.5 cm

Time (Mins)	Conc. (mg/L)	Aluminum			Iron		
		Percent Removal (%)			Percent Removal (%)		
		Flowrate (mL/min)			Flowrate (mL/min)		
		20	25	30	20	25	30
20	5	38	26	18	30	22	14
40	5	50	42	30	42	34	22
60	5	60	50	40	56	44	30
80	5	72	60	52	66	54	40
100	5	82	68	60	70	64	48
120	5	86	74	66	74	68	56
140	5	88	80	70	78	70	62
20	10	28	21	17	23	17	10
40	10	36	36	26	32	26	18
60	10	51	44	36	44	35	26
80	10	62	54	48	52	42	36
100	10	70	62	54	59	50	44
120	10	79	70	58	65	58	51
140	10	82	73	62	71	66	58
20	15	18.7	18.0	14.0	16.0	11.33	7.3
40	15	30.7	30.0	23.3	26.0	20.00	14.7
60	15	44.7	41.3	34.0	34.7	27.33	22.7
80	15	55.3	49.3	46.7	46.0	34.00	30.7
100	15	67.3	59.3	52.7	53.3	41.33	39.3
120	15	72.7	65.3	56.0	61.3	49.33	46.7
140	15	78.7	69.3	60.0	67.3	60.67	53.3

Table B.2 Effect of concentration on boron removal efficiency at various flowrate:
Initial pH 7, current density 12.5 mA/cm², inter-electrode spacing 0.5 cm.

Retention time (Minutes)	Flowrate ml/min	Aluminum			Iron		
		Percent Removal (%)			Removal efficiency (%)		
		Concentration (mg/L)			Concentration (mg/L)		
		5	10	15	5	10	15
20	20	38	28	18.7	30	23	16.0
40	20	50	36	30.7	42	32	26.0
60	20	60	51	44.7	56	44	34.7
80	20	72	62	55.3	66	52	46.0
100	20	82	70	67.3	70	59	53.3
120	20	86	79	72.7	74	65	61.3
140	20	88	82	78.7	78	71	67.3
20	25	26	21	18.0	22	17	11.3
40	25	42	36	30.0	34	26	20.0
60	25	50	44	41.3	44	35	27.3
80	25	60	54	49.3	54	42	34.0
100	25	68	62	59.3	64	50	41.3
120	25	74	70	65.3	68	58	49.3
140	25	79	73	69.3	70	66	60.7
20	30	18	17	14.0	14	10	7.3
40	30	30	26	23.3	22	18	14.7
60	30	40	36	34.0	30	26	22.7
80	30	52	48	46.7	40	36	30.7
100	30	60	54	52.7	48	44	39.3
120	30	66	58	56.0	56	51	46.7
140	30	70	62	60.0	62	58	53.3

APPENDIX C

Table C.1 Pseudo first order kinetic data for boron adsorption onto $\text{Al}(\text{OH})_3$, initial pH 7, inter-electrode spacing 0.5 cm, current density 12.5 mA/cm^2 , Temperature 308K.

Aluminum						
	Boron uptake (mg/g)			Pseudo First Order		
Time (Min)	Concentration (mg/L)			Concentration (mg/L)		
	10	20	30	10	20	30
	q_t			$\log (q_e - q_t)$		
15	4.46	7.87	9.98	0.21	0.52	0.83
30	5.02	8.68	12.15	0.03	0.41	0.66
45	5.70	9.24	13.27	-0.42	0.29	0.536
60	5.95	9.98	15.31	-0.879	0.09	0.136
75	6.08	10.79	15.99	-1.91	-0.36	-0.17

Table C.2 Pseudo first order kinetic data for boron adsorption onto $\text{Fe}(\text{OH})_3$, initial pH 7, inter-electrode spacing 0.5 cm, current density 12.5 mA/cm^2 , Temperature 308K.

Iron						
	Boron uptake (mg/g)			Pseudo First Order		
Time (Min)	Concentration (mg/L)			Concentration (mg/L)		
	10	20	30	10	20	30
	q_t			$\log (q_e - q_t)$		
15	5.99	9.15	14.23	0.19	0.63	0.78
30	6.61	9.92	15.61	-0.03	0.55	0.67
45	7.07	11.30	17.23	-0.34	0.33	0.49
60	7.38	12.15	18.61	-0.81	0.12	0.23
75	7.46	12.61	19.30	-1.11	-0.07	-0.01

Table C.3 Pseudo second order kinetic data for boron adsorption onto $\text{Al}(\text{OH})_3$, initial pH 7, inter-electrode spacing 0.5 cm, current density 12.5 mA/cm^2 , Temperature 308K.

Aluminum						
	Boron uptake (mg/g)			Pseudo Second Order		
Time (Min)	Concentration (mg/L)			Concentration (mg/L)		
	10	20	30	10	20	30
	q_t	q_t	q_t	t/qt	t/qt	t/qt
15	4.46	7.87	9.98	3.36	1.91	1.50
30	5.02	8.68	12.15	5.97	3.46	2.47
45	5.70	9.24	13.27	7.89	4.87	3.39
60	5.95	9.98	15.31	10.08	6.01	3.91
75	6.08	10.79	15.99	12.34	6.95	4.69

Table C.4 Pseudo second order kinetic data for boron adsorption onto $\text{Fe}(\text{OH})_3$, initial pH 7, inter-electrode spacing 0.5 cm, current density 12.5 mA/cm^2 , Temperature 308K.

Iron						
	Boron uptake (mg/g)			Pseudo Second Order		
Time (Min)	Concentration (mg/L)			Concentration (mg/L)		
	10	20	30	10	20	30
	q_t	t/qt	t/qt	t/qt	t/qt	t/qt
15	5.99	9.15	14.23	2.50	1.64	1.05
30	6.61	9.92	15.61	4.54	3.02	1.92
45	7.07	11.30	17.23	6.36	3.98	2.61
60	7.38	12.15	18.61	8.13	4.94	3.22
75	7.46	12.61	19.30	10.05	5.95	3.89

Table C.5 Intra-particle diffusion and Elovich model data for adsorption of boron onto $\text{Al}(\text{OH})_3$, initial pH 7, density 12.5 mA/cm^2 , inter-electrode spacing 0.5 cm, temperature 308K.

Aluminum electrode								
	Boron uptake (mg/g)				Boron uptake (mg/g)			
		Intra-particle diffusion				Elovich model		
Time (Min)	$t^{0.5}$	Concentration (mg/L)			$\ln(t)$	Concentration (mg/L)		
		10	20	30		10	20	30
	$t^{0.5}$	q_t	q_t	q_t	$\ln(t)$	q_t	q_t	q_t
15	3.87298	4.46	7.87	9.98	2.71	4.46	7.87	9.98
30	5.47723	5.02	8.68	12.15	3.40	5.02	8.68	12.15
45	6.70820	5.70	9.24	15.0	3.81	5.70	9.24	13.27
60	7.74597	5.95	9.98	15.31	4.09	5.95	9.98	15.31
75	8.66025	6.08	10.79	15.99	4.32	6.08	10.79	15.99

Table C.6 Intra-particle diffusion and Elovich model data for adsorption of boron onto $\text{Fe}(\text{OH})_3$, initial pH 7, current density 12.5 mA/cm^2 , inter-electrode spacing 0.5 cm, temperature 308K.

Iron electrode								
	Boron uptake (mg/g)					Boron uptake (mg/g)		
		Intra-particle diffusion				Elovich model		
Time (Min)	$t^{0.5}$	Concentration (mg/L)			$\ln(t)$	Concentration (mg/L)		
		10	20	30		10	20	30
	$t^{0.5}$	q_t	q_t	q_t	$\ln(t)$	q_t	q_t	q_t
15	3.87	5.99	9.15	14.23	2.71	5.99	9.15	14.23
30	5.48	6.61	9.92	15.61	3.40	6.61	9.92	15.61
45	6.71	7.07	11.30	17.23	3.81	7.07	11.30	17.23
60	7.75	7.38	12.15	18.61	4.09	7.38	12.15	18.61
75	8.66	7.46	12.61	19.30	4.32	7.46	12.61	19.30

APPENDIX D

Table D1. Data for Langmuir and Freundlich adsorption isotherm for Aluminum electrode

Aluminum electrode					
			Langmuir	Freundlich	
Conc. (mg/L)	q_e (mg/g)	C_e (mg/L)	C_e/q_e	Log q_e	Log C_e
10	6.01	0.26	0.043	0.78	-0.59
20	12.94	2.93	0.23	1.11	0.47
30	14.63	6.3	0.43	1.17	0.80

Table D2. Data for Langmuir and Freundlich adsorption isotherm for iron electrode

Iron electrode					
			Langmuir	Freundlich	
Conc. (mg/L)	q_e (mg/g)	C_e (mg/L)	C_e/q_e	Log q_e	Log C_e
10	7.54	0.19	0.026	0.88	-0.71
20	14.07	1.30	0.09	1.15	0.23
30	20.54	2.90	0.14	1.32	0.46

Table D.3 Thermodynamic data for boron adsorption onto $\text{Al}(\text{OH})_3$, initial pH 7, conc. 20 mg/L, inter-electrode spacing 0.5 cm, current density 12.5 mA/cm².

Aluminum electrode								
Temp (K)	1/T (k)	q _e (mg/g)	C _e (mg/L)	K _c	ln K _c	ΔG° (kJ/mol)	ΔH° (kJ/mol)	ΔS° (J/mol)
298	3.3	10.54	2.93	3.60	1.28	-3.16		
308	3.2	11.22	1.82	6.16	1.82	-4.66		
318	3.1	11.53	1.32	8.75	2.169	-5.73	44.8	125.04
328	3.0	11.78	0.92	12.85	2.55	-6.96		

Table D.4 Thermodynamic data for boron adsorption onto $\text{Fe}(\text{OH})_3$, pH 7, conc. 20 mg/L, inter-electrode spacing 0.5 cm, current density 12.5 mA/cm².

Iron electrode								
Temp (K)	1/T (k)	q _e (mg/g)	C _e (mg/L)	K _c	ln K _c	ΔG° (kJ/mol)	ΔH° (kJ/mol)	ΔS° (J/mol)
298	3.3	12.46	3.80	3.27	1.19	-2.94		
308	3.2	13.46	2.51	5.37	1.68	-4.30		
318	3.1	14.07	1.71	8.25	2.11	-5.58	45.75	135.5
328	3.0	14.53	1.11	13.14	2.58	-7.02		

PUBLICATION

- [1] E. H. Ezechi, M. H. Isa, and S. R. B. M. Kutty, "Boron in Produced Water: Challenges and Improvements: A Comprehensive Review," *Journal of Applied Sciences*, vol. 12, pp. 402-415, 2012.

CONFERENCES

- [1] E. H. Ezechi, M. H. Isa, S. R. Kutty, and N. B. Sapari, "Boron recovery, application and economic significance: A review," in *National Postgraduate Conference (NPC)*, Universiti Teknologi PETRONAS (UTP) Tronoh, Perak, Malaysia, 19-20th September, 2011, IEEE pp. 1-6.
- [2] E. H. Ezechi, M. H. Isa, and S. R. B. M. Kutty, " Box behnken design for the optimization of calcium and magnesium ions removal from produced water by electrocoagulation; "in *World Engineering, Science and Technology congress (ESTCON)*, Kuala Lumpur Convention Centre, Malaysia, 12th-14th June, 2012, pp. 1-6.
- [3] E. H. Ezechi, M. H. Isa, and S. R. B. M. Kutty, " Removal of boron from produced water by electrocoagulation', *Advancs in Environment, Computational Chemistry and Bioscience*, 10th WSEAS International Conference onn Environment, Ecosystems and Development (EED'12), Eden Palace Au Lac Hotel, Montreux, Switzerland. (December 2012).